ABSTRACT

Title of Dissertation:	EXAMINATION OF SOIL GREENHOUSE GAS FLUXES AND DENITRIFICATION TO ASSESS POLLUTION SWAPPING IN AGRICULTURAL DRAINAGE WATER MANAGEMENT
	Jacob Gerrit Hagedorn, Doctor of Philosophy, 2022
Dissertation directed by:	Professor Eric A. Davidson, Marine, Estuarine, and Environmental Science

Increases in agricultural nitrogen (N) inputs driven by synthetic N fertilizer application over the past century have led to higher crop yields but have also intensified riverine nitrate (NO_3^-) loading, contributing to environmental degradation. Drainage water management (DWM) is a best management practice (BMP) implemented on agricultural ditches to reduce downstream NO_3^- loading by slowing ditch discharge with drainage control structures that raise the in-field water table, creating anaerobic conditions. More anaerobic conditions stimulate denitrification and possibly methanogenesis. Denitrification consumes NO_3^-, thereby reducing the downstream N loading, but also increases production of N gases nitric oxide (NO), nitrous oxide (N_2O), and dinitrogen (N_2). This research examined the potential consequence of greenhouse gas (GHG) emissions, specifically methane (CH_4) and N_2O, as a result of DWM-induced low oxygen conditions in a replicated experimental design. Using multiple methods such as soil gas flux measurements, N isotope analyses, gases dissolved in groundwater, and N budgets, this project examined the potential pollution trade-offs between dissolved NO_3^- and soil GHG fluxes.

In chapter 2, I quantified soil N_2O and CH_4 fluxes using static chambers over three years in a corn/soybean rotation system. I also measured soil environmental variables to assess controls on gas production. Results indicated that the DWM treatment raised the groundwater level near the ditch edge but did not increase the surface soil moisture, which likely led to the observation that DWM did not significantly increase soil N_2O and CH_4 emissions. Variation in N_2O fluxes were heavily influenced by N fertilizer application events. A nitrogen budget indicated that this farm site had a lower than average N use efficiency in the U.S. and higher than average soil N_2O emissions.

In chapter 3, I qualitatively and quantitatively examined the role of denitrification in this DWM system by using natural abundance NO_3^- isotopes measured across a leaching continuum (topsoil to deep soil to groundwater to ditch water). Results demonstrated that isotopic values of $\delta^{15}N$ and $\delta^{18}O$ increased in residual NO_3^- along the leaching continuum, providing evidence of denitrification. However, the net effects of nitrification and denitrification resulted in NO_3^- less enriched in ^{15}N than expected by denitrification alone. These isotopic values were then applied to a mass balance of total N and $\delta^{15}N$ to calculate quantitively the magnitude of total gaseous N export and to constrain that estimate using a net N isotopic discrimination factor. The calculated gaseous N export and denitrification rates fell within but toward the high end of previously reported literature ranges. The N budget indicated lower hydrologic N export in the DWM treatment, suggesting increased denitrification, but uncertainty of the corresponding estimates of increased gaseous N export was greater than the difference between treatments, rendering inconclusive the hypothesis that DWM treatment causes more total gaseous N production and

denitrification. Inclusion of isotopes in the N mass balance established a lower bound of total gaseous N export, which was still large relative to other budget terms.

In chapter 4, I synthesized results from the previous two chapters to explore the components of total gaseous N export. I also estimated annual export via dissolved N_2O and N_2 in groundwater entering the drainage ditches. Soil N_2 emissions were estimated by subtracting annual estimates of soil N_2O and groundwater dissolved N_2 and N_2O from the total gaseous N export. Results showed that soil N_2 emissions dominated the gaseous N export. The $N_2O/(N_2 + N_2O)$ ratios of soil emissions were within but on the lower side of the literature range.

This study demonstrated that, at least for this farm, the decrease in hydrologic N loading due to implementation of DWM outweighed the small and statistically non-significant observed increase in GHG production. This result lends support for policies to further incentivize adoption of DWM in ditched agricultural settings. This study also provides a novel, multi-methodological approach for quantitatively assessing and constraining denitrification rates and N_2 emissions. It also is the first study to incorporate measurement of multiple fractions of total gaseous N export on the farm scale as part of annualized agricultural N budget.

EXAMINATION OF SOIL GREENHOUSE GAS FLUXES AND DENITRIFICATION TO ASSESS POLLUTION SWAPPING IN AGRICULTURAL DRAINAGE WATER MANAGEMENT

by

Jacob Gerrit Hagedorn

Dissertation submitted to the Faculty of the Graduate School of the
University of Maryland, College Park, in partial fulfillment
of the requirements for the degree of
Doctor of Philosophy
2022

Advisory Committee:
Professor Eric A. Davidson, Chair
Professor David Nelson
Associate Professor Rebecca Fox
Associate Professor Xin Zhang
Professor Margaret Palmer, Dean's Representative

Dedication

This dissertation is dedicated to Annelise and Alene. This journey would not have been possible without you. You are everything. Here is to a future full of family time, hiking, house building, dreaming, and equally splitting the second shift! Love you!

Acknowledgements

I would like to acknowledge and thank my advisor, Eric Davidson, for an endless amount of support and encouragement. You have guided me through the scientific process with much patience and you have showed me what it means to be a great mentor. I hope to replicate that as I advise students in the future. Also, many thanks to the rest of my committee: Xin Zhang, David Nelson, Rebecca Fox, and Margaret Palmer. Your expertise and insight have been and will be integral to the execution of dissertation.

This project would not have been possible without funding from UMCES, USDA-NIFA, Maryland Water Resources Research Center, and Maryland Sea Grant.

Special thanks to Qiurui Zhu, Mark Castro and Eline Costa for field work assistance, I don't think we will miss dragging electric cords through 9' tall corn. Thanks to Joel Bostic for being technical lab help, exercise buddy, motivator, and moral support; you are true friend. Also, thanks to Stephanie Siemek for being there for technical and emotional support. Thanks to all staff at the Appalachian Lab for dealing with me over the years. Whether it be troubleshooting instrumentation, helping fill out paperwork, or being a listening ear, you are all appreciated.

Thanks to the Horn Point Laboratory team of Tom Fisher, Rebecca Fox, Anne Gustafson, and Erika Koontz and for letting me be a quasi-member of your group, assisting me with field work, data acquisition, interpretation, and writing. Thanks for allowing me to use preliminary data in my analysis.

Big shout out to our collaborating famer, Jim Lewis. Thanks for letting us invade your fields with instrumentation and working your farm management around

our needs. Thanks for just being a text away to answer my many naïve questions about farming and showing me about combine harvester works.

To all my Frostburg friends, thank you for your community. The conversations, distractions, housing, meals, hikes, and laughs were the best part of this journey.

Lastly, thanks to my family (Hagedorn and DeJong). Thanks for believing in me through the brightest and darkest days. A return to the “old” Jake is imminent, so get ready.

Table of Contents

List of Tables

Chapter 2

List of Figures

Chapter 1

Chapter 2

List of Abbreviations

BMP	Best management practice
CH_4	Methane
CO_2	Carbon dioxide
DCS	Drainage control structure
DNRA	Dissimilatory nitrate reduction to ammonium
DWM	Drainage water management
EF	Emissions factor
GHG	Greenhouse gases
GLMER	Generalized linear mixed-effects model
HABs	Harmful algal blooms
KCL	Potassium Chloride
N	Nitrogen
N_2	Dinitrogen gas
N_2O	Nitrous oxide
NH_3	Ammonia
NH_4^+	Ammonium
NO	Nitric oxide
NO_2	Nitrogen dioxide
NO_2^-	Nitrite
NO_3^-	Nitrate
NUE	Nitrogen use efficiency
P	Phosphorus
TDN	Total dissolved nitrogen
UAN	Urea-ammonium-nitrate
VWC	Volumetric water content
WFPS	Water filled pore space

Chapter 1: Introduction

1.1 Nitrogen in Agricultural Settings

With over 1.53 billion hectares of cropland and 3.38 billion hectares of pasture on earth, global agriculture expansion since the mid-nineteenth century has impacted earth's biogeochemical cycles. Agricultural intensification, or increasing crop yield per unit area, has also risen (Matson et al., 1997). In order to accommodate agricultural expansion and intensive crop production, nitrogen (N) fertilizer use has increased by 800% in the past 50 years (Foley et al., 2011), primarily driven by the Haber-Bosch process that captures atmospheric nitrogen and converts it to reactive N (Smil, 1999). N is a key element for ecosystem productivity, particularly within the context of agriculture and this process could provide a practically unlimited source of synthetic nitrogen fertilizer that has been and is used to increase agricultural yield. The problem is that much of the applied N is not incorporated into the crops. Global nitrogen use efficiency (NUE) calculations, a measure used to assess how effectively applied N is absorbed by crops, estimate that 63% (43% in USA) of the applied N is lost to the environment in a variety of pathways such as gaseous emissions and leaching loss (Lasseletta et al., 2014; Zhang et al., 2015).

This loss of N fertilizer to the environment has caused many unintended consequences, which have been termed the “nitrogen cascade” (Galloway et al., 2003). The different chemical forms, magnitudes, transformations, and movement of N impact this cascade and its environmental effects. N can exist in a solid, aqueous, or gaseous state. Common inorganic forms of nitrogen are dinitrogen (N_2), nitrous

oxide (N_2O), nitric oxide (NO), nitrogen dioxide (NO_2), nitrite (NO_2^-), nitrate (NO_3^-), ammonium (NH_4^+), and ammonia (NH_3). The largest pools of nitrogen on earth are in the atmosphere, ocean, and crust. From an agricultural perspective, an important pool of N is soil organic matter which is comprised of decomposing plant matter or microbial biomass (Knoll et al., 2012). As organisms use N compounds, they transform N from one form to another. Common N transformations include mineralization, immobilization, nitrification, dissimilatory nitrate reduction to ammonium (DNRA), denitrification, fixation and anammox. Mineralization refers to the decomposition of organic matter and release of NH_4^+ into soil solution, while immobilization refers to the uptake of NH_4^+ and NO_3^- by microbial biomass. Nitrification is the bacteria-driven process that converts NH_4^+ to NO_3^- in oxic conditions while DNRA converts NO_3^- to NH_4^+ in low oxygen conditions. Denitrification is the bacteria process that reduces NO_3^- to NO_2^- to NO to N_2O to N_2, usually but not exclusively in anerobic conditions. Fixation, either industrially or biologically, is the process by which atmospheric N_2, when combined with other elements, is transformed to a reactive N form such as NH_3. Fixation by lightning, converting N_2 to NO_3^-, is a relatively minor pathway of N fixation. Lastly, anammox, or anaerobic ammonium oxidation, is a bacteria driven process that converts NH_4^+ and NO_2^- to N_2 in anaerobic conditions (Chapin et al., 2002; Hutchinson et al., 1993; Knowles, 1982). These common transformations control how much of and in what form this valuable nutrient is accessible to crops and distributed throughout the agroecosystem.

Via these N transformations, the production of two molecules of N are of particular concern for this study. The first is soluble NO_3^- because it easily moves into waterways. More dissolved NO_3^- leads to human drinking water concerns, and increases the likelihood of eutrophication events, where algae growth and subsequent decomposition of algal necromass consumes available oxygen, reducing water quality for other organisms (Howarth et al., 1996; Kemp et al., 2005; Glibert, 2020). The other molecule of concern is N_2O because it is a greenhouse gas that contributes to climate change and stratospheric ozone depletion. Agricultural soils are the primary anthropogenic source of N_2O over the past century (Lawrence et al., 2021). This gas can also dissolve into water, a phenomenon often overlooked when assessing pollution contributions and distribution.

Managing agricultural nutrients in the interest of water quality and climate change is a critical concern globally, as well as within the Chesapeake Bay watershed. The Eastern Shore, an 11,200 km^2 area on the Delmarva Peninsula that includes parts of western Delaware, eastern Maryland, and the eastern shore of Virginia, comprises only seven percent of the Chesapeake Bay watershed area but receives twice as much N input per unit area of agricultural land compared to the rest of the watershed (Ator, 2015). Agricultural production in this region accounts for about 90% of the N inputs on the Eastern Shore, much of which has contributed to eutrophication and drinking water degradation (Wieczorek and LaMotte, 2010). To reduce nitrogen loading to receiving waters there has been an effort to implement best management practices (BMPs) and stream restoration projects that focus on nutrient

application management and reduction in high-nutrient runoff (Filoso and Palmer, 2011)

1.2 Agricultural Drainage Water Management

A primary reason that high-nutrient runoff has become a problem is agricultural land conversion. Historically, the Eastern Shore was forested with large portions of the region under long periods of inundation (Ator, 2015). To reduce inundation and create arable land for agriculture, artificial drainage and ditching was used to remove water from the fields and create drier soils for crop production. In Maryland, there are over 800 miles of publicly administered drainage ditches and hundreds of miles of privately managed ditches (Needelman et al., 2007). While these ditches create drier field conditions, they are also conduits for applied nutrients to leave the fields in drainage water and quickly move downstream. The drainage ditches and nutrient loading are not just a concern on the Eastern Shore. A significant portion of the springtime NO_3^- loading to the Gulf of Mexico that contributes to hypoxic dead zones is derived from subsurface drainage systems in the Upper Midwest of the U.S. (David et al., 2010)

To reduce nutrient loading to nearby bodies of water, a BMP called drainage water management (DWM) or controlled drainage was designed. DWM consists of a drainage control structure (DCS) that is installed at the end of drainage ditches to regulate the discharge from the field. The DCS consists of a box inserted into the ground with stackable boards inside that control the height of the water table in the ditch. Figure 1 shows a cross-sectional view of a DCS in a drainage ditch. The goal of DWM is to decrease the amount of dissolved N that leaves the fields to improve

overall water quality for the downstream watershed (Skaggs et al., 1994; Skaggs et al., 2012; Evans et al., 2007). Research has shown that this BMP has been effective for reducing NO_3^- loading by either decreasing hydrologic discharge and/or decreasing NO_3^- concentration (Fisher et al., 2010; Schmidt et al., 2007; Gilliam et al., 1979; Evans et al., 1995; Drury et al., 2014). When managed correctly, DWM does not adversely affect crop yield and in some instances increases yield by increasing subsurface water available for crop growth (Schott et al., 2017; Jaynes 2012).

1.3 Denitrification

The mechanism for DWM's effectiveness at reducing NO_3^- concentrations is that slowing water flow increases the soil water residence time, creating more anaerobic conditions that could facilitate denitrification in the soil subsurface (Skaggs et al., 2012). Denitrification is the microbially-driven process of respiratory reduction of NO_3^- or NO_2^- to gaseous NO, N_2O, or N_2. The key environmental conditions that control denitrification are microbial diversity, soil temperature, oxygen availability, organic carbon availability, pH, and NO_3^- availability (Nommik, 1956; Knowles, 1982; Firestone and Davidson, 1989). Denitrifying organisms are considered ubiquitous in most environments, although some do not have the full suite of enzymes for carrying out each reductive step from NO_3^- to N_2. Most are facultative aerobes that activate denitrifying enzymes when oxygen becomes limiting (Hutchinson et al., 1993; Tiedje, 1988). Peak bacterial activity for denitrification occurs between 10-35ºC and rates decrease below and above this temperature range. Labile organic carbon serves as an electron donor in denitrification. Since organic carbon is more

prevalent in surface soils, denitrification is expected to be more prevalent there compared to deeper soils or groundwater. Lower oxygen content is more suitable for denitrification, although the presence of O_2 can vary in soil microsites. Water filled pore space (WFPS) of soil, as a proxy for oxygen content, controls denitrification rates and gas diffusion from soils (Knowles, 1982; Davidson et al., 2000; Morse et al., 2012). Research has demonstrated that different WFPS contents yield different proportions of gaseous by-products from denitrification (Amundson et al., 1990; Davidson et al., 1991, Davidson et al., 2000). As the electron acceptor, NO_3^- availability is central to denitrification and is often abundant in fertilized agricultural settings.

Quantifying in-situ denitrification is challenging because of the variety of gaseous by-products produced and environmental condition heterogeneities. There have been many strategies used to estimate denitrification, from direct flux measurements to tracers to stable isotope techniques. Directly measuring the dominant end product of denitrification, N_2, is difficult because high atmospheric N_2 background means measuring detectable changes in concentration in situ is currently not possible (Groffman et al., 2006, Fisher et al., 2019). Denitrification in soils is also highly variable, both spatially and temporally. Much work has been dedicated to evaluating the spatial and temporal extent of denitrification, which led to the terms "hotspots" and "hot moments" (McClain et al., 2003). Recently, it has been proposed to transition from this language and use "control points" to describe spatial and temporal heterogeneity (Bernhardt et al., 2017). No matter the terminology, soil microsite variations in carbon, oxygen, and NO_3^- control the spatial and temporal

occurrence of denitrification in soils. Temporally, seasons with higher precipitation, NO_3^-, and temperature would be expected to have higher denitrification rates. In agriculture, irrigation and fertilization events, particularly during the spring and summer, would likely promote denitrification (Dobbie et al., 1999). Spatially, lower topographic positions with higher moisture content or locations with higher N addition would have more denitrification potential. Because of these spatial and temporal heterogeneities most denitrification measurements, depending on scale, have high uncertainties. For this reason, it is important to combine multiple approaches when attempting to quantify denitrification to help frame inherent heterogeneity and uncertainty (Groffman et al., 2006).

Denitrification is an important biogeochemical process within the N cycle that regulates the accumulation of NO_3^- by reduction to NO, N_2O, and N_2. From an agricultural perspective, denitrification promoted by DWM could alleviate N loading to downstream waters. However, an important consideration must be given to the magnitude of an intermediate denitrification product, N_2O, which can diffuse to the atmosphere when denitrification is incomplete. As a consequent, denitrification could cause harmful environmental effects by producing this potent greenhouse gas and reactant in stratospheric ozone depletion. The tradeoff between NO_3^- reduction to improve water quality and N_2O production that could exacerbate climate change, presents a case of potential pollution swapping.

1.4 Nitrous Oxide

Nitrous oxide is the denitrification by-product of focus in this study because N_2O is a greenhouse gas 265 times more potent than carbon dioxide (CO_2) on a 100-

year time frame (Pachuri et al., 2014). Since agricultural soil management is responsible for 74% of 2020 U.S N_2O emissions (US EPA, 2020) understanding the influence of agricultural management practices on N_2O emissions presents a valuable area of research. The average N_2O concentration in the atmosphere in 2018 was 330 ppb with an upward trajectory of 1.3% per year (US EPA, 2019). The primary reason agriculture is responsible for the majority of anthropogenic N_2O emissions is synthetic fertilizer usage, which provides ample NO_3^- that can help stimulate the denitrification process.

While the emphasis of this research is on N_2O production by denitrification, N_2O can also be produced by nitrification, a biological aerobic process that oxidizes NH_4^+ to NO_3^-. It can be difficult to decipher which molecule of N_2O is derived from which biogeochemical process. Both processes can co-occur in agricultural fields depending on the spatial distribution of oxygen and soil microsite conditions. Soil N_2O emissions are impacted by similar environmental variables as denitrification such as soil temperature, available nitrogen, pH, and water content (Skiba et al.,1998; Castellano et al., 2010). In general, as WFPS rises above 60-70%, depending on the soil type, denitrification is most responsible for N_2O emissions. Below 60% WFPS, nitrification becomes the dominant N_2O producing process (Bateman et al., 2005; Davidson et al., 2000). Because DWM and the subsequent influence on soil moisture is the focus of this research, the assumption is that N_2O production from incomplete denitrification is usually more important than N_2O production from nitrification, although the sum is measured. Evidence of the importance of denitrification will be

provided by complementary measurements of the $\delta^{15}N\text{-}NO_3^-$, a stable isotope of NO_3^-, as described later.

1.5 Methane

Another consideration when implementing DWM is that increased anoxic conditions could also create conditions suitable for methane (CH_4) production by methanogenesis (Nykanen et al., 1998; Nangia et al., 2013). Methane is a greenhouse gas 25 times more potent than carbon dioxide on a 100-year time frame (IPCC 2014). Agriculture accounts for 47% of national CH_4 emissions, but that is primarily because of enteric fermentation and manure management (US EPA, 2019). In soils, methanogens produce CH_4 via reduction of organic substrates when there is an abundance of organic C along with a depletion of preferred electron acceptors like O_2, NO_3^-, and sulfate, which often occurs in saturated wetland landscapes (Chapin et al., 2002; Brevik et al., 2012). Methane is also oxidized by methanotrophs, which requires oxygen, and therefore typically occurs in the soil surface where oxygen can more easily diffuse. Since the presence or absence of oxygen is so vital, soil moisture plays a large role in the consumption, production, and movement of CH_4. Methane fluxes into the atmosphere are usually highest when it escapes through plant tissues or as bubbles that bypass zones of CH_4 consumption (Walter et al., 2006). Other factors that control CH_4 production and consumption include temperature, pH and NH_4^+ content. In general, temperature and pH impact the function of the microbes that produce or consume CH_4. Ammonium can compete with methanotrophs for CH_4, inhibiting CH_4 oxidization.

1.6 Natural Abundance Nitrate Isotopes

In agricultural systems, N pools, flows and transformations have been measured using different methodological techniques to answer pertinent questions about biogeochemical processing. One such method is the application of natural abundance isotopes to identify and quantify distinct sources and transformations of N, particularly denitrification. Isotopes of an element have the same number of protons but a different quantity of neutrons. The most abundant N isotope and O isotope are ^{14}N and ^{16}O, respectively. ^{15}N and ^{18}O are less abundant isotopes of N and O and the ratio of $^{15}N/^{14}N$ or $^{18}O/^{16}O$ can be used to evaluate specific environmental processes that impact that ratio. Isotopic methods can be suitable for detecting and quantifying denitrification because denitrifying bacteria prefer to consume NO_3^- with the ^{14}N isotope (Kendall et al., 2007; Groffman et al., 2006). This preference causes isotopic fractionation which leaves behind residual NO_3^- with a relatively enriched ^{15}N isotopic value. Denitrification also fractionates the oxygen atoms when reducing NO_3^-, preferring ^{16}O, thereby leaving behind residual NO_3^- with an enriched ^{18}O isotope value. Using a dual isotope ($\delta^{15}N\text{-}NO_3^-$ and $\delta^{18}O\text{-}NO_3^-$) approach, denitrification is expected to leave an isotopic imprint on both atoms during microbial NO_3^- consumption. By assessing the relationship between the dual isotopes, denitrification can be qualitatively inferred (Fang et al., 2015; Granger et al., 2010; Hall et al., 2016). This inference is primarily derived from the notion that denitrification can be described by examination of the $\delta^{18}O\text{-}NO_3^-$: $\delta^{15}N\text{-}NO_3^-$ slope. Previous studies have demonstrated that the range of denitrification signal occurs between the slopes of 0.5 and 1.0 (Figure 2) (Kendall et al., 2007; Houlton et al., 2006). However, other N

transformation processes can impact the isotopic signature of NO_3^-. Nitrification, the oxidation of NH_4^+ to NO_3^-, can also fractionate NO_3^-, but produces isotopically lighter ^{15}N-NO_3^-. Nitrification does not fractionate the oxygen atom of NO_3^- because it derives oxygen from surrounding soil air and soil water, which has its own unique isotopic values. For this reason, $\delta^{18}O$-NO_3^- might maintain the denitrification imprint in residual NO_3^- but for $\delta^{15}N$-NO_3^- there is a possibility of overprinting of lighter NO_3^- (nitrification) on heavier residual NO_3^- (denitrification), masking the denitrification signal (Granger et al., 2008).

1.7 Mass Balance of Total N and ^{15}N

Another methodological technique used to assess N processing in agroecosystems is N mass balance derived from N budgets. This accounting technique has been used since the 1800's, (Meisinger et al., 2008; Allison et al., 1955) but more recently it has been supplemented to include $\delta^{15}N$, which allows for a more detailed analysis of specific N flows (Bai et al., 2012; Fang et al., 2015). Mass balances require defining the temporal and spatial boundaries of a system, then quantifying the inputs and outputs of that system. The internal N cycling of the system is typically assumed to be at steady state, which allows for the output, which is difficult to measure, to be estimated by difference (Zhang et al., 2020; Groffman et al., 2006). This is the case for the quantification of the N output of denitrification or gaseous export for many N balances in a variety of ecosystems, with most using total N for the mass balance (David et al., 2000; Pribyl et al., 2005; David et al., 2001). Recent isotopic measurement advancements have allowed for $\delta^{15}N$ to be incorporated into mass balance analyses. This is important, particularly when characterizing

gaseous N export in a mass balance because N processes isotopically fractionate when producing N_2, N_2O, NH_3 and NO. When isotopic fractionation occurs, the residual substrate becomes relatively enriched and the product relatively depleted in $\delta^{15}N$. The difference between the initial substrate enrichment and the depleted product is the discrimination factor, or isotope effect (Craine et al., 2015). While multiple N processes, such as denitrification, nitrification and volatilization, can be responsible for the production of N gases and isotopic fractionation, assessment of $\delta^{15}N$ and discrimination factors help constrain the limits of gaseous emissions and denitrification. This aids the mass balance goal of quantifying specific N outputs without direct measurement. While promising, one characteristic of most mass balances is uncertainty. Most inputs variables in mass balances have some error associated with their measurement, the error representing temporal, spatial, or technological variation. When calculating an output by difference, the resulting value encapsulates the propagation of all input variable errors, usually leading to large uncertainty (Davidson et al., 2006; Groffman et al., 2006; Fisher et al., 2019). Despite high uncertainty, this mass balance technique is valuable for assessing N cycling in agroecosystems and provides an analytical foundation for when uncertainty can be reduced with technological advancements, more intensive measurement, or new approaches.

1.8 Study Site

This research occurred on a private farm that is artificially drained with ditches in the Choptank basin on the Eastern Shore of Maryland, USA. This region's land use is dominated by agriculture, both crop and poultry production (Ator, 2015).

The collaborating farmer has been performing the same farm management strategy of corn/soybean rotation since 2004 and operated the DWM BMP since 2006. Regional watersheds including this site have historically had high nutrient loading into downstream water, which has contributed to Chesapeake Bay eutrophication and algal bloom events (Testa et al., 2017). There has been general improvement, with local variation, in nutrient loading in the past 30 years (Murphy et al., 2022; Sabo et al., 2022), and some of that is attributed to the implementation of BMP's incentivized by federal and state programs (Fisher et al., 2021; Fox et al., 2021). The experimental design at the study site consisted of field scale DWM and non-DWM treatment with two replicates per treatment. Soil gas emissions, soil extractions, groundwater, and surface ditch water were measured and sampled in the execution of this study.

1.9 Research Overview

Given that DWM has the potential to decrease NO_3^- but also produce N_2O and CH_4, this research explored the magnitude and mechanisms of potential pollution-swapping, or trading reductions in dissolved NO_3^- export for increases in greenhouse gas emissions, occurring in an agricultural field that uses DWM. This research contributes to understanding soil gas dynamics and denitrification in an operational agricultural setting. This was executed according to the three objectives described below, each corresponding to a respective chapter.

1) Quantify how DWM impacts soil greenhouse gas fluxes using static soil chambers (chapter two)

2) Determine how DWM affects denitrification using a dual isotope technique and mass balance for both qualitative and quantitative denitrification assessment (chapter three)

3) Integrate the quantitative estimates with soil N_2O emissions and hydrologic dissolved gases to examine the gaseous N export component of the N budget (chapter four)

In chapter two, I evaluated if DWM increased soil N_2O and CH_4 emissions at the field scale. I used static soil chambers to manually sample soil gas fluxes over three years. I also measured soil parameters such as NO_3^- content, temperature and moisture to evaluate environmental drivers of soil N_2O emissions. I showed that while there was evidence that DWM raised the groundwater table near drainage ditches, that impact was not observed in surface soil moisture within the fields. The active periods of DWM did not result in significantly higher N_2O and CH_4 emissions, indicating that at this site, pollution swapping is not a serious concern. Soil N_2O emissions were driven by N fertilization events, moderate soil moisture conditions, higher NO_3^- content, and higher soil temperature, aligning with previous literature. Multiple techniques for the calculation of annual N_2O estimates revealed consistent values, which were above average in comparison to other N fertilized corn sites. This farm also had above average N surplus and below average N use efficiency.

In chapter three, I examined the impact of DWM on denitrification and total gaseous N export. I used a natural abundance NO_3^- isotope technique to examine relationships between $\delta^{15}N\text{-}NO_3^-$, $\delta^{18}O\text{-}NO_3^-$, and NO_3^- in soils, groundwater and ditch water to qualitatively describe the impact of denitrification at different spatial

locations. I combined this isotopic assessment with a N mass balance to quantitatively describe total gaseous N export and denitrification. I presented isotopic evidence that denitrification and nitrification are co-occurring in soils, groundwater and ditch water, in both treatments. There was also evidence that denitrification isotopic signal intensifies along a continuum from surface soils to ditch water. Additionally, dissolved gases in groundwater supported evidence of denitrification as elevated excess N_2 concentrations were associated with lower oxygen saturations, lower NO_3^- concentrations and more enriched $\delta^{15}N\text{-}NO_3^-$ values. For both treatments, the N mass balance showed that gaseous N export was the second largest export besides crop N export and fit within the range of values found in other fertilized agricultural systems. An estimate of net N discrimination factors based on isotope mass balance helped constrain the uncertainty of the magnitude of denitrification-derived gaseous N emissions. A sensitivity analysis showed that even if there were underestimates in hydrologic N export, substantial gaseous N export would still be indicated by constraints of reported discrimination factor on the ^{15}N mass balance. Although the DWM treatment had less hydrologic N export compared to the non-DWM treatment, which suggested that DWM treatment had more gaseous N export, the propagation of errors required for mass balance showed that the uncertainties of total gaseous N export were as large as the difference between treatments.

In chapter four, I synthesized total annual gaseous N export from the mass balance analysis with measured soil N_2O emissions and groundwater dissolved N_2 and N_2O estimates. I explored the relationships between the components of the gaseous N export and showed that soil N_2 emissions likely dominated gaseous N

export, implying that denitrification played a large role in this agroecosystem although the role was not substantially different between treatments.

In summary, I showed that the DWM treatment impacted groundwater near the ditch edge, but not in the surface soil moisture. There was not a statistically significant increase in N_2O and CH_4 soil gas emissions in the DWM treatment, suggesting that pollution swapping was not a serious concern. There was evidence for denitrification from the isotopic evaluation of variety of media (soils, groundwater, ditch water) and in groundwater dissolved N gas measurements, although no difference by treatment. The hydrologic N export was lower in the DWM treatment compared to non-DWM treatment, but the gaseous N export estimates had greater uncertainty than difference between treatments. Gaseous N export was likely dominated by soil N_2 emissions.

This research has implications for agricultural water management strategies on the Eastern Shore and in the Upper Midwest USA, where extensive ditch networks continue to function. This study added to other work demonstrating that the concern of swapping decreases in NO_3^- export for increases in N_2O and CH_4 emissions when employing DWM was not found. While NO_3^- export was decreased, soil GHG emissions were not significantly greater as a result of DWM. This finding adds to the growing body of literature evaluating the effectiveness of BMPs. From a fundamental agroecosystem N cycling perspective, this research contributes an applied, intensively sampled, field scale, multi-methodological example for quantifying the key components of a N budget. This study adds to previous literature that used N mass and natural abundance N isotopes to qualitatively and quantitatively assess the role of

gaseous N production and denitrification. This work advances the scientific knowledge by synthesizing multiple direct gaseous N measurements with a full N budget, which better frames the intricacies and uncertainties surrounding N cycling in an agroecosystem.

1.10 Figures

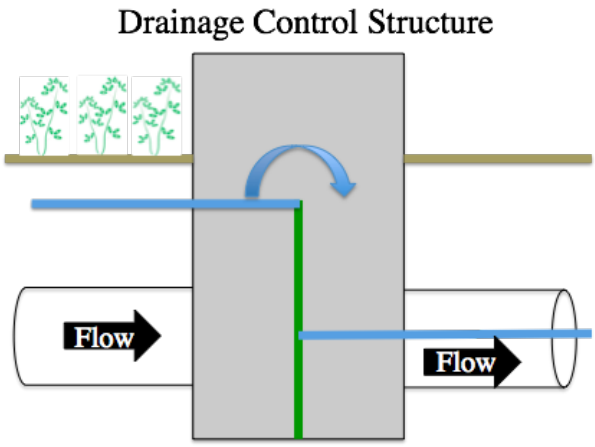

Figure 1: Cross-sectional depiction of a drainage control structure placed at the end of agricultural drainage ditches, controlling the water table height and water flow. The panel shows stacked boards (green) that slow or stop ditch water flow and raise the water table (blue) in the soil behind the structure.

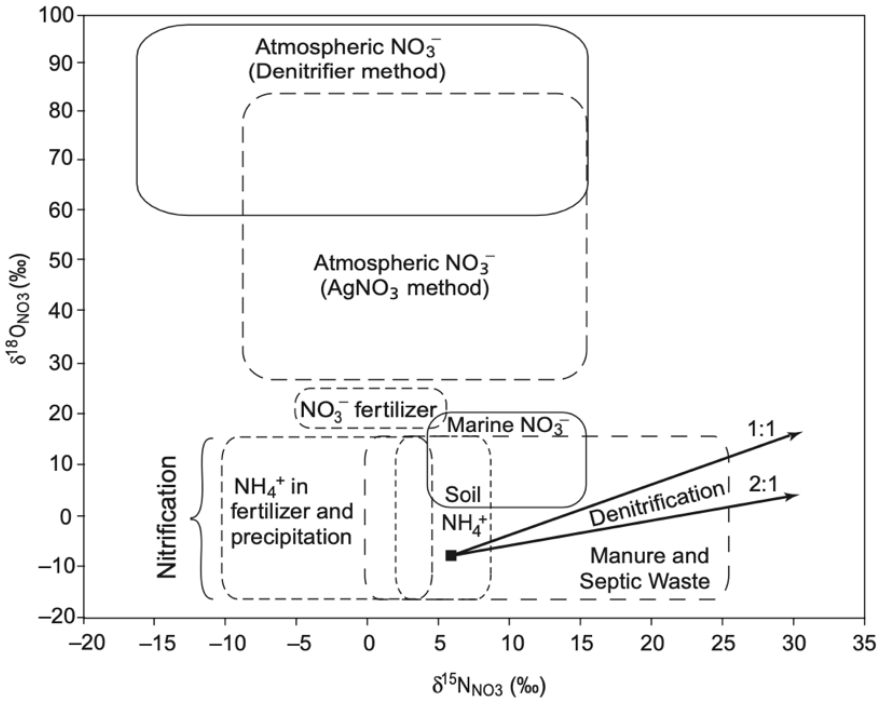

Figure 2. Graphic by Kendall et al. (2007) illustrating the relationship between the $\delta^{15}N\text{-}NO_3^-$ value and the $\delta^{18}O\text{-}NO_3^-$ value. The boxes within the plot show the relative ranges of isotopic values associated with certain pools and processes. The 1:1 (1.0) and 2:1 (0.5) denitrification slopes are labeled.

Chapter 2: Effects of Drainage Water Management in a Corn–Soy Rotation on Soil N_2O and CH_4 Fluxes

Chapter Note

This chapter was published in the journal *Nitrogen* (2022, 3, 128–148. https://doi.org/10.3390/nitrogen3010010) with co-authors Eric Davidson, Thomas Fisher, Rebecca Fox, Qiurui Zhu, Anne Gustafason, Erika Koontz, Mark Castro, and James Lewis.

Abstract

Drainage water management (DWM), also known as controlled drainage, is a best management practice (BMP) deployed on drainage ditches with demonstrated success at reducing dissolved nitrogen export from agricultural fields. By slowing discharge from agricultural ditches, subsequent anaerobic soil conditions provide an environment for nitrate to be reduced via denitrification. Despite this success, incomplete denitrification might increase nitrous oxide (N_2O) emissions and more reducing conditions might increase methanogenesis, resulting in increased methane (CH_4) emissions. These two gases, N_2O and CH_4, are potent greenhouse gases (GHG) and N_2O also depletes stratospheric ozone. This potential pollution swapping of nitrate reduction for GHG production could negatively impact the desirability of this BMP. We conducted three years of static chamber measurements of GHG emissions from the soil surface in farm plots with and without DWM in a corn–soybean rotation on the Delmarva Peninsula. We found that DWM raised the water table at the drainage ditch edge, but had no statistically significant effect on water-filled pore space in the field soil surface. Nor did we find a significant effect of DWM on GHG emissions. These findings are encouraging and suggest that, at least for this farm site,

DWM can be used to remove nitrate without a significant tradeoff of increased GHG emissions.

2.1 Introduction

Excess agricultural nitrogen (N) and phosphorus (P) addition to the environment has been a long-term problem in the United States, contributing to algal blooms and eutrophication (Glibert, 2020). Within the Chesapeake Bay watershed agricultural production on the Delmarva peninsula accounted for ~90% of the nitrogen inputs (Wieczorek and LaMotte, 2010; Ator and Denver, 2015; Sabo et al., 2019), much of which is derived from synthetic nitrogen fertilizer (Smil, 1999). Despite the need for nitrogen to increase crop yields, more than half of the N applied can be lost to the environment in a variety of pathways such as leaching and gas emissions (Lassaletta et al., 2014; Zhang et al., 2021). Surface ditches and tile drains installed to remove water from wet fields act as conduits for export of dissolved nutrients. Drainage water management (DWM) is a best management practice (BMP) designed to slow this movement and thereby reduce reactive N loss from agricultural fields that have drainage ditches (Skaggs et al., 1994; Evans et al., 1995).

Drainage water management (DWM) functions by placing drainage control structures (DCS) at the end of drainage ditches with the goal of slowing water discharge and raising water levels in ditches. By keeping water in the field for longer, the water table upstream of the ditch rises, creating more widespread anaerobic soil conditions (Skaggs et al., 2012). When N, as nitrate, is exposed to more reducing conditions microbially driven denitrification is more likely (Firestone and Davidson, 1989; Nömmik 1956). Some studies have demonstrated that DWM has been effective

at reducing nitrate loading into downstream waters (Carstensen et al., 2020; Drury et al., 2009; Sunohara et al., 2014), including preliminary results from the farm of present study (Hagedorn et al., 2019). However, incomplete denitrification can result in nitrous oxide (N_2O) production, a potent greenhouse gas (GHG) and a reactant in stratospheric ozone destruction (Kanter et al., 2021; Prather et al., 2015). In addition, nitrification has also been documented to produce N_2O as a byproduct (Firestone and Davidson, 1989). Agricultural soil management, driven by anthropogenic nitrogen inputs, is responsible for 75% of the total N_2O emissions in the US and 45% of total N_2O emissions in North America (US EPA, 2021; Xu et al., 2021). In addition to N_2O, reducing conditions can also create higher methane (CH_4) emissions via methanogenesis (Knowles 1993). Methane is the second most important GHG, with potency 25-fold greater than CO_2 in a 100 year time frame (Pachauri and Meyers 2014).

Broadly, soil N_2O fluxes are controlled primarily by inorganic-N content, carbon availability, soil moisture, microbial community abundances/composition, soil temperature, soil pH, and soil texture (Firestone and Davidson, 1989; Nömmik 1956). Fertilizer N can be rapidly converted to nitrate, through nitrification, and nitrate can then become substrate for denitrification. Both nitrification and denitrification can contribute to large N_2O emission spikes (Bateman and Baggs, 2005), especially denitrification when high soil nitrate concentrations co-occur with high soil moisture conditions (Fisher et al., 2018; Dobbie et al., 1999). The combination of high N input with DWM that retains water in the field could result in lower hydrologic losses of N as nitrate through the ditch but with the tradeoff of higher losses of N_2O.

Previous work examining the impact of water table changes and DWM on GHG emissions in agriculture fields has yielded contradictory results. Some studies found that undrained fields had higher N_2O emissions than drained fields (Kumar et al., 2014; Fernández et al., 2016; Kliewer and Gilliam 1995; Elmi et al., 2005) while other studies found that there was no difference in N_2O emissions between drained and undrained fields (Nangia et al., 2013; Crézé and Madramootoo 2019; Datta et al., 2013; Van Zandvoort et al., 2017). For CH_4, one study (Kumar et al., 2014) found higher emissions in undrained fields while others found no drainage effect on CH_4 emissions (Nangia et al., 2013; Crézé and Madramootoo 2019; Datta et al., 2013). Some of these studies did not directly evaluate DWM manipulations, creating higher and lower water tables at specific times of the year, rather they explored drainage impact in general (Kumar et al., 2014; Fernández et al., 2016; Datta et al., 2013), or drainage impact with subsurface irrigation (Elmi et al., 2005; Crézé and Madramootoo 2019). The variability in conclusions and paucity of direct assessments of DWM mean that further research is needed to understand the impacts of this particular BMP on the potential for increased GHGs. Here, we compare measured soil emissions of N_2O and CH_4 in corn and soybean fields with controlled drainage (DWM) and free drainage (non-DWM) at a farm in eastern Maryland, on the Delmarva Peninsula. We hypothesized that DWM would increase soil GHG emissions.

2.2 Methods

2.2.1 Study site location

The research site was located on a private farm within the Choptank watershed on the coastal plain of the Delmarva Peninsula on the Eastern Shore of Maryland (Figure 1, N 39.11973, W 75.8069). Historically a wet landscape, the land was made arable by installing drainage ditches. Harvested crops mostly contribute feed to nearby concentrated poultry production. Precipitation averages 110 cm per year. This study site is an operational farm with a collaborating farmer willing to accommodate our research needs while working within the timing of standard agricultural management. A DWM system was already in place and a direct evaluation of that system was possible in a relatively small area. The ditches split the site into four similarly sized fields ranging from 3 to 6 hectares each, with an average length of 220 m. The dominant soil type is a Fallsington series on 0–2 percent slopes classified as fine-loamy, mixed, active, mesic Typic Endoaquults.

2.2.2 Farm management

The crop management plan was a no-till, corn–soybean rotation with a winter radish cover crop. The typical growing season ranged from April to October. Approximately 213 kg ha^{-1} of synthetic urea-ammonium nitrate (UAN) was applied during corn years and no N fertilizer was applied during soybean years. Approximately 22 kg N ha^{-1} was knifed-in during corn planting, and the other 191 kg N ha^{-1} was broadcast-applied in late May or early June. During corn planting, the fields received a sulfur addition of 15 kg S ha^{-1}. Liquid or dry potash was applied

during corn and soybean years. Herbicide was applied prior to or soon after planting and sometimes in June to suppress undesired vegetative growth. Prior to harvest, daikon radish seed was applied by air to serve as the winter cover crop. Manure and lime were applied every 5 years, which did not occur during this project's duration. The site had pivot irrigation that was used to supplement natural precipitation events in the summer months. All the research fields had the same crop rotation schedule, N fertilization rate, and irrigation rate from 2017 to 2019.

2.2.3 DWM management

The DWM strategy consisted of inserting and removing boards within the drainage control structures (DCS) to slow the ditch discharge while accommodating standard farm practices (Figure S1). For farm activities such as planting, N fertilization, and harvest, the DCS boards were removed and fields were drained to create a drier condition for equipment use. This management timeline was dependent on precipitation events, groundwater levels, and evapotranspiration; therefore the strategy was modified to adapt to changing environmental conditions. We refer to the time period when the boards were in place in the DWM DCS as "active" and the period when they were removed from the DWM DCS as "inactive".

2.2.4 Experimental design

Figure 1 shows a site map depicting the static chamber transect locations and borders of study plots. Non-DWM, or free drainage, was implemented on two fields (A and B) and controlled drainage, or DWM, implemented in the other two fields (C and D). In each field the soil chamber sampling design consisted of a transect of eight

chambers installed perpendicular to the ditch. Each transect was approximately 12 m in length and the soil chamber collars were equally spaced. The replicate plots were adjacent to each other in order to increase the horizontal fetch of micrometeorological measurements of a companion part of this study that will be reported elsewhere.

Soil and soil gas flux measurements were taken approximately monthly, depending on climatic conditions, but more temporally intensive sampling was done around planting, irrigation, N fertilization, and harvest to better characterize trace gas dynamics during those periods. Because preliminary studies showed some diel variation (Figure S2), the order of chamber sampling was randomized to ensure that the same field was not measured at the same time of day during every sampling date, thus minimizing potential sampling biases due to diel variation. Fluxes were sampled starting at approximately 8:00 EST and extended until approximately 17:00 EST.

Two slotted PVC (5 cm diameter) piezometers, used to measured groundwater levels, were installed approximately 1.5–2 m deep in the four research fields. One piezometer was installed within 1 m of the perimeter of the ditch while another was placed in the field 15 m perpendicular to the ditch piezometer (Figure 1). The piezometers were located within 15 m of the chamber transect. Solinst water level data loggers were placed in each piezometer which recorded pressure and temperature every 30 min. The pressure was then converted to depth of water below the surface by subtracting barometric pressure recorded separately by a Solinst barologger. Thirty-minute water depths were aggregated to daily mean for this analysis.

There were four primary controls on the statistical power of this experimental design: (1) plot replication, (2) number of chamber measurements in each plot, (3)

number of days of sampling over three years and (4) number of gas concentration measurements used to calculate each flux. This experimental design was limited to two replicate plots per treatment because four was the maximum number of flux towers that could be established in the companion micrometeorological study. The within-plot statistical power of this study was provided by eight chambers per field, which was needed for measurements known to have high spatial variability, as is the case with N_2O and CH_4 (Kravchenko and Robertson 2015). This study had excellent statistical strength in the number of gas concentration measurements per flux calculation, as there was a single chamber headspace concentration recorded every second (1Hz), which increased the flux estimation accuracy, lowered the flux detection limit, reduced the time needed for each flux measurement, and afforded improved statistical analysis (Levy et al., 2011).

2.2.5 Flux measurements

A Picarro G2308 cavity ringdown spectrometer and a static soil chamber system were used to measure N_2O and CH_4 soil gas fluxes. The instrument specifications state that the raw precision (1σ) of the instrument was <25 ppb + 0.05% of the reading for N_2O and <10 ppb + 0.05% of the reading for CH_4. The chambers consisted of a PVC chamber top with a curled vent, 12 cm length and 1 mm ID, and a matching PVC chamber collar. The chamber was approximately 25 cm in diameter. The chamber collar height was 5 cm and was inserted 3–4 cm into the soil. The chamber top height was 2.5 cm and had a rubber gasket around the perimeter to ensure a tight fit onto the collar. The approximate total volume of the chamber, dependent on insertion depth into the soil, was 4 L. The flux measurement system

used a recirculation technique through inlet and outlet tubing connected to the instrument, air pump, and the chamber top. Twenty-meter lengths of 6 mm OD polyethylene tubing connected the gas analyzer to the chamber top. Given the average flow rate of the pump (~230 mL min^{-1}), the tubing diameter, and length, it took approximately 45 s for gas to reach the analyzer from the chamber. Because of the high frequency (1 Hz) of reporting concentration by the instrument and its high sensitivity to change in concentration, the chamber top was left on each collar for only ~5 min, which was sufficient time to detect a non-zero slope of increasing or decreasing headspace concentrations, while minimizing a potential chamber artifact of altering the concentration gradient between soil and headspace gas. The slope was used to calculate a flux using equation 1

$$Flux\ (\mu mol\ m^{-2}\ min^{-1}) = \frac{dConc}{dt} * \frac{P * V}{A * R * T} \quad (1)$$

where dConc/dt = slope (μL L^{-1} min^{-1}), P = air pressure (atm), R = gas law constant (L atm mol^{-1} K^{-1}), T = air temperature (K), V = chamber volume (L), and A = chamber area (m^2). Flux units of μmol m^{-2} min^{-1} were used for statistical analyses, but when flux interpolations and annual estimates were conducted, the flux units were converted to μg N_2O-N m^{-2} min^{-1}.

2.2.6 Soil chemical and physical characteristics

Volumetric water content (VWC) of the soil was measured using a manual Decagon 5TM soil moisture probe. The probe was inserted vertically into the soil surface to a depth of 5 cm. At each chamber location (n = 32), three VWC measurements were taken outside the chamber area, and the mean calculated. The

probe calibration was checked in the laboratory prior to field usage and the VWC was obtained using the Topp equation (Topp et al., 1980).

Soil samples used for gravimetric soil moisture, nitrate and ammonium concentration analyses were taken using a 2.2 cm diameter soil push probe during each gas flux measurement. At each chamber (n = 32) three, 5 cm deep soil plugs surrounding the chamber were collected and placed together into a labeled bag. The bag was placed in a refrigerated cooler, transported back to the laboratory and processed within 48 h. At the lab, the soil within each bag was homogenized and sieved using a 10 mesh (2 mm) pan. Six grams of the field-moist sieved soil were extracted in 30 mL of 2M potassium chloride (KCL), placed on an oscillating shaker table for at least 2 h, and vacuum filtered through a Whatman No. 42 filter paper. Extracts were then analyzed for nitrate, nitrite, and ammonium concentration using flow injection analysis Lachat autoanalyzer (Maynard et al., 1993). If samples were not processed in the analyzer within 12 h, they were stored at 4°C until analysis within 30 days of soil collection. Soil push probe samples from five sampling dates selected over the three-year study were also analyzed for total soil carbon and total soil nitrogen using a Carlo Erba NC2500 elemental analyzer.

The surface bulk density of the soil was measured using a 5 cm length, 5 cm diameter PVC core. Air-dried soil was sieved with 10 mesh (2 mm) pan and weighed. The bulk density was calculated as the < 2 mm air-dried mass divided by the volume. Two bulk density surface cores were taken in each field for two years of this study and averaged by field and year. Surface bulk density measurements were used to convert VWC to water-filled pore space (WFPS) by calculating the total porosity

assuming a particle density of 2.65 g cm^{-3} (Robertson et al., 1999). Soil texture was assessed twice using hand augered soil samples at 10 cm intervals to an approximate depth of 1 m, twice, in each field. The soils were sieved using a 10 mesh (2 mm diameter) pan, air-dried for at least 72 h, and measured for soil texture using the hydrometer method (Gavlak et al., 2005).

2.2.7 Non-parametric DWM impact model

The purpose of this model was to determine if the dependent variables (gas fluxes, piezometer depth, soil moisture) were impacted by DWM. Because of non-normality and heteroskedasticity of the dependent variable data, a non-parametric Wilcoxon test was used. The piezometer water depth, soil moisture and fluxes were assessed separately as dependent variables of interest. The independent variables were treatment (DWM/controlled drainage; versus non-DWM/free drainage) and board period (ac-tive—DCS boards inserted in the DWM plots; versus inactive—DCS boards removed for the farmer's management activities). A pairwise post hoc test was performed to estimate p-values assessing the difference between board periods under both treatment conditions.

2.2.8 Mixed-effects model

A generalized linear mixed-effects model (GLMER) in R program was used to assess the impact of treatment and other predictor variables on N_2O and CH_4 fluxes. Both N_2O and CH_4 fluxes were non-normal and right skewed, so a natural log transformation was applied. A small positive offset was added to make all values

positive before log transformation (Van der Weerden et al., 2020). A gamma log link distribution was applied in the GLMER model (Bolker et al., 2009).

For N_2O, the independent variables of treatment, fertilization period, year, and board period were categorical variables assessed as fixed effects. Chamber location (1–8, with 1 being closest to the ditch and 8 being furthest) was a continuous variable serving as a measure of distance from ditch edge. After distance from the ditch was found to not be a significant fixed effect ($p > 0.05$), chamber number was then considered a random effect. Sampling dates were considered part of the fertilization period if they occurred within a window of 4 weeks after a fertilization event. Several studies have shown a peak of N_2O emissions within days of fertilization, followed by a gradual decline over 2–4 weeks (Fisher et al., 2018; Jankowski et al., 2018; Matson et al., 1996). Board period was the same categorical variable as described in Section 2.7. Interaction effects between all fixed effects were also evaluated. Final models were selected based on the lowest AIC value of multiple fixed effect combinations and interactions. An estimated marginal means post hoc test was conducted when p-values of main effects were less than 0.05. Model residuals were visually analyzed for normality and heteroskedasticity.

For CH_4, the independent variables of treatment, seasonal period, board period, and year were categorical variables assessed as fixed effects. Chamber location (1–8, with 1 being closest to the ditch and 8 being furthest) was initially tested as a continuous variable serving as a measure of distance from ditch edge but was not significant ($p>0.05$), therefore distance was considered a random effect. Seasonal period was assigned a value based on inclusion within the data range of

April 1–June 30. These dates were selected because they corresponded to the beginning of the warmer spring season with wet soil conditions, prior to drier summer months. The final model was selected based on the lowest AIC value of multiple fixed effect combinations and interactions. An estimated marginal means post hoc test was conducted when p-values of main effects were less than 0.05. Model residuals were visually analyzed for normality and heteroskedasticity.

2.2.9 Regression statistics

To examine how environmental variables controlled N_2O emissions, a stepwise linear regression was created using soil temperature, soil water-filled pore space (WFPS), and nitrate concentration as the predictor variables for N_2O emissions. The data were unaggregated, so each chamber flux measurement was an observation, for a total of 536 measurements with a complete suite of data for all dependent and independent variables. All data were tested for normality using the Shapiro–Wilk normality test and were log-transformed. For WFPS, a quadratic term was added to the model to account for an expected non-linear response (Firestone and Davidson, 1989). The stepwise regression created multiple models with different combinations of predictor variables. The model with the lowest AIC was selected. Homoscedasticity and normality were assessed in the final model residuals.

2.2.10 Annual flux calculations – Seasonally based flux interpolation

To estimate an annual N_2O gas flux, each year was divided into 3–4 periods, detailed in Table S1, bounded by farm management events (such fertilization events and harvest) and observed seasonal impacts (such as spring warming) of patterns of

measured fluxes. For periods in which no visually obvious N_2O spikes occurred, an arithmetic mean was taken of all the flux measurements within that time period and multiplied by the number of days within that period. For periods in which a spike of N_2O flux was observed followed by a sustained drop in flux values, usually within days or weeks after N fertilization in corn years or shortly after temperature and moisture increase in the soybean year, a decay curve and function were fitted to the data for the duration of those observations (Figure S3). Daily fluxes were then summed to obtain a total period value. The emission values in each period (both arithmetically derived and decay curve derived) were summed to obtain an annual flux measurement. There were 3–4 periods per year with 2 to 5 flux measurements per period. This procedure was repeated to calculate an annual flux for each chamber. The chamber annual fluxes were averaged by treatment and a 95% confidence interval (CI) was calculated, representing spatial flux variability.

For CH_4, each year was divided into 3 periods bounded by seasonal impacts on measured fluxes (Table S2). A mean flux was calculated for each period, multiplied by the number of days within that period, and period fluxes were summed to obtain an annual CH_4 flux. This procedure was repeated for each chamber and the chambers were averaged by treatment to obtain a 95% CI representing the spatial variation within the treatment.

2.2.11 Annual flux calculations – Mixed-effects model extrapolation

For an independent check on the interpolation method, annual CH_4 and N_2O fluxes were also calculated by extrapolating the mean flux values reported in the mixed-effects model results for each year. This more simplistic approach did not

account specifically for observed spikes in gas fluxes but represented the spatial and temporal variation accounted for in the mixed-effects model. An error term for each annual estimate was calculated based on the standard errors of the estimates of the mixed-effects model output.

2.2.12 Annual flux calculations – Regression model N_2O flux interpolation

A regression-based model was used to obtain another independent annual N_2O flux estimate using environmental variables of soil moisture, soil nitrate, and soil temperature. Linear interpolations were made between each of the measured data points for these environmental drivers. The interpolated daily variable values were applied to a stepwise linear regression equation. Predicted hourly N_2O fluxes were summed to an annual flux. This was done for each chamber (n = 32) and an average and standard error were calculated by treatment.

2.3 Results

2.3.1 Environmental variables

The following section describes the climatic and soil variables measured to complement the flux measurements (Figure 2).

2.3.1.1Precipitation and air temperature

Daily precipitation and irrigation amounts were recorded over the course of this study (Figure 2A). The highest daily rainfall was 7.84 cm in February 2018. Seasonally averaged over three study years (2017–2019), March–May had the highest average rainfall with 31.8 ± 1 cm, followed by December-February with 26.4 ± 3.6 cm, June–August with 19.1 ± 8.6 cm, and September–November with 9.0 ± 1.9 cm.

The daily average air temperature over three years was 14.1 °C and ranged from −13.0 to 30.1 °C (data not shown).

2.3.1.2 Soil temperature and moisture

Soil temperature and moisture at 5 cm depth were measured at the same frequencies as chamber fluxes. Soil temperature ranged from 2.1 to 29.1 °C and followed expected seasonality trends (Figure 2B). The measured mean percent water-filled pore space (%WFPS) by treatment ranged from 13% to 67% over the study period (Figure 2C). The highest recorded soil moisture contents occurred in the winter (Dec–Feb) and spring (March–May), and the lowest soil moisture contents occurred during the summer (June–Aug) and fall (Sep–Nov). There was a particularly dry period in July 2018, when the lowest soil moisture content of this study was recorded. Statistical analysis of WFPS can be found in results Section 3.4.

2.3.1.3 Soil extractable nitrogen

The soil extractable nitrate in the top 5 cm, measured at each chamber sampling, ranged from 0.38 to 34.6 mg N kg^{-1} (Figure 2D). In April 2017 and 2019, 22 kg N ha^{-1} as UAN fertilizer were applied during planting and in June 2017 and 2019 200 kg N ha^{-1} as UAN were applied, as indicated by arrows in Figure 2. In general, there was a positive association between N fertilization and soil nitrogen concentration. Soil nitrate values increased soon after application of N fertilizer in April and June of 2017 and 2019. After this period, the soil nitrate concentrations decreased throughout the remainder of the year. In the 2018 soybean crop, the soil nitrate values rose in the spring but did not reach concentrations as high as the years with N fertilization. For soil extractable ammonium values, the concentrations

remained below 10 mg N kg^{-1} during the study period, except one measurement in June 2018 (data not shown). Ammonium values were more variable than nitrate and higher during summer than during winter.

2.3.1.4 Soil texture and bulk density

Soil texture varied spatially within and between the four fields. Augered soil cores in field C had higher clay and silt content compared to fields A, B, and D at depths ranging from 20 to 60 cm (Figure S4 and Table S3). The 5 cm surface bulk density values, %C, and %N also varied by field, with higher %C and %N values associated with higher clay content (Table S4).

2.3.2 Piezometers

The daily mean piezometer water depth was aggregated by treatment and piezometer location during the inactive and active DWM DCS board periods (Figure 3). In the ditch piezometers, in the DCS inactive (unshaded) periods, the DWM depth values were generally deeper than the non-DWM plot values, indicating spatial heterogeneity across the field. During the DCS active (shaded) periods, however, the lines on Figure 3 tend to converge, indicating that the DCS active installation of boards in the DWM plots increased the ditch piezometer water levels. In the field piezometers, the effect of board placement is less clear. The statistical evaluation of these piezometer data were combined with analysis of WFPS data and are found in Section 3.4.

2.3.3 Chamber flux summary

From 2017 to 2019, 959 chamber flux measurements were taken. Most fluxes were small and the data had right-skewed distribution. When calculating the fluxes using the change in slope over time, assessed by linear regression, 96% of the methane slopes were significantly different from zero ($p < 0.05$) and of those 21% were negative, indicating CH_4 consumption events. For N_2O, 85% of the N_2O slopes were significantly different from zero ($p < 0.05$) and 15% of those were negative. Because of the data skew, a log transformation was applied for parametric statistical analyses. An analysis of the minimum detectable flux (MDF) is provided in the supplementary materials (Table S5).

Figure 2E shows the N_2O-N flux data, averaged by treatment. The highest emissions occurred after N fertilization events (planting or broadcast) in the April–July period of 2017 and 2019, marked by arrows. In 2017, the larger N_2O peak occurred during the second fertilization and in 2019, after the first fertilization. The large response to the first fertilization in April 2019 N application may have resulted from co-occurrence of a precipitation event the day following application. Soil N_2O consumption events occurred at various times throughout this study at the individual chamber scale, but never as the average flux from all chambers at the field scale. This indicates small scale flux variability within a field, but not net negative fluxes at the field scale.

For CH_4, the highest CH_4 emissions occurred in the spring period (April–June; Figure 2F). Several individual chambers showed net consumption of atmospheric

CH_4, but only rarely did this translate to net consumption as the mean at the field or treatment scale.

2.3.4 Non-parametric DWM model for effects on piezometers, WFPS, and gas fluxes

The non-parametric statistical analysis results for dependent variables of ditch piezometer, field piezometer, and surface WFPS showed differences in the interaction of treatment and board period (Figure 4). For the ditch piezometers, the mean water depth below ground was significantly deeper during the inactive DCS period than the active DCS period in the non-DWM sites. However, this trend was reversed in the DWM sites, with a higher mean water depth in the active DCS period compared to the inactive DCS period, indicating that the additional boards in the DWM sites raised the water table near the ditch, even during the dry summer. The field piezometer water levels showed the same trends as the ditch piezometers, except that the mean water level between active and inactive DCS periods was not significantly different in the DWM condition, indicating that the additional boards in the DWM sites had less of an effect on the water table in the mid-field, approximately 15 m from the ditch. The DWM only raised the water table in the mid-field piezometers to the same level as the non-DWM plots in the active DCS season, but did not exceed it, as was the case for the ditch piezometers (Figure 4). The WFPS showed no significant differences by treatment or board period, indicating the DWM did not affect near surface moisture content. The same non-parametric analysis for gas fluxes showed no significant differences by treatment or board period, indicating the DWM did not impact the soil gas fluxes in the fields (Figure 5).

2.3.5 Mixed-effects model results for N_2O and CH_4 fluxes

The purpose of the mixed-effects model was to assess the impact of the DWM treatment and other dependent variables. For N_2O fluxes, the effects of the post-N fertilization period, year, chamber location, and interactions were assessed using two sub-models. In the first sub-model, the N fertilization effect was evaluated using only 2017 and 2019 data (corn years) because 2018 data (soybean year) did not have a N fertilization period. In the second sub-model the effects of treatment and year were assessed using all years' data, but N fertilization variable was not included. The mixed model results (Table 1) show that DWM did not significantly affect N_2O fluxes, which is consistent with the non-parametric model results (Figures 4 and 5). Year had a significant effect on N_2O fluxes, as the fertilized corn years of 2017 and 2019 had higher N_2O fluxes compared to the unfertilized soybean year of 2018. The post hoc test showed that the N_2O fluxes in 2017 and 2019 were not significantly different. Using the sub-model with only data from N fertilization years, the post-N fertilization period had significantly higher N_2O fluxes than the non-fertilization period (Table 2). No interaction effects between independent variables were significant.

For CH_4, DWM treatment, year and season were tested. CH_4 emissions did not have significant differences based on year or treatment (Table 1). The spring seasonal period had higher CH_4 emissions compared to the non-spring periods (Table 2).

2.3.6 N_2O multiple regression

There was a weak positive linear relationship ($r^2 = 0.12$, $p < 0.001$, Figure S5) between soil nitrate and N_2O fluxes. The largest N_2O fluxes occurred when soil nitrate concentrations were high, but some large N_2O fluxes also occurred at lower soil nitrate concentrations. For soil temperature, the higher N_2O emissions occurred above 12°C, although it should be noted that N fertilization events also only occurred during periods above this temperature. For WFPS, the highest N_2O emission events occurred at intermediate WFPS values, but not all N_2O flux events between those WPFS values resulted in high emissions. The highest N_2O emissions typically occurred when the following combination of conditions existed: the soil temperature was above 12°C, nitrate concentration was at least 10 mg N kg^{-1}, and WFPS was between 35% and 60% (Figure 6).

The stepwise linear regression yielded the lowest AIC when the model included all terms, including a quadratic term for WFPS. The most important predictor variable was soil nitrate followed by soil temperature, and WFPS. The full model (Equation 2) and each predictor variable were significant ($p < 0.001$), and the full model yielded an r^2 value of 0.23 (Table S6).

$$\ln(N_2O + 1) = (0.029 * NO_3N) + (0.021 * \text{soil temp}) + (0.056 * \text{WFPS}) - (0.001 * \text{WFPS}^2) - 1.37 \quad (2)$$

where N_2O is N_2O flux (μg N_2O-N m^{-2} min^{-1}), NO_3-N is concentration of nitrate (mg NO_3-N kg^{-1} dry soil), WFPS is water-filled pore space (%), soil temp is soil temperature (°C).

2.3.7 Annual soil emission flux estimates

Annual soil gas flux estimates were derived from the three methods described in Section 2.10 (Tables 3 and 4). All the methods indicated that the N_2O-N emissions in the corn years of 2017 and 2019 were elevated in both the DWM and non-DWM conditions compared to the soybean year of 2018. While the annual estimates show higher emissions in 2019 compared to 2017, which is a result of a higher peak N_2O emission and nitrate measurements after the first fertilization event in 2019 (Figure 2), the non-parametric and the mixed-effects model tests discussed above indicated that the difference between 2017 and 2019 fluxes was not significant. The seasonally-based interpolation method yielded higher annual flux estimates, but there was generally broad agreement between the three methods, given the uncertainty terms.

The seasonally-based interpolation method permitted partitioning fluxes into periods. Individual seasonal period estimates (mean ± 95% CI) for N_2O showed that brief (6–8 weeks) seasonal periods following the fertilization events, which were quantified by the decay function, contributed nearly half of the total annual N_2O flux (Table S1).

There were small net positive annual CH_4 fluxes in each year and treatment (Table 4 and Table S2). Consistent with the mixed-effects model, there were no clear differences between years and treatments, except that the seasonally-based interpolation estimates were higher for 2019. This may be an artifact caused by unusually high fluxes measured in a few chambers during a period with sparse temporal coverage.

2.4 Discussion

2.4.1 Impact of drainage water management

2.4.1.1 *Groundwater level*

The DWM treatment raised the near-ditch water table when the DCS were active (Figure 4). This effect was also observed in the field piezometers but was weaker, indicating that DWM had an impact on the groundwater storage, with the strongest effect close to the ditch. In contrast, the DWM did not affect the surface soil moisture within the agricultural fields. The observed effectiveness of DWM to reduce nitrate load in previous studies may be due to denitrification occurring in the ditches or in the elevated groundwater leading to the ditches (Carstensen et al., 2020; Hagedorn et al., 2019; Fisher et al., 2010; Williams et al., 2015; Lavaire et al., 2017; Smit and Kellman 2011; Lalonde et al., 1996). It is likely that the DWM reduced nitrate leaching into the ditches but did not significantly affect surface (5 cm) soil moisture and rates of denitrification within the surface soils of cropped fields between the ditches where the chamber flux measurements were conducted.

2.4.1.2 N_2O and CH_4 fluxes

Soil GHG emissions were not significantly impacted by DWM or the interaction of board period and treatment (Figure 5 and Table 1). While DWM affected the depth of the water table, and preliminary results showed that hydrologic nitrate export was reduced (Hagedorn et al., 2019), DWM did not impact the surface soil moisture or the GHG fluxes from the soil in the cropped areas (Figure 4 and Table 1). Hence, the results do not support the hypothesis that DWM would increase CH_4 or N_2O soil emissions. This null impact of DWM on GHG emissions confirms

other literature findings, particularly those evaluating field scale DWM manipulations (Nangia et al., 2013; Crézé et al., 2013; Datta et al., 2013; Van Zandvoort et al., 2017). Other studies found some increase in CH_4 and N_2O emissions in undrained fields, but were not evaluating the effect of DWM manipulations per se, but rather the effect of tile drainage in general, by comparing drained fields to undrained fields. In those instances, the undrained fields had higher N_2O and CH_4 emissions, although the differences were seasonally variable and not consistent over multiple years (Kumar et al., 2014; Fernandez et al., 2016).

2.4.2 Farm management impact on GHGs

For N_2O fluxes, in both DWM and non-DWM fields, the mixed model results (Tables 1 and 2) demonstrated that N fertilization during corn years had the greatest impact on N_2O emissions. Soon after each of the N fertilization events, we observed a pulsed increase in both soil nitrate concentrations and N_2O emissions, which then declined over a period of 1-2 months as soil nitrate declined during crop development (Figures 2D and 2E). This finding confirms existing literature that shows that N_2O fluxes are highest in the days and weeks following N fertilization (Jankowski et al., 2018; Parkin and Kaspar, 2006; Baggs et al., 2003; Bremner et al., 1981).

For all N fertilization events in this study, fluxes were measured 1 day and again 3 or 4 days after. The largest fluxes were observed at 3–4 days after N fertilization. A study of corn/soybean in Brazil demonstrated a similar lag of a few days between fertilization and subsequent N_2O flux spikes, which they attributed to the time it took for nitrification to convert fertilizer-N to nitrate (Jankowski et al., 2018).

The multiple regression results align with the published literature demonstrating that key variables of soil nitrate, temperature, and soil moisture play a role in controlling N_2O emissions (Figure 6; Equation 2) (Jankowski et al., 2018; Ullah and Moore, 2011). The variation in these parameters fit within the context found for N-fertilized agricultural fields (Venterea and Coulter, 2015).

There was not a specific farm management action that most controlled CH_4 fluxes in this study. Seasonality explained most of the CH_4 flux trends. The highest CH_4 emissions occurred during the period from April to July in all three years of this study. This period corresponded with a time when the temperature had already increased above winter lows but WFPS still remained high (≥55%) due to spring rain and low rates of evapotranspiration before and for a few weeks following planting. The relatively warm and wet conditions were sufficiently conducive to methanogenesis within the soil to produce a period of somewhat elevated emissions relative to other seasons. No DWM effect occurred, and the spring seasonal effect occurred in both treatments.

2.4.3 Comparing annual soil emission estimates

For N_2O, all three interpolation methods produced lower annual estimates in the 2018 soybean year compared to the corn years of 2017 and 2019. The higher emissions in the corn years were driven by N fertilization. There was an appearance of a possible difference in treatment means (albeit with overlapping standard errors) in the seasonally-based interpolation in 2017, but this was not observed in 2018 or 2019, nor in the other two annual estimate techniques (Table 3). The non-parametric model and the mixed-effects model did not show significant differences in N_2O gas

fluxes between treatments in any year, which suggests that the interpolated treatment means in 2017 should not be considered different. The regression-based interpolation produced similar annual estimates to the mixed-effects model mean extrapolation, and both were somewhat lower than the seasonally-based interpolation. A lower annual estimate for the regression model is likely because non-linear responses to soil nitrate and lack of continuous nitrate data may cause underestimation of the N_2O fluxes. Similarly, extrapolation of the means of the mixed-effects model gives more weight to mean responses rather than pulse (spike) events. Despite limitations for each of the three methods for estimating annual fluxes, they are in broad agreement and therefore represent the likely range of annual fluxes for each year and treatment. Because it captures the post-N fertilization N_2O peaks, we used the seasonally-based interpolation estimate for comparison to the literature in Section 4.4.

For CH_4, the seasonally-based annual interpolation had somewhat higher annual estimates compared to the mixed-effects model mean extrapolation, but all estimates indicated a very small net source, which is consistent with other studies of agricultural soils (Cowan et al., 2021). There were no differences in treatment in any year for either interpolation technique.

2.4.4 Comparison to regional and global nitrogen budget measurements

2.4.4.1 N_2O emissions factor

The nitrous oxide emission factor (EF) was calculated by dividing the seasonally-based interpolated N_2O annual flux, averaged over treatment and year, for the corn years reported in Table 3, by the average N fertilization rate of 213 kg N ha^{-1}. This resulted in an EF of 3.0%. This calculation method does not account for

N_2O emissions from a background, unfertilized agriculture site, likely leading to an EF overestimate. To partially account for this, the soybean N_2O emissions in 2018 were used as an unfertilized control, and subtracted from the averaged N_2O emissions in 2017 and 2019. This may overcompensate for the expected flux from an unfertilized soil control because the previous year's fertilization could have had a residual impact on soil N availability in 2018 and because biological N fixation likely added soil N during the soybean year. However, subtracting the entire annual flux from the soybean year provides a lower bracket estimate for the EF during the corn years. This correction yields an EF of 2.2%. A N_2O EF in fertilized agriculture is influenced by a range of environmental variables such as soil type, N input type, and precipitation. The current IPCC guidelines use a default EF range of 1.3–1.9% for synthetic fertilizer agriculture in climates with greater than 1000 mm precipitation (Reddy et al., 2019; Hergoualc'H et al., 2021). The EF estimate from this research is slightly higher than the upper limit of the uncertainty range of IPCC recommendation.

2.4.4.2 Nitrogen balance

We calculated a nitrogen balance and nitrogen use efficiency (NUE) based upon average data from the two corn years. The average total amount of nitrogen applied during fertilized corn years was 213 kg N ha^{-1}. The average corn yield was 13,800 kg ha^{-1} (~220 bushels ac^{-1}). The harvested corn had an average (across treatments) nitrogen content of 0.84 ± 0.18% (n = 8), resulting in removal of 91–141 kg N ha^{-1}, the range representing the variation in the measured nitrogen content. The nitrogen balance (also known as N surplus), defined as the amount of N applied minus the amount of N removed via harvest, was estimated to be 97 ± 20 kg N ha^{-1}.

Using these estimates of N inputs and outputs, and assuming that annual N deposition rate at this site of 6 kg N ha^{-1} (Fisher et al., 2021) had a negligible impact, and that N fixation was only applicable during soybean crop years, the average nitrogen use efficiency (NUE) for the corn years, defined as the N removed in the harvest divided by the N additions, was 54 ± 11%. This value is somewhat low for the U.S. but falls within the range of values calculated nationally and globally in irrigated maize systems (Lassaletta et al., 2014; Conant et al., 2013; Zhang et al., 2015; Basso et al., 2019; Roy et al., 2021). Ours is the first study known to us on N budget estimates from corn grown in the U.S. Mid-Atlantic region. Compared to the dataset compiled by (Eagle et al., 2020) from the U.S. cornbelt, which supported a non-linear correlation between annual N_2O emissions and N balance, the annual N_2O emission estimates from the present study fall within the range reported by (Eagle et al., 2020), but are higher than predicted based on their reported relationship with N balance (Figure S6). This result is consistent with the lower than average NUE reported here.

2.5 Conclusions

The DWM condition did not increase soil N_2O and CH_4 emissions. While there was evidence that DWM impacted the groundwater table near the drainage ditches, this impact was not evident in the surface soil moisture nor the surface soil GHG fluxes themselves. This finding spanned multiple years of corn and soybean crop rotation.

Three independent methods for deriving annual flux estimates revealed consistent estimates within their uncertainty ranges. Comparing the annual N_2O flux estimates and related measures of N cycling to other studies on corn fields in the U.S.,

this farm had above average N surplus, below average NUE, and above average annual N_2O fluxes, although these values fell within reported regional and global ranges.

Follow-up studies will address the possibility of N_2O accumulation within the groundwater near the ditch areas and degassing of ditch water and will also report on the effect of DWM on export of dissolved N and P. For the cropland soil surface studied here, DWM did not have an unintended consequence of increased greenhouse gas emissions. This study provides evidence that DWM may be an effective BMP to reduce hydrologic nitrate export from crop fields without concerns of significant pollution swapping of increased greenhouse gas emissions from the soil surface.

2.6 Supplementary Materials

The following supporting information can be downloaded at: www.mdpi.com/xxx/s1, Figure S1: Detail of DCS and DWM technique; Figure S2: Summary of diel variation of N_2O fluxes; Figure S3: Visual of decay curve fitting for annual N_2O estimate; Figure S4: Clay size fraction by depth and field; Figure S5: Summary of individual regression results for input variables into multiple linear regression; Figure S6: Plot of N balance versus N_2O emissions; Table S1: N_2O seasonally-based annual estimate details; Table S2: CH_4 seasonally-based annual estimate details; Table S3: USDA soil textural class description; Table S4: Soil characterization results; Table S5: Summary of minimal detectable flux calculations; Table S6: Summary results of multiple linear regression model.

2.7 Author Contributions

Conceptualization, E.A.D., T.R.F., R.J.F., M.S.C., J.L., and J.G.H.; methodology, J.G.H., E.A.D., T.R.F., R.J.F., Q.Z., A.B.G., E.K., M.S.C., and J.L.; formal analysis, J.G.H. and E.A.D.; investigation, J.G.H., T.R.F., R.J.F., Q.Z., A.B.G., E.K., and M.S.C.; data curation, J.G.H.; writing—original draft preparation, J.G.H. and E.A.D.; writing—review and editing, J.G.H., E.A.D., T.R.F., R.J.F., Q.Z., A.B.G., E.K., M.S.C., and J.L.; visualization, J.G.H. and E.A.D.; supervision, E.A.D., T.R.F., R.J.F., M.S.C., and J.L.; project administration, E.A.D., T.R.F., R.J.F., M.S.C., and J.L.; funding acquisition, E.A.D., T.R.F., R.J.F., M.S.C., J.L., and J.G.H. All authors have read and agreed to the published version of the manuscript.

2.8 Funding

This research was funded by USDA NIFA, grant number 2016-67019-25263, Maryland SeaGrant R/E-22F, Maryland Water Resources Research Center Z9212103, and the UMCES Appalachian Laboratory.

2.9 Data availability statement

Data available in a publicly accessible repository. The data presented in this study are openly available in [FigShare] at [10.6084/m9.figurshare.19349828].

2.10 Acknowledgments

We would like to acknowledge training and technical support from Katie Kline at UMCES Appalachian Laboratory. We acknowledge data collection work performed by Michelle Lepori-Bui through UMCES Horn Point Laboratory. We

acknowledge Dr. Nick Nickerson for the loaning of the Eosense automated chamber gas flux equipment for a period of this research.

2.11 Conflicts of interest

The authors declare no conflict of interest. The funders had no role in the design of the study; in the collection, analyses, or interpretation of data; in the writing of the manuscript, or in the decision to publish the results.

2.12 Tables

Table 1. Mixed-effects model results for N_2O-N and CH_4-C mean fluxes (± SE) aggregated by year and treatment. For N_2O-N, years 2017 and 2019 were significantly different from 2018, but not significantly different from each other. The effects of year and DWM treatment were not significant for CH_4 fluxes.

	N_2O-N (μg N m^{-2} min^{-1})		CH_4-C (μg C m^2 min^{-1})	
Year	**DWM (A)**	**Non-DWM (A)**	**DWM (A)**	**Non-DWM (A)**
2017	0.94 ± 0.38 (a)	0.81 ± 0.38 (a)	0.03 ± 0.01 (a)	0.02 ± 0.01 (a)
2018	0.48 ± 0.40 (b)	0.39 ± 0.39 (b)	0.03 ± 0.01 (a)	0.02 ± 0.01 (a)
2019	1.20 ± 0.39 (a)	1.02 ± 0.39 (a)	0.04 ± 0.01 (a)	0.03 ± 0.01 (a)

Uppercase letters (A,B) indicate statistical difference ($p < 0.05$) by treatment, within each gas type. Lowercase letters (a,b) indicate statistical difference ($p < 0.05$) by year.

Table 2. Modeled mean ± SE of N_2O-N and CH_4-C fluxes aggregated by N fertilization period for years 2017 and 2019 for N_2O-N and by season for CH_4. The post-fertilization period had significantly higher N_2O emissions compared to the non-N fertilization period. The spring seasonal period had higher CH_4 emissions compared to the non-spring periods.

N_2O-N (μg N m^{-2} min^{-1})		CH_4-C (μg C m^{-2} min^{-1})	
N Fertilization period	**Mean ± SE**	**Seasonal period**	**Mean ± SE**
Post-fertilization	2.15 ± 0.38 (a)	Spring	0.04 ± 0.001 (a)
Non-fertilization	0.21 ± 0.38 (b)	Non-spring	0.02 ± 0.001 (b)

Lower case letters (a,b) next to mean ± SE indicate statistical difference ($p < 0.05$) by period within gas type.

Table 3. Comparison between annual N_2O flux measurement methods. The SE associated with the seasonally-based interpolation and regression-based interpolation means represent spatial heterogeneity among chambers. The mixed-effects model mean extrapolation error represents the reported model mean error.

	N_2O-N kg ha^{-1} yr^{-1} (Mean ± SE)					
	Seasonally-Based Interpolation		**Mx Effects Model Mean Extrapolated**		**Regression-Based Interpolation**	
Year	**DWM**	**Non-DWM**	**DWM**	**Non-DWM**	**DWM**	**Non-DWM**
2017	6.4 ± 1.1	4.3 ± 0.8	4.9 ± 1.9	4.3 ± 1.9	3.9 ± 1.0	3.8 ± 0.7
2018	2.1 ± 0.3	1.2 ± 0.3	2.5 ± 2.1	2.0 ± 2.0	1.5 ± 0.2	1.8 ± 0.2
2019	7.7 ± 1.4	7.2 ± 3.5	6.3 ± 2.0	5.7 ± 2.0	5.7 ± 1.3	6.4 ± 2.3

Table 4. Summary of comparison between the two annual CH_4 flux calculation methods. The SE associated with the seasonally-based interpolation represents the spatial heterogeneity among chambers. The mixed-effects model mean extrapolation error was derived from the model output error term.

	CH_4-C kg ha^{-1} yr^{-1} (Mean ± SE)			
	Mx Effects Model Mean Extrapolated		**Seasonally-Based Interpolation**	
Year	DWM	Non-DWM	DWM	Non-DWM
2017	0.16 ± 0.05	0.11 ± 0.05	0.18 ± 0.10	0.19 ± 0.06
2018	0.16 ± 0.05	0.11 ± 0.05	0.17 ± 0.15	0.15 ± 0.06
2019	0.21 ± 0.05	0.16 ± 0.05	0.56 ± 0.73	0.42 ± 0.12

2.13 Figures

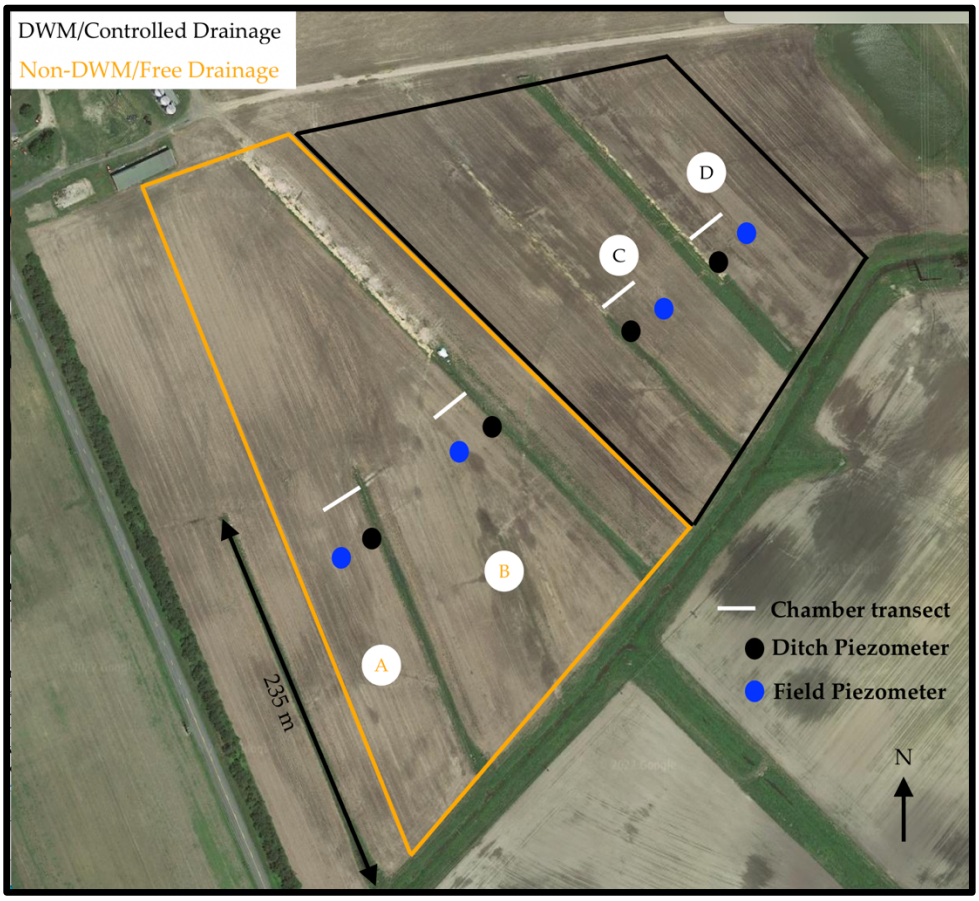

Figure 1. Aerial image of the research site showing the approximate piezometer locations, chamber transect locations, and treatment area borders. Fields A and B were free draining (non-DWM); fields C and D had controlled drainage (DWM).

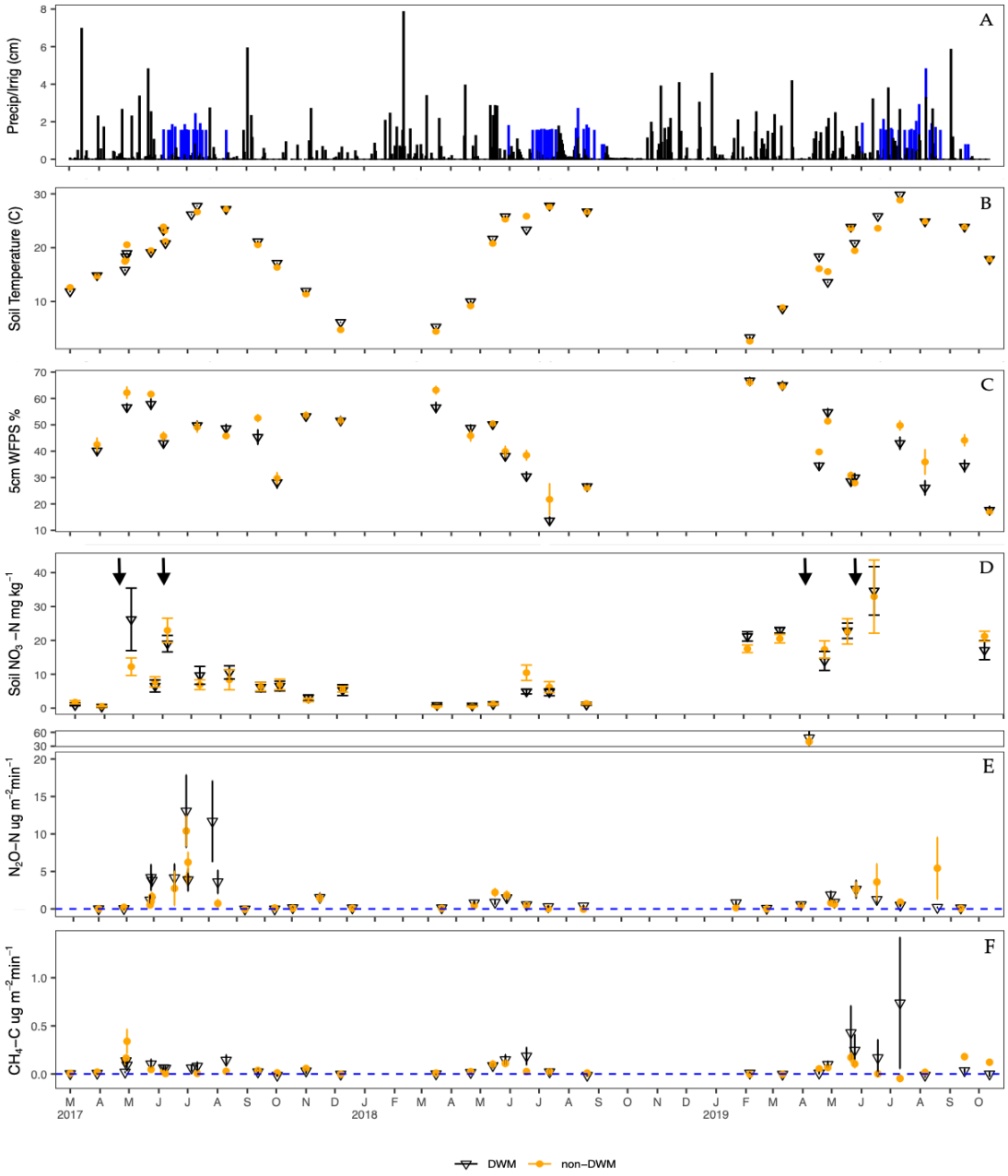

Figure 2. Climactic, soil, and flux variables measured over the course of this study. Arrows mark N fertilization events. Blue bars in (A) are irrigation events and black bars are precipitation events. The other measured variables are soil temperature (B), WFPS (C), soil nitrate (D), N_2O-N flux (E) and CH_4-C flux (F). Dashed blue lines in (E) and (F) mark the value of zero net flux. Mean + SE bars.

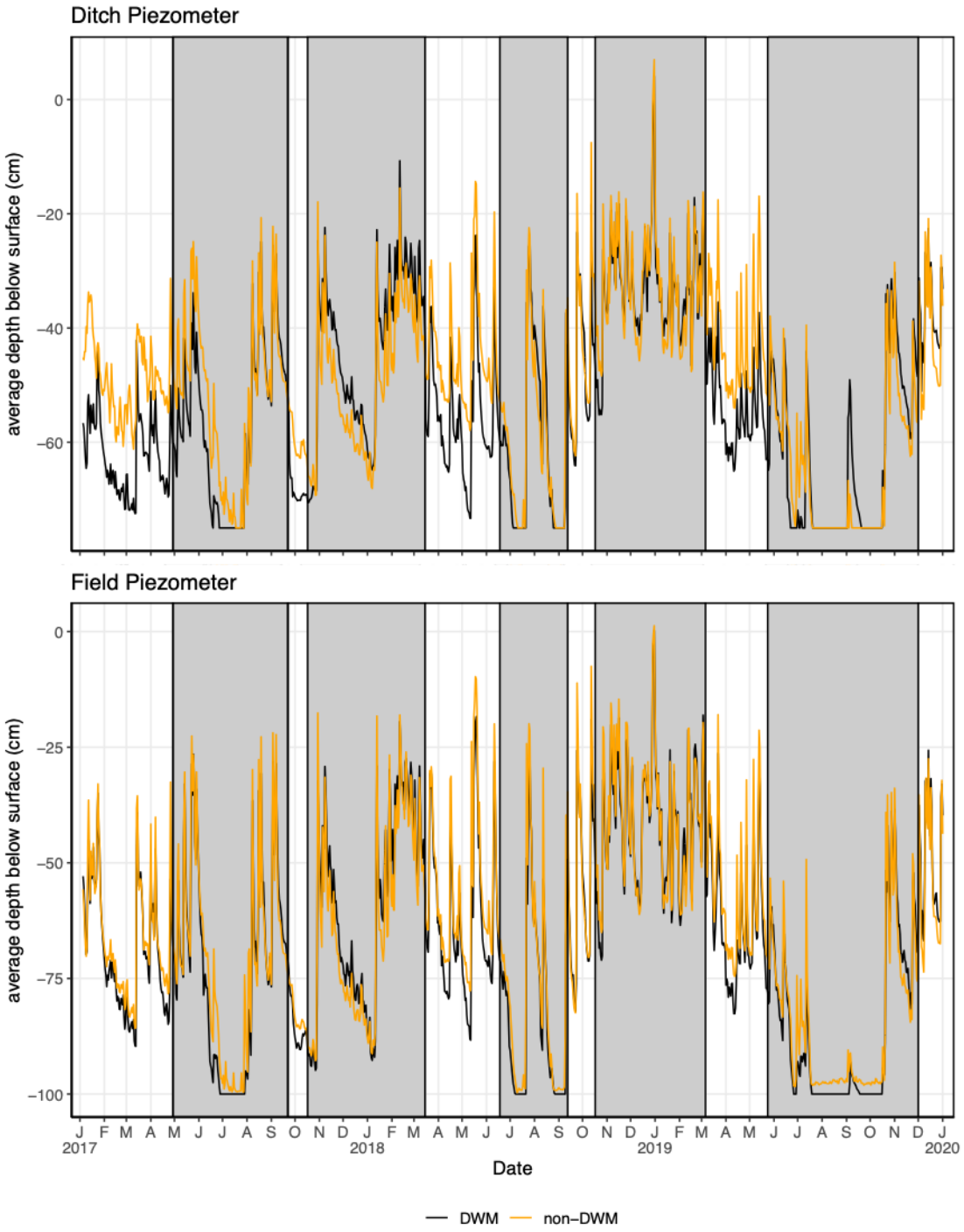

Figure 3. Mean piezometer water depth (cm) colored by treatment and piezometer location. The shaded time frame represents the active DWM DCS period and unshaded the inactive DWM DCS period.

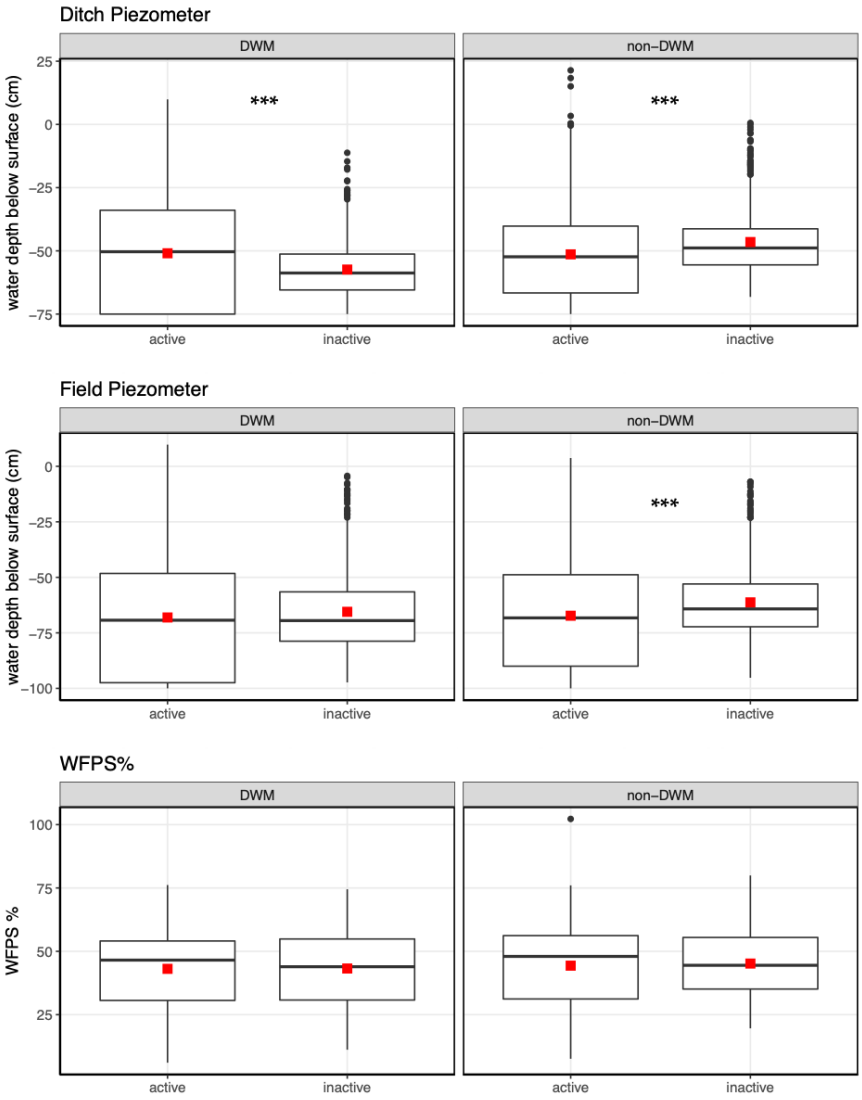

Figure 3. Box plot of the ditch piezometer, field piezometer and %WFPS in surface soil. Data were aggregated by treatment and board period. Asterisks indicate the significance of a Wilcoxon rank sum test for comparison between active DCS versus inactive DCS periods within each treatment (*** indicate $p < 0.001$; no asterisks indicate $p>0.05$). Red squares represent means.

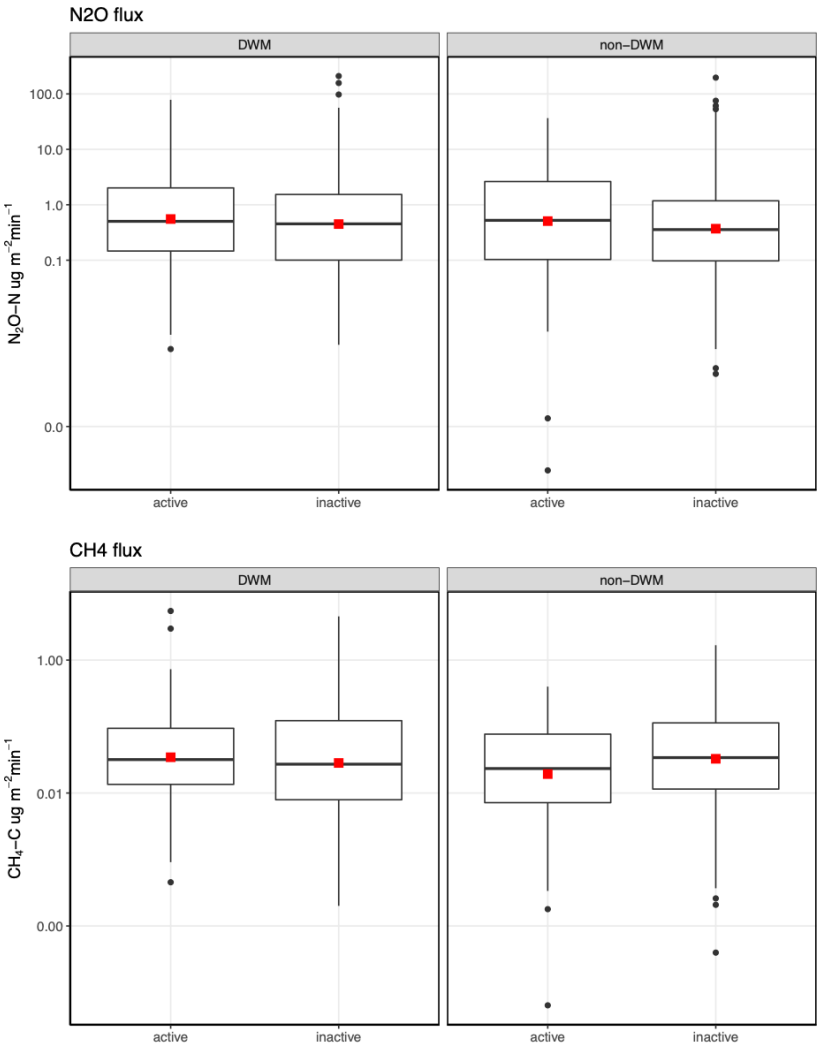

Figure 4. Box plot of gas flux data aggregated by board period and treatment. There were no significant differences ($p > 0.05$) between board period in either of the treatments according to the Wilcoxon rank sum test. Red squares represent means.

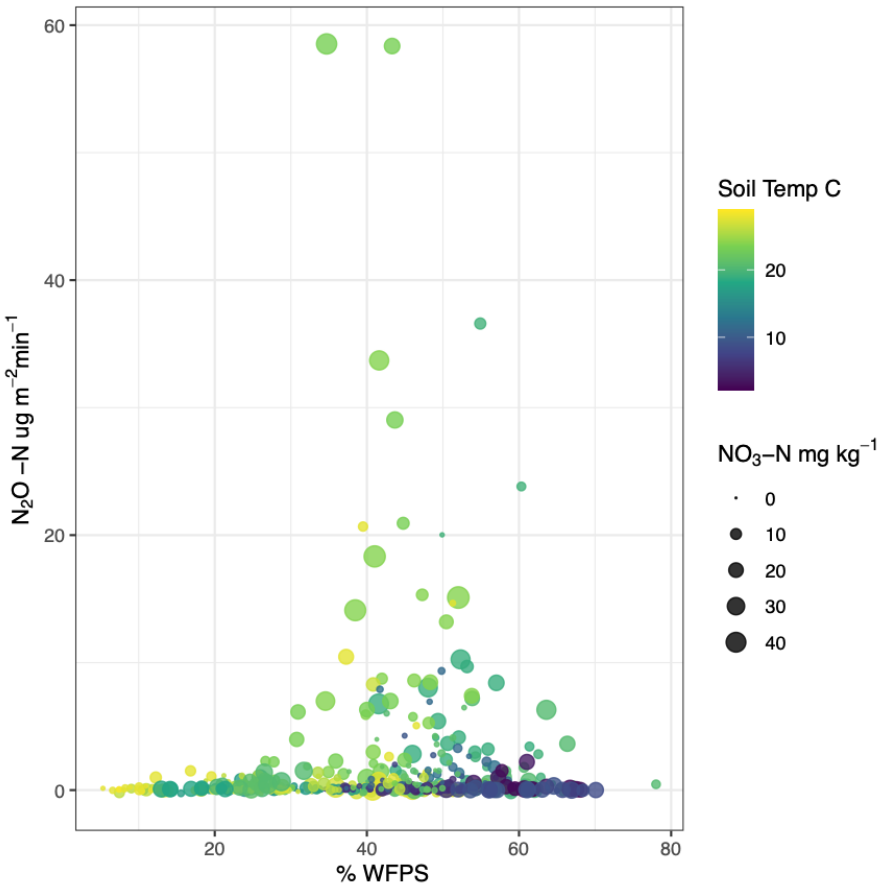

Figure 6. Bubble scatter plot showing the relationship between N_2O fluxes (y-axis), WFPS (x-axis), soil NO_3-N content (circle size), and soil temperature (color range).

2.14 Supplementary Tables

Table S1. Details of specific periods used to calculate the seasonally based annual N_2O estimates each year by treatment. Mean ± 95% CI reported.

Period Start	Period End	# days	# obs	Mean or Decay Function	Non-DWM (kg N_2O-N ha^{-1} $period^{1}$)	DWM (kg N_2O-N ha^{-1} $period^{1}$)
2017 Corn						
1/1/17	4/27/17	116	3	Mean	0.4 ± 0.3	0.7 ± 0.7
4/27/17	6/5/17	39	3	Mean	1.0 ± 1.0	2.3 ± 1.1
6/5/17	8/10/17	66	4	Decay	2.0 ± 0.9	2.5 ± 1.4
8/10/17	1/1/18	144	4	Mean	0.9 ± 0.6	0.9 ± 0.7
				2017 Annual Estimate	***4.3 ± 0.8***	***6.4 ± 1.1***
2018 Soybean						
1/1/18	5/14/18	133	2	Mean	0.7 ± 0.5	0.9 ± 0.6
5/14/18	7/11/18	58	3	Decay	0.5 ± 0.2	0.4 ± 0.1
7/11/18	1/1/19	174	2	Mean	0.0 ± 0.1	0.9 ± 0.4
				2018 Annual Estimate	***1.2 ± 0.3***	***2.1 ± 0.3***
2019 Corn						
1/1/19	4/26/19	115	3	Mean	0.3 ± 0.2	0.8 ± 0.4
4/26/19	6/17/19	52	3	Decay	3.7 ± 2.5	4.7 ± 2.1
6/17/19	1/1/20	198	4-5	Decay	3.2 ± 4.4	2.3 ± 1.2
				2019 Annual Estimate	***7.2 ± 3.5***	***7.7 ± 1.4***

Table S2. The season period boundaries used for the CH_4 seasonally-based annual flux estimate. Mean ± SE.

Period Start	Period End	# days	# flux observations	DWM (CH4-C kg ha^{-1} $period^{-1}$)	Non- DWM (CH4-C kg ha^{-1} $period^{-1}$)
1/1/17	4/26/17	115	2	0.01 ± 0.01	0.02 ± 0.03
4/26/17	7/15/17	80	6	0.08 ± 0.09	0.10 ± 0.11
7/15/17	1/1/18	170	5	0.09 ± 0.13	0.06 ± 0.07
			2017 Annual Estimate	**0.18 ± 0.10**	**0.19 ± 0.06**
1/1/17	4/26/17	115	2	0.01 ± 0.03	0.03 ± 0.03
4/26/17	7/15/17	80	4	0.15 ± 0.18	0.09 ± 0.07
7/15/17	1/1/18	170	2	0.01 ± 0.03	0.04 ± 0.10
			2018 Annual Estimate	**0.17 ± 0.15**	**0.15 ± 0.06**
1/1/17	4/26/17	115	2	0.01 ± 0.03	0.03 ± 0.04
4/26/17	7/15/17	80	5	0.29 ± 0.84	0.08 ± 0.10
7/15/17	1/1/18	170	3	0.02 ± 0.10	0.31 ± 0.23
			2019 Annual Estimate	**0.56 ± 0.73**	**0.42 ± 0.12**

Table S3. USDA soil textural class description as derived from sand, silt, and clay fractions obtained by hydrometer method for each study plot.

	Study Plot			
	Non-DWM		DWM	
Depth (cm)	**A**	**B**	**C**	**D**
0-10	Loamy fine sand	loamy fine sand	loam	sandy loam
10-20	Loamy fine sand	loamy fine sand	loam	sandy loam
20-30	fine sand	fine sand	silty clay loam	sandy clay loam
30-40	fine sand	fine sand	silty clay loam	sandy loam
40-50	fine sand	fine sand	silty clay loam	loamy fine sand
50-60	loamy fine sand	fine sand	clay loam	fine sand
60-70	loamy fine sand	sandy clay loam	clay loam	fine sand
70-80	fine sand	sandy loam	loamy fine sand	loamy fine sand
80-90	fine sand	sandy loam	sandy loam	loamy fine sand
90-100	sandy loam	sandy loam	fine sand	loamy fine sand

Table S4. %C, %N, and bulk density measurements (mean ± SD) at 5 cm depth. N = 40 for %C and %N. N= 4 for BD.

	Study Plot			
	Non - DWM		DWM	
Variable	**A**	**B**	**C**	**D**
%C	1.37 ± 0.06	1.47 ± 0.07	2.17 ± 0.05	2.08 ± 0.07
%N	0.12 ± 0.01	0.13 ± 0.01	0.18 ± 0.00	0.17 ± 0.01
BD (g cm-3)	1.13 ± 0.03	1.17 ± 0.01	1.05 ± 0.03	1.11 ± 0.04

Table S5. Summary of minimum detectable flux (MDF) calculation methodologies and resulting percentages of measured fluxes over the MDF. The two methods show that between 70 and 90% of the flux measurements were above the detection limit, which is in broad agreement with the percentage of concentration slopes that were significantly different from zero. Two methods were used to calculate the minimum detectable flux (MDF) of the chamber design. The first method adopted by Verchot et al. (1999) used calculated CH_4 and N_2O fluxes binned at 0.01 ug m^{-2} hr^{-1} intervals and 95% confidence intervals of those fluxes. The lowest flux bin with at least 67% of the 95% confidence intervals of individual flux measurements not including zero was deemed the MDF. The second method is derived from Courtois et al. (2019) based on a method developed by Christiansen et al. (2015) for use with small numbers of syringe samples but modified by Nickerson (2016) to account for the high frequency measurements of the Picarro G2308 instrument.

	MDF Method (μg m^{-2} hr^{-1})	
	Courtois 2019	**Verchot 1999**
CH_4-C MDF +/-	0.21	0.12
N_2O-N MDF +/-	1.2	2.5
CH_4-C > |MDF|	83%	92%
N_2O-N > |MDF|	92%	84%

Table S6. Summary of multiple linear regression results of ln N_2O flux data, showing the coefficients (columns) of the independent model variables. The full model had a residual standard error of 0.644 on 531 degrees of freedom with an $r^2 = 0.23$ and a p-value <0.001. The full model described by equation 2 in the main text is listed above the table below.

$$\ln(N_2O + 1) = (0.029 * NO_3N) + (0.021 * \text{soil temp}) + (0.056 * \text{WFPS}) - (0.001 * \text{WFPS}^2) - 1.37$$

Variable	Estimate	Std. Error	P-value
Intercept	-1.37	0.2150	<0.001
NO_3-N	0.029	0.0031	<0.001
Soil Temp	0.021	0.0041	<0.001
WFPS	0.056	0.0097	<0.001
WFPS ^ 2	-0.001	0.0001	<0.001

2.15 Supplementary Figures.

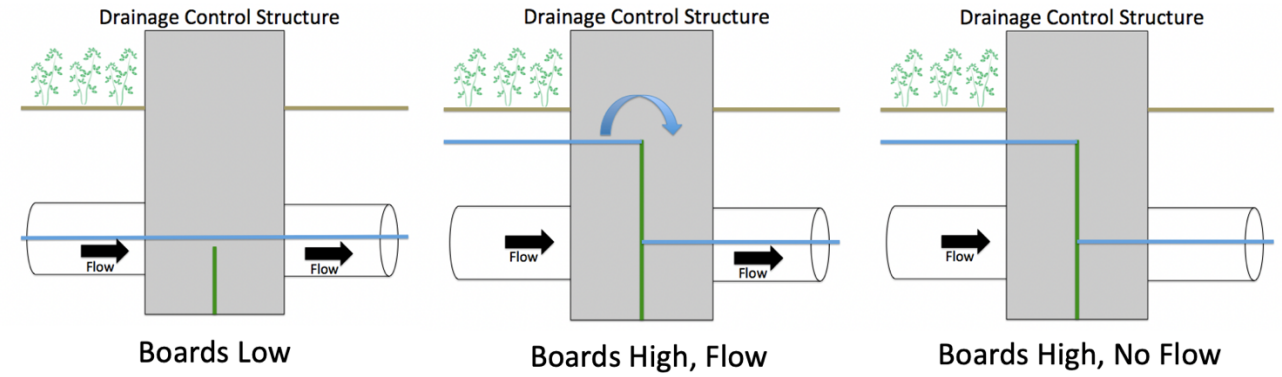

Figure S1. Detail of cross-section of drainage control structures that implements DWM. Low board and high board (green) conditions as well as theoretical water tables (blue).

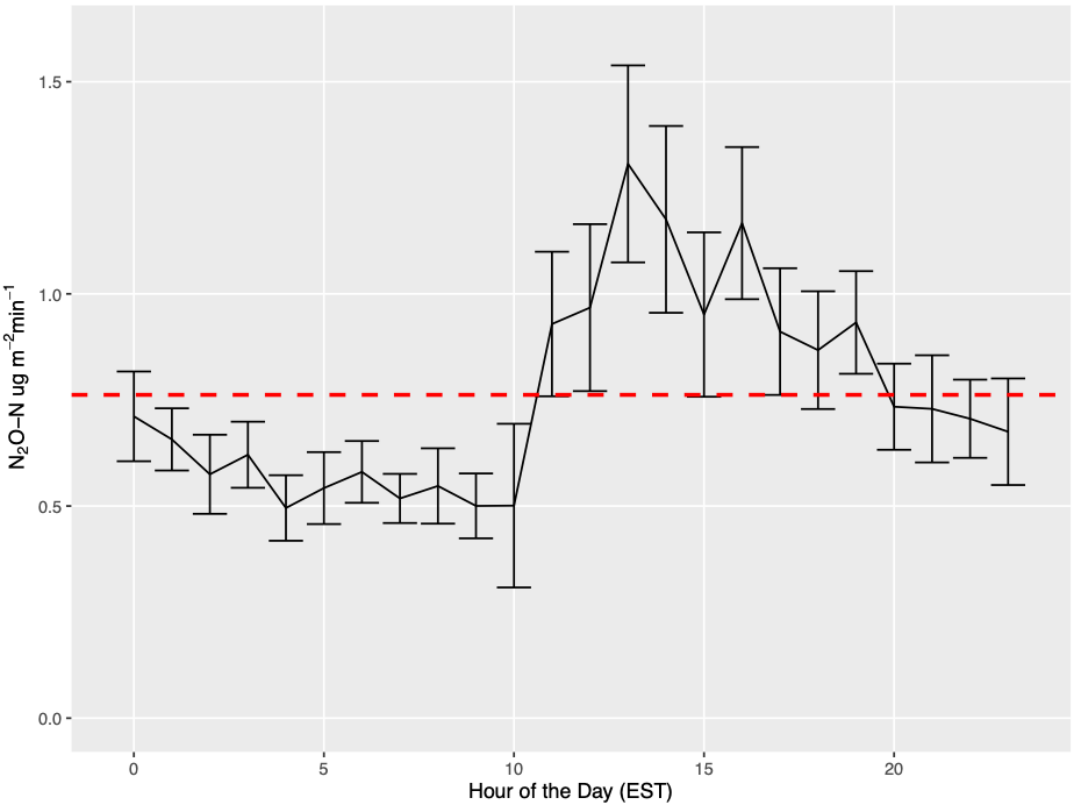

Figure S2. Summary of diel variation of N2O fluxes in a preliminary sampling campaign from 05/19/2019 to 05/22/2019 using an Eosense automated chamber. Each point is a mean (± SE error bar) from four chambers over four days for each hour of the day. This period did not include precipitation or N fertilization events. The red dashed line represents the mean flux of all chambers over the entire 4-day period.

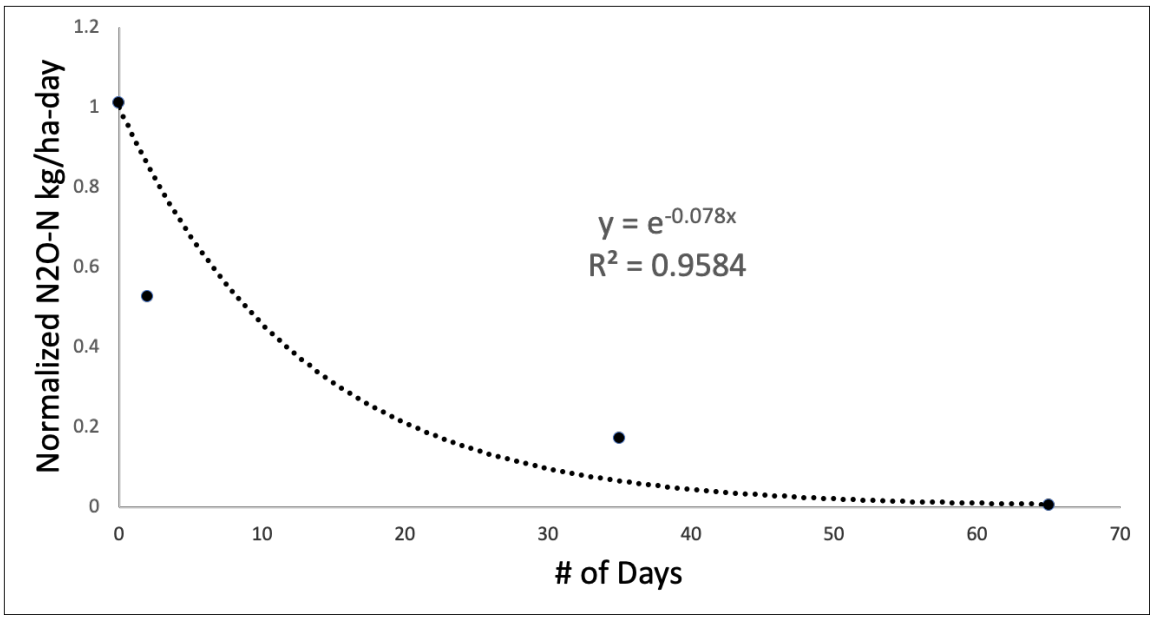

Figure S3. Demonstration of decay curve fit to a particular period of time after N fertilization to estimate annual N_2O fluxes.

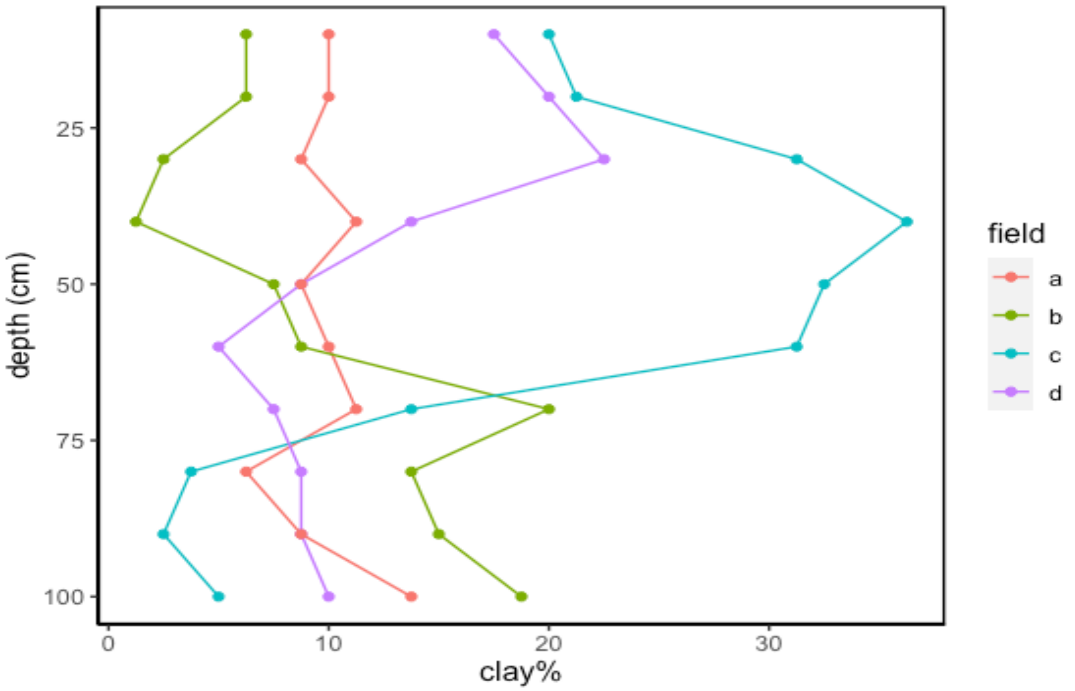

Figure S4. Clay size fraction percentage at each depth for each field.

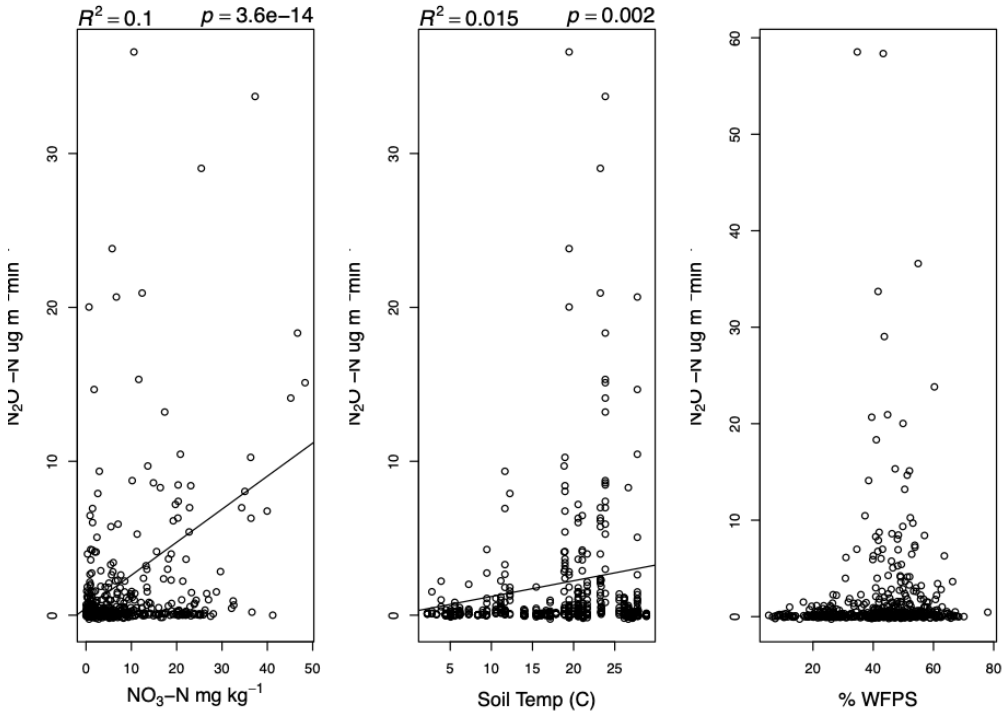

Figure S5. Three panels showing describing the individual relationships between N_2O gas fluxes and variables used in the multiple linear regression model. Linear regression p-values and r^2 values reported at the top of each panel.

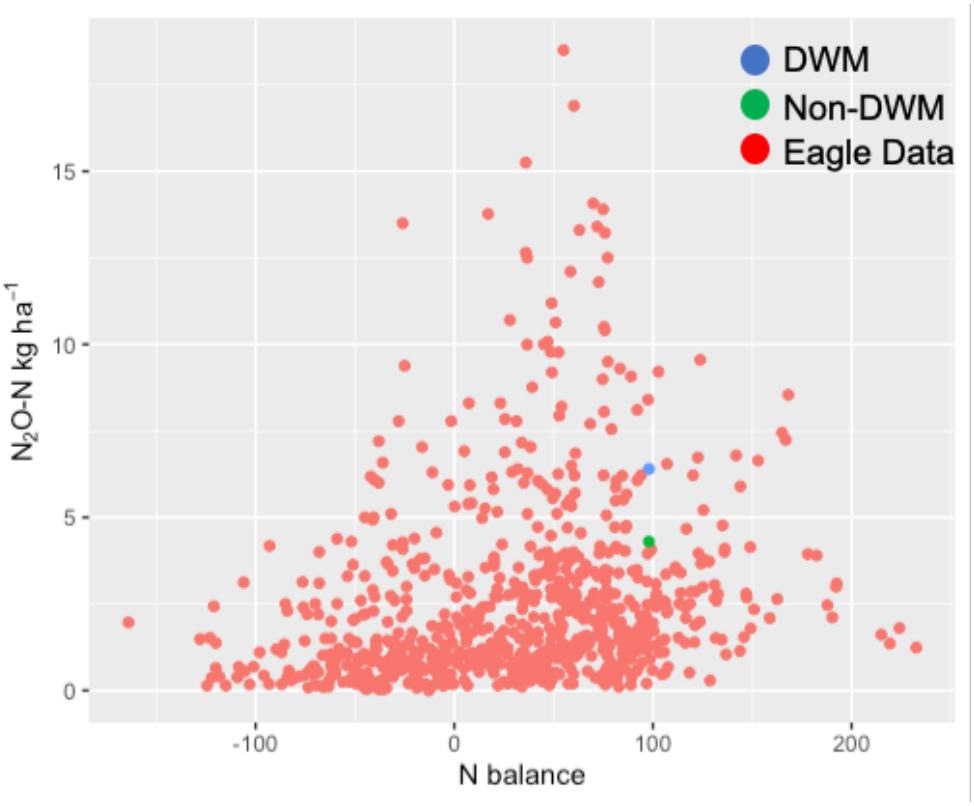

Figure S6. Comparison of study data to Eagle et al. (2020) review of studies from the U.S. cornbelt evaluating N balance versus N_2O emissions.

Chapter 3: Using Natural Abundance Nitrate Isotopes to Assess Denitrification Impact in an Agricultural Drainage Water Management System

Chapter Note

This chapter has been written in preparation for submission as a manuscript to the journal *Biogeochemistry*. Upon submission to the journal, components of dissertation chapter 4 will be added to the discussion and conclusion sections of this chapter.

Abstract

Drainage water management (DWM) is a best management practice (BMP) that can reduce nitrogen (N) export from agricultural ditches to downstream waters. By slowing water flow and increasing water tables, nitrate (NO_3^-) can be removed via denitrification. As denitrification reduces NO_3^- to nitrous oxide (N_2O) and dinitrogen (N_2), these gases are emitted from soil or dissolved in groundwater. N_2O is a potent greenhouse gas and a reactant in stratospheric ozone depletion. Here we evaluated evidence for denitrification using natural abundance of $\delta^{18}O$ and $\delta^{15}N$ in NO_3^- in a corn-soybean rotation on a working farm in eastern Maryland. We measured soil extracts, piezometer groundwater, and ditch water samples in plots with and without active DWM. The results demonstrated an increase in fractionation of both isotopes consistent with denitrification along a leaching continuum from surface to deep soil, mid-field to edge-of-ditch groundwater, and in the ditchwater. However, the net effects of nitrification and denitrification resulted in NO_3^- somewhat less enriched in ^{15}N than expected by denitrification fractionation alone. Based on preliminary mass

balances of both total N and $\delta^{15}N$, the calculated net N isotopic discrimination was within the range of published values for denitrification, indicating a significant role for denitrification in all study fields. Excess N_2 dissolved in groundwater piezometers also indicated denitrification. Although lower observed NO_3^- export from ditches in the DWM fields would suggest higher rates of denitrification, propagation of uncertainties of multiple mass balance terms in a Monte Carlo analysis resulted in error terms for denitrification that were as large as the difference between treatments in NO_3^- export. The dual isotopic analyses provided corroboration of denitrification and bounded quantitative estimates of denitrification derived from mass balances.

3.1 Introduction

Nitrogen (N) is a key element for ecosystem productivity, particularly within the context of agriculture (Galloway, 2003). The rise of modern agriculture has impacted the N cycle in a variety of ways. One such impact is industrial N fixation which created synthetic N fertilizer production by using the Haber-Bosch process to convert atmospheric dinitrogen (N_2) gas to ammonia (NH_3) (Vitousek et al., 1997; Fowler et al., 2013). Abundant use of synthetic N fertilizers since the 1950's has increased crop yields but has also led to pollution issues such as eutrophication and greenhouse gas emissions. When N fertilizer is applied to crop fields, but not assimilated by the plants, it becomes excess nutrient content in the soil where it can leach into groundwater, concentrate in surface water bodies, or be transformed to a gas and emitted into the atmosphere (Schlesinger, 2009).

Agricultural expansion in the U.S. included the conversion of many wetland landscapes to arable land through the installation of drainage ditches, particularly in

the Midwest and coastal regions. These ditches served as conduits to drain water from soil for the purpose of creating drier conditions for crop growth (Webb et al., 2021). These conduits not only moved water from fields, they also moved dissolved nutrients, like N, downstream, contributing to eutrophication of aquatic ecosystems (Skaggs et al., 2012; Gilliam et al., 1979). Eutrophication has been documented in every U.S. state and is correlated with the increased frequency and spread of coastal and freshwater harmful algal blooms (HAB's). These events have closed fisheries, caused human health issues because of impacts on drinking water, and have led to a detrimental ecological cascade of environmental concerns (Glibert, 2020; Galloway, 2003).

As this nutrient issue has persisted, agricultural best management practices (BMP) have been designed and implemented to reduce nutrient loads and concentrations entering downstream waters. One such BMP is drainage water management (DWM). The purpose of DWM is to use drainage control structures to slow down the water flow from agricultural fields by raising the water table behind the structure (Gilliam et al., 1986). By keeping more water in the field for longer, higher moisture conditions and lower oxygen content can create an environment more conducive for denitrification. This microbially driven process that consumes nitrate (NO_3^-), a nutrient of concern for eutrophication, can reduce NO_3^- to N_2 in agricultural soil (Nommick, 1956, Firestone, 1982). Many studies have demonstrated the effectiveness of this BMP at reducing hydrologic N export from agricultural ditches, either by reducing the total discharge (Williams et al., 2015; Helmers et al., 2022), reducing the NO_3^- concentration (Fisher et al., 2010; Skaggs et al., 2012, Drury et al.,

1996), or both (Carstenson et al., 2016; Smith et al., 2011). While DWM has shown promise at reducing N export (Drury et al., 2009; Jaynes et al., 2012), a concern is that the mechanism that consumes NO_3^-, denitrification, can also produce nitrous oxide (N_2O), a potent greenhouse gas. This could be an example of unintended pollution swapping by trading decreases in hydrologic NO_3^- export for increases in soil N_2O production. However, in a companion study at the same research site, we found that soil N_2O emissions were not significantly higher in the DWM treatment, suggesting that pollution swapping (nitrate leaching versus. greenhouse gas emissions) may not be a serious concern, at least on this study farm (Hagedorn et al., 2022). Preliminary estimates of hydrologic N export indicate the DWM treatment decreased N export via NO_3^- concentration reduction rather discharge reduction, indicating that denitrification may have been stimulated.

This research examines the effect of DWM on denitrification and gaseous N export in a fertilized N agricultural system through a novel combination of measuring dissolved gases, dual NO_3^- isotopes at multiple locations (soil profile, piezometer, ditch outflow), and components of a total N and $\delta^{15}N$ mass balance. The purpose of this research was to qualitatively and quantitatively assess the occurrence and magnitude of denitrification within the context of DWM. Denitrification is difficult to quantify because of its temporal and spatial heterogeneity, and the technological challenges in measuring the primary end product, N_2, in a N_2 -rich atmosphere (Davidson et al., 2006; Groffman et al., 2012; Seitzinger et al., 2006). Relatively recent methodological advances have enabled detecting and measuring denitrification through natural abundance isotopes. Dual isotopes of NO_3^- ($\delta^{18}O$-NO_3^- and- $\delta^{15}N$-

NO_3^-) can be used to qualitatively assess the influence of denitrification across spatial scales, because denitrifying enzymes discriminate against ^{18}O and ^{15}N, preferring ^{16}O and ^{14}N, which results in the isotopic enrichment of residual NO_3^- (Groffman et al., 2006; Kendall et al., 2007). Previous work has demonstrated that $\delta^{18}O$ and $\delta^{15}N$-isotopes can be used to infer specific N sources and processes along a hydrologic pathway in evaluating progressive denitrification (Lohse et al., 2013, Osaka et al., 2010). Evidence of isotopic enrichment has been found in soils, soil water, shallow groundwater, and streams to varying degrees (Xu et al., 2021; Yu et al., 2019; Ostrom et al., 1998; Clague et al., 2019). However, denitrification is not the only process that impacts residual NO_3^- isotopes. The production of NO_3^- via nitrification, the two-step oxidative process that transforms ammonium (NH_4^+) to NO_3^-, also isotopically discriminates, resulting in NO_3^- that is depleted in ^{15}N (Mariotti et al., 1981; Casciotti et al., 2003; Kendall et al., 2007; Högberg et al., 1997). Within agricultural DWM, only a few isotopic NO_3^- studies exist, and they either did not observe isotopic evidence of denitrification (Smith et al., 2011; Kelly et al., 2013), or did not find that DWM enhanced denitrification (Carstensen et al., 2019; Carstensen et al., 2016), although most of these studies only sampled NO_3^- isotopes from ditch water.

This isotope analysis can be merged with a mass balance approach for measuring components of the agricultural N cycle, which can lead to insightful research about how N moves in the environment (Gentry et al., 2009). Mass balances rely on developing a budget of inputs and outputs, then directly quantifying the budget terms that are possible to measure, and solving for unknown variables by difference (Reinhardt et al., 2006). However, accurate field-scale nitrogen balances

can seldom be developed because many pools/flows of N remain difficult to measure directly, and propagating multiple parameter errors within a mass balance budget results in large uncertainties of the term (often denitrification) that is calculated by difference. This conundrum was noted nearly 70 years ago by Allison (1955) and more recent reviews noted that it still remains true today (Davidson et al., 2006). Integrating multiple methodological techniques, such as both N mass balance and isotopic measurements, across scales may offer a new approach to elucidate whether and where denitrification occurs, and help constrain quantitative estimates of denitrification.

The two objectives of this study were 1) to evaluate use variation in the natural abundance of $\delta^{18}O\text{-}NO_3^-$ and $\delta^{15}N\text{-}NO_3^-$ as a qualitative indicator of the presence of denitrification in the soil, groundwater, and stream water in a N fertilized, DWM agricultural system; and 2) to use an isotopic N mass balance to quantify if and how DWM impacts the relative proportions of hydrologic and gaseous N export. For the first objective, the natural abundance NO_3^- isotopic technique was implemented to describe the patterns of residual $\delta^{18}O\text{-}NO_3^-$ and $\delta^{15}N\text{-}NO_3^-$ across the field-to-ditch spatial continuum and to evaluate the degree to which fractionating N processes, like denitrification and nitrification, impart an isotopic signature. To assess this signal, NO_3^- samples were analyzed from the soil profile, piezometers and ditch water. The hypotheses within this objective are associated the conceptual isotopic continuum diagram (Figs. 1-3), and are described as follows:

Hypothesis #1: Progression within dual isotope slope range: We expected that denitrification imparts a positive slope relationship between $\delta^{18}O\text{-}NO_3^-$ and $\delta^{15}N\text{-}$

NO_3^-. We hypothesized that most NO_3^- samples would fall between slopes of 0.5 and 1.0 ($\delta^{18}O\text{-}NO_3^-$: $\delta^{15}N\text{-}NO_3^-$), indicating that denitrification is the dominate N processing mechanism (Kendall et al., 2007; Mengis et al., 1999; Bolhke and Denver, 1995; Granger et al., 2008). Deviations from that slope would demonstrate the impact of other N processes, such as nitrification.

Hypothesis #2: Progression along spatial continuum: We hypothesized that the dual isotope enrichment would increase progressively, with more enriched NO_3^- isotope values moving along the idealized hydrological flow path from surface soil to deep soil to field piezometer to ditch piezometer to ditch water, as indicated by the trend to the upper right in Fig. 1 (Jung et al., 2020).

For the second objective, we hypothesized that DWM would stimulate denitrification and subsequently a higher fraction of gaseous N export compared to hydrologic N export. Here we explore whether isotopic methods provide an opportunity to overcome difficulty in constraining estimates of flows for N budgets (Zhang et al., 2020). Some studies have shown that combining isotopic data with mass balances can be used to infer large gaseous emissions, although much of this previous work occurred in forested or tropical environments (Houlton et al., 2006; Fang et al., 2015). Given the strong isotope effect denitrification imparts on NO_3^-, combining a N mass balance with isotopic N balance could help constrain estimates of denitrification.

3.2 Methods

3.2.1 Research Site

The site was located at a private agricultural farm on the Eastern Shore of Maryland, USA (N 39.11973, W 75.8069) that has operated under a corn-soybean rotation since 2004. The ~12 hectare research area had four drainage ditches. Drainage control structures (DCS) were installed in 2006 and were used according to the drainage water management (DWM) protocol since inception. The farm site had pivot irrigation that was used during dry periods in summer. For corn crops, the site was fertilized with a split application of urea ammonium nitrate (UAN) totaling 213 kg ha^{-1} yr^{-1}. Every 4-5 years, sludge was applied to the field, which did not occur during this study period, though it did occur two years prior. The soils were predominately Fallsington sandy loams, 0 to 2 percent slopes, Mid-Atlantic Coastal Plain (Soil Staff, NRCS).

3.2.2Experimental Design

Two ditches and their respective drainage/field areas (A and B) were assigned as non-DWM treatment plots. Two other ditches and drainage/field areas (C and D) were assigned as DWM treatment plots (Figure 2). Beginning in April 2017, this experimental design was applied and maintained throughout the project duration. This consisted of inserting 3-4 boards and a v-notch weir into the DWM treatment DCS (which allows the water table to be raised) and removing them (which allows the lowering of the water table) during periods of farm management such as planting and harvesting, as determined by the collaborating farmer. The non-DWM treatment DCS

only had a single board with a v-notch weir. Soil and water were sampled at locations within each field along the conceptual continuum sequence from surface bulk soil, soil profile, field piezometer, ditch piezometer, and ditch (Figures 1-3) from April 2017 to October 2018 with variable timing and frequency (Table 1).

3.2.3 Sampling Techniques

3.2.3.1 *Soil Profile Samples*

The soil profile samples were removed using a 4.5 cm diameter auger down to one meter depth, and were separated into 10 cm intervals. Samples were stored in plastic bags and placed in a cooler for transport to the laboratory. Within 36 hours of collection, subsamples were assessed for soil extractable NO_3^- content and isotopic values, as described in the analytical methods section. All remaining sample material was frozen. To get a larger sample number for bulk surface soil estimates, three 2.5 cm diameter by 10 cm long soil plugs were taken at 8 locations within in each field plot, aligning with gas sampling chambers described in companion study (Hagedorn et al., 2022, Supplementary Fig. S2). Soil samples were analyzed for $\delta^{15}N$ of total soil N as described below, which was used as a parameter for calculating the net N isotopic discrimination factor described later.

3.2.3.2 Piezometers

The 5 cm diameter PVC piezometers were installed with 30 cm slotted screens about one meter beneath the soil surface. The ditch piezometers were placed ~ 70 meters upstream of the ditch outlets, on the edge of the ditches. The field piezometers were placed about 20 meters inward along a line perpendicular to each ditch and approximately in the middle of the fields. The piezometers were pumped dry prior to

sampling, and once sufficiently recharged, usually 1-2 hours later, groundwater samples were acquired in acid-washed bottles for nutrient analysis using a positive pressure pump. The sample was stored on ice, transported back to the lab, filtered using 0.4 μM Whatman glass fiber filters and frozen for later analysis. For dissolved gas sampling, six 12-mL exetainer tubes were filled per piezometer, allowing the tube to overflow at least three times to minimize atmospheric contamination, capped and placed in ice water (Fox et al., 2014).

3.2.3.3 Ditches

At the outlet of the drainage ditches, a v-notch weir was installed to quantify flow rates and discharge. A water sample was taken from water overflowing the v-notch. The collection bottles were rinsed three times before a sample was taken. All samples were stored on ice, transported back to the lab, filtered, and frozen prior to analyses. Ditch gas samples were acquired by inserting a narrow diameter piece of tubing attached to a centrifuge tube to the bottom of an exetainer, which acted as a vent. The exetainer and the vent were inserted upside down into the ditch water carefully. As the exetainer was submerged, the water entered the exetainer because the air in the tube was expelled through the vent. After the exetainer was filled, the vent tubing was removed, and the exetainer was capped underwater. The exetainers were then placed in ice water and samples were usually analyzed within 24 hours of collection. This method minimized both atmospheric gas contamination and water turbulence while filling the exetainer (Fox et al., 2014).

3.2.4 Analytical Techniques

3.2.4.1 Bulk Soil N, Crop Grain N, and Isotopes

Bulk soil samples were air-dried, homogenized by plot, and sieved (10 mesh). For grain samples, four ears of corn in each field were randomly collected and the kernels of the ears were stripped, dried, and homogenized. All solid samples (bulk soil and grain) were analyzed for %N with a Carlo Erba NC 2500 Elemental Analyzer and $\delta^{15}N$ with the Thermo Delta V+ isotope ratio mass spectrometer, both conducted at the Central Appalachians Stable Isotope Facility (CASIF) in Frostburg, MD.

3.2.4.2 Soil Profile Extracts

Soil samples were subsampled and measured for gravimetric water content. The samples were air-dried and passed through a 2 mm sieve. Extractions in 2M potassium chloride (KCL) were performed to measure NO_3^- content according to the following protocol: 5 grams of air-dried soil and 25 mL of 2M KCL were placed into a 50 mL polypropylene bottle. The bottle was placed on a reciprocating shaker and agitated for 1 hour. After shaking, the sample was centrifuged and filtered through a Fisherbrand 0.45 um filter. Filtrate was collected and analyzed for NH_4^+ and NO_3^- using a colorimetric Lachat technique (Maynard et al., 1993), then converted to units of mg kg^{-1}. Filtrate was then frozen until isotopic analysis. Measured moisture content was used to convert mg NO_3^--N kg^{-1} dry soil to mg NO_3^--N L^{-1} to make more direct comparisons of soil extractions to piezometer samples.

3.2.4.3 Water Chemistry

Samples from ditches and piezometers were collected and stored on ice until the end of the sampling day. The samples were filtered and frozen for up to a month, before automated colorimetric analysis (Fisher et al., 2010; Sutton et al., 2010). The analysis was conducted at UMCES Horn Point Laboratory for NH_4^+, NO_3^-, and total

dissolved nitrogen (TDN). Irrigation samples were analyzed at UMCES Appalachian Laboratory for TDN, NO_3^- and NH_4^+. Samples were collected, filtered and analyzed using a colorimetric Lachat technique (Maynard et al., 1993).

3.2.4.4 Dissolved Gases

Dissolved N_2, O_2, and Argon (Ar) concentrations were measured at the Horn Point Laboratory using the membrane inlet mass spectrometry (MIMS) technique (Kana et al., 1994; Fox et al., 2014). An argon (Ar) recharge temperature was then used to calculate the background N_2 based upon solubility data at the recharge temperature (Colt, 1984). Excess N_2 was calculated by subtracting the equilibrium background N_2 concentration from the measured N_2 concentration. Oxygen levels were expressed as % saturation (100 * observed O_2 concentration/background O_2 concentration). Dissolved N_2O concentrations were measured using a Shimadzu 2014 gas chromatograph (GC) and electron capture detector and flame ionization detector (Fox et al., 2014). Gas standards were used to establish the linear range of the GC prior to and after each analysis. Sample concentrations were calculated using the solubility data of Weiss and Price (1980) and corrected to standard temperature and pressure conditions.

3.2.4.5 Nitrate Isotopes

All NO_3^- isotope samples were analyzed at the CASIF lab. For both soil extracts and water samples a bacterial denitrifier method was used to convert NO_3^- to N_2O, which was then analyzed for isotopic values upon thermal decomposition of N_2O to N_2 and O_2 (Kaiser et al., 2007). Volume and mass of nitrate added were corrected for variations in sample concentrations. A ThermoFisher Delta V+ isotope

ratio mass spectrometer was used, and the analytical precision of $\delta^{15}N$ was 1.5 ‰ and $\delta^{18}O$ was 2.8‰ as determined by repeated measurements (n ≅ 14) of an internal reference ("Chile NO_3^-", Duda Energy 1sn 1 lb. Sodium Nitrate Fertilizer 99+% Pure Chile Saltpeter from Amazon.com). Measured nitrogen and oxygen isotope ratios were calibrated using international reference standards, USGS 32 ($\delta^{15}N$ = 180 ‰), USGS 34 ($\delta^{15}N$ = -1.8 ‰, $\delta^{18}O$ = -27.9 ‰) and USGS 35 ($\delta^{18}O$ = 57.5 ‰) (Bohlke et al., 2003). Data were corrected for detectable instrument drift. For piezometer and ditch water samples, deionized (DI) water standards were used while KCL standards were used for soil extract samples (Rock and Ellert, 2007). The delta values were defined by Eq. 1, where R is the $^{15}N/^{14}N$ or $^{18}O/^{16}O$ ratio of the sample and a standard. Isotopic values are expressed on a per mil (‰) basis.

Equation 1 (Eq. 1) $$\delta_{sample}\ (‰) = \left(\frac{R_{sample}}{R_{standard}} - 1\right) * 1000$$

3.2.5 Isotopic N mass Balance

3.2.5.1 Description

A N mass balance was combined with a $\delta^{15}N$ isotope balance to estimate the magnitude and mean $\delta^{15}N$ value of gaseous N export. The $\delta^{15}N$ gaseous N export isotopic value, calculated by difference, was then used with the measured surface bulk soil $\delta^{15}N$ value to determine a net N discrimination factor representing the net isotopic effect of total gaseous N production (Eq. 4). This mass balance was conducted for the April 2017 – March 2018 corn year. Quasi-steady state of soil N

was assumed, as the farm had been under a same fertilization and crop corn/soybean rotation since 2004. Mineralization of soil organic-N, and input of previous year's crop residue, was likely a source of N for crop uptake, but internal cycling of N (mineralization-immobilization-turnover) was assumed not to affect the system mass balance if soil N stocks are at quasi steady-state. The following equations were applied with estimates calculated or measured for each parameter.

Equation 2 (Eq. 2): N Mass Balance:

$$\text{Gaseous N Export} = \text{Fertilizer N Input} + \text{Atmospheric N Input} + \text{Irrigation N Input} - \text{Hydro N Export} - \text{Crop Grain N Export}$$

Equation 3 (Eq. 3): δ^{15}N Isotope Balance:

$$\frac{(\text{FertN} * \delta^{15}\text{N fert}) + (\text{AtmN} * \delta^{15}\text{N atm}) + (\text{IrrigN} * \delta^{15}\text{N irrig}) - (\text{HydroN} * \delta^{15}\text{N hydro}) - (\text{CropN} * \delta^{15}\text{N crop})}{\text{Gaseous N Export}} = \delta^{15}\text{N gas}$$

Equation 4 (Eq. 4): Gaseous N net discrimination factor:

$$\text{net N discrimination factor} = \delta^{15}\text{N gas} - \delta^{15}\text{N bulk surface soil}$$

Below is a description of the parameters' values used in the aforementioned equations.

3.2.5.2 Parameters

1. Fertilizer N Input (mass and $\delta^{15}N$): This information was provided by the collaborating farmer who, during corn crop years, applied UAN fertilizer. Split application of the UAN was conducted with one application knifed-in during planting and another side-dressed around the V6 stage corn growth. Fertilization rates did not differ by treatment. Synthetic fertilizer $\delta^{15}N$ values were derived from the literature. We assumed a ± 10% error due to fertilizer application variability for a total of 213 ± 21 kg N ha^{-1} (discussed further in chapter 4). Given the source of synthetically applied UAN is the atmosphere, it was assumed the $\delta^{15}N$ value was 0 ± 2 ‰ (Michalski et al., 2015).

2. Atmospheric N Input (mass and $\delta^{15}N$): The mass was obtained via estimates from interpolated estimates conducted by the National Atmospheric Deposition Program (NADP). For the period of analysis, the study site was estimated to have had 8.2 ± 1.3 kg ha^{-1} of total N deposition (NADP, 2020; Schwede et al., 2014). Given the source of natural N deposition is the atmosphere, it was assumed the $\delta^{15}N$ value was 0 ± 2 ‰ (Michalski et al., 2015, Elliot et al., 2007)

3. Irrigation N Input (mass and $\delta^{15}N$): Irrigation N concentration was averaged with two samples taken a year apart during the study. The irrigation water was sourced from two wells at 120 and 105 meters deep. Irrigation occurred uniformly across treatments. The volume of irrigation precipitation was recorded each year by the collaborating farmer and was combined with average TDN concentrations to obtain a mass. Irrigation $\delta^{15}N$ was measured at the CASIF using analytical protocol described in the methods section. The site received 29.0 cm of irrigation. The average TDN

concentration of irrigation was 1.36 ± 0.1 mg L^{-1} and was dominated by NO_3^- (> 98%). This equated to a total N mass of 4.2 ± 0.5 kg N ha^{-1}. Nitrate $\delta^{15}N$ was averaged to be 7.5 ± 0.2 ‰.

4. Hydro N export (mass and $\delta^{15}N$): This parameter was calculated by the collaborating Horn Point Laboratory team using discharge and N concentration data from v-notch weirs in the control structures. Water level above v-notch in the drainage control structure was measured every 30 min using a Solnist logger. For baseflow, water samples for chemical analysis were collected monthly. For storm water flow, ISCO samplers collected water samples once per hour beginning at the anticipated start of the event. These concentrations were combined with discharge and catchment area to obtain flow-weighted hydrologic export as kg N ha^{-1} yr^{-1}. NO_3^- isotopes from v-notch ditch samples were measured 9 times for each field. Preliminary estimates from the Horn Point Lab team found TDN export (of which NO_3^- concentration was dominant) of 10.2 ± 3.4 kg N ha^{-1} for DWM and 29.1 ± 1.2 kg N ha^{-1} for non-DWM (Fisher et al., (in prep); Hagedorn et al., 2019).

5. Crop N Export (mass and $\delta^{15}N$): This parameter was calculated by measuring %N of crop grain at random locations in all study plots. The %N was converted to kg N by multiplying %N by the grain yield (bushels ac^{-1} reported by the collaborating farmer and converted to kg ha^{-1}) to obtain kg N ha^{-1} of crop export. Grain yield was provided by the collaborating farmer based on the output logged by the combine harvester. Grain $\delta^{15}N$ was measured at the same time as %N, according to analytical protocol previously described. The corn grain had an average N content of 0.84 ± 0.18% and the average corn yield was 13,800 kg ha^{-1} resulting in an average crop N

export of 118 ± 12 kg ha^{-1}(Hagedorn et al., 2022). The average $\delta^{15}N$ corn grain value was 3.4 ± 0.4 ‰.

6. Gaseous N Export (mass and $\delta^{15}N$): These are the unknown parameters being solved for in Eq. 2 and Eq. 3. Total gaseous N export in an agriculture system can occur as NH_3, NO, N_2O or N_2, which we do not differentiate in the mass balance calculation. The average $\delta^{15}N$ of total gaseous N export was calculated from Eq. 3, and was used in Eq. 4 to estimate a net N discrimination factor. These results are reported in Table 2.

7. Bulk surface soil ($\delta^{15}N$): A $\delta^{15}N$ value of total N in the top 10 cm of soil was used as the reference point for net N discrimination factor. The bulk soil surface values were 8.5 ± 1.0‰ for DWM and 9.1 ± 1.4 for non-DWM, and were input to solve for Eq. 4. By subtracting these $\delta^{15}N$ value from the calculated gaseous $\delta^{15}N$ export values, net N discrimination factors associated with N transformation to gaseous N, were calculated (Eq. 4).

3.2.5.3 Monte Carlo Technique

A two-step Monte Carlo (MC) analysis was used to constrain the isotopic N mass balance estimates (Eq. 2 and Eq. 3). The first step was to calculate the gaseous N export using Eq. 2. Using measured data mean ± SD (standard deviation), a normal distribution was created for each input parameter. The output distribution for total gaseous N export then served as an input parameter for the second MC that solved for the $\delta^{15}N$ gas value in Eq. 3. Each MC step was run for 10,000 iterations. The mean of the $\delta^{15}N$ gas value output was combined with the surface bulk $\delta^{15}N$ soil value to solve Eq. 4.

3.2.5.4 Sensitivity Analysis

A sensitivity analysis was conducted to evaluate how uncertainties in hydrologic N export would impact the mass balance gaseous N export value and subsequent net N discrimination factor for both treatments. A range of hydrologic N export values, from 5 to 60 kg ha^{-1} yr^{-1}, were evaluated using Eqs. 2 and 3 in the sensitivity analysis.

3.3 Results

3.3.1 Soil Profile Samples

The soil profile extractions ranged from 0.4 to 26.8 NO_3^--N (mg kg^{-1}), -6.7 ‰ to 18.7 ‰ $\delta^{15}N$-NO_3^-, and -2.5 ‰ to 33.9 ‰ $\delta^{18}O$-NO_3^-. There was a general decrease in NO_3^--N content with depth for both treatments (Figure 4). There was a slight increase in $\delta^{15}N$-NO_3^- with depth, mostly from 0-10 cm to 10-20 cm, and a general increase in $\delta^{18}O$-NO_3^- values with depth for both treatments. In the DWM treatment, the $\delta^{15}N$-NO_3^- and $\delta^{18}O$-NO_3^- values generally had higher magnitudes compared to the non-DWM treatment, but the standard deviations (which represent the variation from multiple sampling dates; Figures S1, S2, S3), overlapped (Figure 4).

3.3.2 Piezometers

The piezometer water samples ranged from 0.1 to 42.1 NO_3^--N mg L^{-1}, 6.7 ‰ to 79.2 ‰ $\delta^{15}N$-NO_3^-, and -2.8 ‰ to 22.2 ‰ $\delta^{18}O$-NO_3^- (Figure 5). There was a strong L-shaped relationship between NO_3^--N concentration and $\delta^{15}N$-NO_3^- value. The field piezometer had high NO_3^--N concentrations with the low $\delta^{15}N$-NO_3^- values

while the ditch piezometer had low NO_3^--N concentrations with the enriched $\delta^{15}N$-NO_3^- values.

3.3.2.1 *Dissolved Gases*

The dissolved gases in the piezometers ranged from 0.2 to 5.0 excess N_2-N (mg L^{-1}), 0.01 to 0.15 N_2O-N (mg L^{-1}), and 7.5% to 71.5 % O_2 saturation. A positive relationship was observed between residual $\delta^{15}N$-NO_3^- and excess N_2-N, driven largely by a ditch piezometer in the non-DWM treatment. In contrast, dissolved N_2O-N was low when $\delta^{15}N$-NO_3^- was high. The elevated $\delta^{15}N$-NO_3^- values occurred only when % O_2 saturation was less than 40%. The excess N_2-N and N_2O-N concentrations indicated on the x-axes (Figure 6) show that excess N_2-N concentrations were one to two orders of magnitude larger than N_2O-N concentrations. In evaluating the relationships between $\delta^{15}N$-NO_3^-, NO_3^--N content, O_2 content, and excess N_2-N, the highest $\delta^{15}N$-NO_3^- values occurred at lower residual NO_3^--N concentrations and lower O_2 content. This pattern was most strongly found in the non-DWM ditch piezometer (Figure 7).

3.3.3 Ditches

The ditch v-notch samples ranged from 0.1 to 10.7 NO_3^--N mg L^{-1}, 9.1 ‰ to 17.2 ‰ $\delta^{15}N$-NO_3^-, and 4.6 ‰ to 13.0 ‰ $\delta^{18}O$-NO_3^--N (Figure 8). There are fewer points for the DWM treatment because by design it was backing up water behind the DCS and did not always have water flowing over the v-notch weir. The DWM samples when there was flow over the weir generally had lower NO_3^--N^- concentrations compared to the non-DWM samples. There was generally a negative relationship between NO_3^--N concentration and $\delta^{15}N$-NO_3^- value.

3.3.4 Isotopic Relationships

3.3.4.1 NO_3^--N versus $\delta^{15}N$-NO_3^-

Some of the highest NO_3^--N concentrations, regardless of treatment, occurred in the surface soil, deep soil and field piezometer, which also had some of the lowest $\delta^{15}N$-NO_3^- values. The lowest NO_3^--N concentrations, generally found in the deep soil, ditch piezometers, and ditches, were where the highest $\delta^{15}N$-NO_3^- values were observed, although not all low NO_3^--N concentrations had enriched $\delta^{15}N$-NO_3^- values (Figure 9). The L-shaped relationship between $\delta^{15}N$-NO_3^- and NO_3^--N content shown for piezometer samples (Figure 5) is also apparent when the soil and ditch samples are included (Figure 9).

3.3.4.2 $\delta^{15}N$-NO_3^- versus $\delta^{18}O$-NO_3^-

The relationship between $\delta^{15}N$-NO_3^- and $\delta^{18}O$-NO_3^- was evaluated for each replicate field according to the conceptual isotopic continuum (Figure 10). Additionally, all replicate data were aggregated by sample location and treatment (Figure 11). There were positive relationships observed in all treatment replicates. The isotopic relationship was examined according to the fit within the 0.5 to 1.0 slope range. The two lines were set to cross at isotope values of 0 ‰ $\delta^{15}N$ of the fertilizer-N (Michalski et al., 2015) and at the minimum observed value in surface soil extracts for $\delta^{18}O$-NO_3^-, which represent the starting point for enrichment of residual NO_3^- caused by denitrification. The data showed a general dual isotope enrichment along the conceptual isotopic continuum with some deviation. Some data points fell within denitrification slope range, but many points fell to the upper left of the slope line, indicating that $\delta^{15}N$-NO_3^- did not become as enriched as expected if denitrification

were the only fractionating process. An exception was the ditch piezometer in field B (non-DWM #2), which was highly enriched in $\delta^{15}N\text{-}NO_3^-$.

3.3.5 Isotopic N Mass Balance

Fertilizer N input, atmospheric N input, irrigation N input, and crop N export were the same for both treatments. Fertilizer application dominated N input into the system while crop and gaseous N export dominated outputs. Irrigation N input and hydrologic N export played relatively minor roles in terms of magnitude of N budget terms. Hydrologic N export was the only mass balance variable that differed by treatment. Given the definition of the mass balance approach in Eq. 2, a difference between the hydrologic N export terms controls the difference in gaseous N export terms, assuming a near steady state system.

3.3.5.1 Monte Carlo Model

The Monte Carlo (MC) simulations of the combined total N and $\delta^{15}N$ mass balances in Eq. 2 and 3 indicate estimates (mean ± SD) of gaseous N export (97.5 ± 23.8 and 78.3 ± 24.1 kg N ha^{-1} yr^{-1} for DWM and non-DWM, respectively) and $\delta^{15}N$ of gas export (-6.0‰ ± 5.0‰ and -10.2‰ ± 6.3‰ for DWM and non-DWM, respectively, Table 2). The coefficient of variation (SD/mean) associated with the gaseous N export estimates was about 30%. Hence, the variation around the mean gaseous N export estimate was larger than the difference between the treatment means for hydrologic N export and total gaseous N export. This result is the product of error propagation in the MC analysis. To solve for Eq. 4, the surface bulk soil $\delta^{15}N$ value was subtracted from the mean output value for the gaseous $\delta^{15}N$ distribution

from Eq. 3 to produce the net N discrimination factor, where -6.0 - 8.5 = -14.5 ‰ and -10.2 – 9.1 = -19.3‰ for DWM and non-DWM, respectively.

3.4 Discussion

3.4.1 Qualitative Indication of Denitrification

3.4.1.1 Decrease in NO_3^- Content

A decrease in NO_3^- concentration in an agricultural system can occur through plant uptake, immobilization (microbial uptake), leaching loss, and denitrification. However, denitrification imparts a large positive enrichment of N and O isotopes on residual NO_3^-. In the soil profile, a decrease in NO_3^- concentration with depth along with slight enrichment in $\delta^{15}N\text{-}NO_3^-$ with depth and moderate enrichment in $\delta^{18}O\text{-}NO_3^-$ with depth, suggests denitrification was active in the soil profile (Figure 4) (Hobbie et al., 2009). Examining this relationship across the sampling continuum, a negative relationship, whether linear or exponential, between NO_3^- concentrations and $\delta^{15}N\text{-}NO_3^-$ values is expected in a system with denitrification present (Koba et al., 1997; Wexler et al., 2012; Nestler et al., 2011). This is consistent with the L-shaped pattern demonstrated in Figure 9.

3.4.1.2 Collective Dual NO_3^- Isotopic Signal

Evaluating the isotopic relationship between $\delta^{18}O\text{-}NO_3^-$ and $\delta^{15}N\text{-}NO_3^-$ provides a qualitative indication of the influence of nitrification and denitrification in this system. Previous studies showed that denitrification can be inferred when the dual isotope enrichment causes the residual NO_3^- to fall between the 1.0 and 0.5 slopes of this relationship (Kendall et al., 2007; Burns et al., 2009). In applying the

data aggregated by sample location along the conceptual isotopic continuum diagram (Figure 11), the hypotheses of the first objective were evaluated as follows:

Hypothesis 1) Progression within denitrification slope range: The means of the data aggregated by sampling locations along the conceptual drainage continuum fell both outside and inside the denitrification slope area. These observations could be explained by the co-occurrence of nitrification and denitrification. In some cases, denitrification dominated nitrification showing highly enriched values of both isotopes within the denitrification slope range, as for the non-DWM ditch piezometer (Fig. 11, unfilled purple circle). One of the non-DWM ditch piezometers showed the most enriched values within the range. For the other spatial locations, any nitrification occurring along the leaching continuum would have diluted the ^{15}N isotopic signal of denitrification. Nitrification discriminates against the heavier N isotope, not the O isotope, conferring depleted $\delta^{15}N\text{-}NO_3^-$ values to the NO_3^- produced, which, when combined with enriched residual NO_3^- following denitrification, moves the mean measured isotopic values to the upper left of the 1.0 slope line (Figure 11). The combined effect of nitrification and denitrification produces less enriched $\delta^{15}N\text{-}NO_3^-$ values (driven by nitrification masking denitrification) but more enriched $\delta^{18}O\text{-}NO_3^-$ values (driven by denitrification), as seen in the both treatments' ditch samples. Nitrification (red arrow, Fig. 11) moderated the denitrification-only signal (blue arrow) by pushing $\delta^{15}N\text{-}NO_3^-$ values lower despite relatively enriched $\delta^{18}O\text{-}NO_3^-$ values (Granger et al., 2016). While the non-DWM ditch piezometer showed highly enriched isotopic values that overcame the nitrification isotopic impact, the overall

masking effect of nitrification impacted treatments similarly at the majority of spatial locations.

Hypothesis 2) Progression along the spatial continuum: There was some variability in the positive isotopic enrichment progression described in along the spatial leaching continuum (Fig. 1), which could be caused by nitrification or by other confounding factors such as spatial heterogeneity. With the exception of the non-DWM ditch piezometer, both treatments generally showed surface soils (start of the continuum) with the lowest NO_3^- isotope values while the ditches (end of the continuum) had the highest isotope values, which aligned with the hypothesis. The other spatial locations fell between those endmembers and had overlapping error bars (representing variability by sampling date and replicate), making it difficult to decipher a definitive order of progression within the conceptual continuum. The high isotopic values of non-DWM ditch piezometer NO_3^- were likely evidence of a hotspot, which is a commonly observed characteristic of denitrification within a landscape (Bernhardt et al., 2017; Weitzman et al., 2021).

3.4.1.3 Dissolved Gases in Piezometers

The main products of denitrification are N_2 and N_2O, but N_2O can also be produced via nitrification. The ratio of production of these gases varies with environmental conditions such as O_2 content and NO_3^- concentrations. Lower O_2 conditions with higher NO_3^- concentrations favor denitrification, rather than nitrification, and N_2 production relative to N_2O is favored by higher moisture content, lower O_2 content, and lower NO_3^- concentrations, assuming ubiquitous bacteria and carbon availability (Firestone and Davidson, 1989). The most enriched $\delta^{15}N\text{-}NO_3^-$

values correlating with lower residual NO_3^- concentrations and lower % O_2 saturation implies elevated N processing via denitrification that consumed NO_3^-, producing N_2 as the end product (Figure 7). This denitrification signal is reinforced by the observation that dissolved excess N_2-N concentrations were highest at relatively lower % O_2 saturation in conjunction with moderate NO_3^- concentrations suggesting that when denitrification occurred, N_2 was the primary end product of denitrification.

3.4.2 Quantitative Indication of Denitrification

3.4.2.1 Gaseous N Export Mass

Because there was less hydrologic N export in the DWM treatment (10.2 ± 3.4 kg ha^{-1} for DWM and 29.1 ± 1.2 kg N ha^{-1} for non-DWM), the mass balance indicated that there was more gaseous N export in the DWM treatment (97.5 ± 23.8 kg ha^{-1} for DWM and 78.3 ± 24.1 kg ha^{-1} for non-DWM), assuming near steady state soil N. However, the uncertainty of the gaseous N export estimate was large because of the compounding nature of propagation of all N mass balance parameters' errors (Soper et al., 2018). Since the error terms for each mean gaseous N export estimate are larger in magnitude than the difference between the treatment means, the study did not definitively support the hypothesis that the DWM treatment resulted in more denitrification, as indicated by increased gaseous N export. Few studies have quantified total gaseous N export, but compared to denitrification rates, which are often presumed to dominate gaseous emissions, the estimates of the present study are on the high end of the range for fertilized N agricultural systems (Sigler et al., 2022; Gentry et al., 2009, Phillips et al., 2008, Seitzinger et al., 2006).

3.4.2.2 Other Components of Gaseous N Export Term

The qualitative isotope analysis indicated that both nitrification and denitrification were likely present in the system, in both treatments, but the estimates of total gaseous N export analysis do not distinguish between N gas derived by different processes. N gases are produced primarily via nitrification (N_2O, NO), denitrification (N_2, N_2O, NO) and ammonia volatilization (NH_3). Emissions of NH_3 were likely small at this site because the average soil pH was 6.1 (Hagedorn et al., 2022), which likely reduced volatilization compared to high soil pH conditions (Rochette et al., 2013). Soil emissions of NO from this mesic and irrigated site were likely to be lower than soil N_2O emissions (Davidson and Verchot, 2000), which a companion study reported in the range of 4.3 to 6.4 kg N ha^{-1} yr^{-1} (Hagedorn et al., 2022). Hence, it is likely that N_2 from denitrification was the dominant gaseous N product, which will be considered further in chapter 4.

The gaseous N term also encapsulates the potential error associated with other unaccounted N export pathways. For example, hydrologic N export used in this N mass balance could be an underestimate if there was significant N that was leached to deep regional groundwater or groundwater seepage around the ditch outlet. Further, vegetation N uptake by plants, such as ditch algae or ditch bank vegetation, or immobilization of N in ditch sediments was not included in the N mass balance. If significant, this would lower the magnitude of the gaseous N export term.

3.4.2.3 Net N Discrimination Factor

The calculated $\delta^{15}N$ values for gaseous N export from Eq. 3 were -6.0 ± 5.0 ‰ (DWM) and -10.2 ± 6.3 ‰ (non-DWM). These values fell within the ranges

reported in the literature for denitrification products (Barford et al., 1999; Snider et al., 2015). For the net N discrimination factor, we assumed the bulk soil N represented the reference point for total gaseous N transformation (Eq. 4). It is plausible that N fertilization would lower the $\delta^{15}N$ isotope reference point, but because bulk soil is such a large stock of N which influences all N cycling processes, including mineralization, immobilization, plant uptake, nitrification, ammonia volatilization, and denitrification, the bulk soil N likely best represents the $\delta^{15}N$ value encompassing the balance between all soil N processing. Using these estimates of gaseous $\delta^{15}N$, a net N discrimination factor relative to the $\delta^{15}N$ value of bulk soil N was calculated to be -14.5 ‰ for DWM and -19.3 ‰ for non-DWM. This factor encapsulates the net N isotopic signal that was imparted from gas transformation via denitrification and any other contributing processes. These values for net isotopic discrimination are consistent with reported values for denitrification from a variety of systems, ranging from -13 ‰ to -35‰ (Barford et al., 1999; Sigler et al., 2022; Denk et al., 2017), but somewhat on the low end due to the confounding effect of nitrification also affecting the $\delta^{15}N\text{-}NO_3^-$, as indicated by the $\delta^{18}O\text{-}NO_3^-$ versus $\delta^{15}N\text{-}NO_3^-$ relationship results (Figure 11).

This net N discrimination factor calculation is sensitive to changes in the N mass balance inputs and outputs. For example, the N mass balance made the assumption that leaching losses apart from ditch weir discharge, such as seepage or underflow, were negligible. However, this could lead to an underestimate of total hydrologic N export which would impact the N mass balance calculation of gaseous N export and net N discrimination factor. A sensitivity analysis showed how changes

in hydrologic N magnitude, ranging from 5 to 60 kg ha^{-1} yr^{-1}, would impact the net N discrimination factor by treatment following Eqs. 2-4 (Figure 12). It revealed that even if hydrologic N export was underestimated by a factor of two because it didn't account for unmeasured underflow or seepage, the resulting net N discrimination factor would still be within the literature range for denitrification (-13 ‰ to -35‰), albeit nearer the lower end of that range. Because the calculated net discrimination factor decreases nonlinearly with increasing hydrologic N export, hydrologic export exceeding 55 kg ha^{-1} yr^{-1} would require unrealistically depleted values of $\delta^{15}N$ gas in Eq. 3 (Denk et al., 2019; Barford et al., 1999; Sigler et al., 2022). A hydrologic N export value of 55 kg ha^{-1} yr^{--1} corresponds to a gaseous N export value of 50 kg ha^{-1} yr^{-1} therefore this isotopic constraint suggests that gaseous N export much less than 50 kg ha^{-1} yr^{-1} in the DWM treatment would be unlikely. Hence, employing mass balance of both total N and $\delta^{15}N$ helps bracket the gaseous N export estimate, providing a lower bound for denitrification.

3.4.2.4 Limitations of N Mass Balance Approach

Some aspects of the assumptions and estimates required for a mass N balance have limitations that could be improved in future work. For example, this study's mass balance approach examined N dynamics over a single corn year of the corn/soybean rotation system. However, unharvested crop residue from one year might play a role in the N budget of the following year's crop. This study assumed that the internal N cycling processes of mineralization, immobilization, and transformation of organic N in and on the soil (crop residue) is at a dynamic steady state and does not affect the N mass balance of inputs and outputs. Including the

second year of a two-year crop rotation might help strengthen the steady state assumption because it accounts for a longer period of time and includes possible residual N from one crop contributing to the N budget of the other crop. However, because soybean is leguminous N fixer, an additional input parameter would be needed for soybean N fixation, which is challenging to measure. Soybean N fixation has been estimated in a variety of ways, but each with significant uncertainties (Unkovich et al., 2008). Therefore, including a soybean year could increase the overall uncertainty of the mass balance.

Another area for future improvement is in the measurement and estimation of the components of the N mass balance and their uncertainties (Table 3). For example, the source of uncertainty for irrigation N was temporal variation while it was spatial variation for crop N export. It might be valuable to make the source of uncertainty uniform across variables (either spatial, temporal, or measurement variation), to increase confidence in what each mean value's uncertainty represents. Further, the assumed normal distribution for each variable could be modified if additional data warranted an alternative distribution type.

A reduction in the uncertainty of the estimated mean of each parameter would further this research and perhaps narrow the uncertainty of the estimate of gaseous N production by difference of the other terms. The ± 10% uncertainty assumed for fertilizer N inputs may be high given the GPS based pump flow technology used by the farmer for N application. A sensitivity analysis was performed to evaluate how reductions in the assumed uncertainties of the fertilizer N input and crop N export (the two largest magnitude variables in the N mass balance) would impact the

calculated gaseous N export values. For each of those two variables two scenarios were assessed: one with 50% of the original uncertainty assumed in the initial mass balance analysis and the other with 10% of the original uncertainty. A fifth scenario was a combination with 50% of the original uncertainty in both crop N export and N fertilizer input. Results show that the N export uncertainty is most sensitive to the assumed uncertainty of fertilizer N input (Table 4). If the N input uncertainty could be reduced to 10% of the original assumption, then the overlap of the means and their uncertainties of gaseous N export by DWM treatment narrows considerably. Similarly reducing the uncertainties of both N fertilizer input and crop N export to 50% of the originally assumed value also reduced the N gas export uncertainty by about half.

There are ways to improve uncertainties of the mass balance parameters. For example, the crop N export uncertainty could be lowered if a larger number of corn grain samples were collected from the fields and analyzed for %N content. This might have reduced the impact of some of the variation in %N content which could impact the crop N export value. For the fertilizer N content, an assessment of the uniformity of the application rate at different points in the field would increase confidence of the error surrounding that mean estimate.

3.5 Conclusion

3.5.1 Lines of Evidence of Denitrification

The first objective of this study was to use the natural abundance dual NO_3^- isotope technique to evaluate the signal of denitrification at a variety of spatial

locations within an agricultural DWM system. One line of evidence of denitrification was found in the soil profile that showed a decrease in NO_3^- content with depth accompanied by a slight to moderate enrichment of $\delta^{15}N\text{-}NO_3^-$ and $\delta^{18}O\text{-}NO_3^-$ with depth. Further, it was shown that among all spatial locations (soil profile, field and ditch piezometers, ditch water) the highest $\delta^{15}N\text{-}NO_3^-$ values occurred when NO_3^- concentrations were lowest, suggesting that NO_3^- was consumed and the residual became enriched in $\delta^{15}N$, consistent with denitrification.

A second line of denitrification evidence was found in the evaluation of the collective dual NO_3^- isotope analysis corresponding to the conceptual isotopic continuum diagram. The first hypothesis, regarding the slope of the $\delta^{18}O\text{-}NO_3^-$:$\delta^{15}N\text{-}NO_3^-$ relationship, demonstrated strong evidence for denitrification occurrence across spatial locations, as some points fell within the denitrification-only signal range, while others showed evidence of nitrification moderating the expected signal of denitrification. Values of $\delta^{15}N\text{-}NO_3^-$ falling above the literature-derived $\delta^{18}O\text{-}NO_3^-$:$\delta^{15}N\text{-}NO_3^-$ slope of 1.0 indicated that nitrification was influencing the isotopic signal. The mixed isotopic signal with values both above and below the 1.0 slope showed that nitrification and denitrification were co-occurring. The second hypothesis about the isotope enrichment signal following the idealized hydrologic pathway was partially supported. Enrichment of both isotopes generally increased along the spatial continuum from surface soils to deep soils, to field piezometer to ditch piezometer, and to ditch water, albeit with some variation likely due to spatial hotspots impacting the local intensity of N processing.

A third line of denitrification evidence was found in the dissolved gases in the piezometers. The highest dissolved excess N_2-N concentrations occurred under lower % O_2 saturation conditions and moderate NO_3^- concentrations. Further, the highest $\delta^{15}N\text{-}NO_3^-$ values also co-occurred with the low relative % O_2 saturation and low NO_3^--N concentrations, supporting the notion that denitrification occurred and imparted enriched $\delta^{15}N\text{-}NO_3^-$ on residual NO_3^- while producing mostly N_2 as the dominant end product.

A fourth line of denitrification evidence was found in the isotopic N mass balance results. The calculated $\delta^{15}N$ of gaseous N export and the calculated net N discrimination factors both fell within literature ranges for denitrification measured at variety of scales and settings. Furthermore, the isotopic mass N balance and calculated net discrimination factors enabled estimation of a lower bound estimate of denitrification in this system.

3.5.2 Treatment Effect on Denitrification

Both treatments showed multiple lines of evidence for substantial denitrification with co-occurrence of nitrification. Less hydrologic N export in the DWM treatment relative to non-DWM treatment suggested that there was more gaseous N export in the DWM, likely caused by increased denitrification. However, the N mass balance combined with Monte Carlo propagation of errors showed that uncertainties in the total gaseous N export estimate were as large as the difference between treatments. In both treatments, estimates of isotopic N mass balance and net N isotopic discrimination factors were in alignment with previously published values

for denitrification, thus corroborating a major role for denitrification with a quantified lower bound in the N mass balance of this agriculture landscape.

3.6 Tables

Table 1: Description of the sampling location, measured N constituents and frequency of sampling.

Location	Measured N Constituents	Frequency
Bulk surface soil	%N, $\delta^{15}N$	Bi-Monthly
Soil Profile (0-100 cm, 10 cm intervals)	NO_3^--N, $\delta^{15}N$-NO_3^-, $\delta^{18}O$-NO_3^- (KCl extracts)	Bi-Monthly
Piezometers	NO_3^--N, $\delta^{15}N$-NO_3^-, $\delta^{18}O$-NO_3^- , dissolved N_2O-N and excess N_2-N	Monthly
Ditch (v-notch weir)	NO_3^--N, $\delta^{15}N$-NO_3^-, $\delta^{18}O$-NO_3^-	Monthly

Table 2. Parameters and results (mean ± SD) of Monte Carlo analyses that solved for Eq. 2 and Eq. 3.

	DWM		Non-DWM		Type of Data
Variable	Mass (kg ha^{-1})	$\delta^{15}N$ (‰)	Mass (kg ha^{-1})	$\delta^{15}N$ (‰)	
Fertilizer N Input	213 ± 21.0	0.0 ± 2.0	213 ± 21.0	0.0 ± 2.0	Measured
Atmospheric N Input	8.2 ± 1.3	0.0 ± 2.0	8.2 ± 1.3	0.0 ± 2.0	Literature values
Irrigation N Input	4.2 ± 0.5	7.5 ± 0.2	4.2 ± 0.5	7.5 ± 0.2	Measured
Hydrologic N Export	10.2 ± 3.4	13.3 ± 2.1	29.1 ± 1.2	12.6 ± 2.4	Measured
Crop N Export	118 ± 12	3.7 ± 0.4	118 ± 12	3.7 ± 0.4	Measured
Gaseous N Export	97.5 ± 23.8	-6.0 ± 5.0	78.3 ± 24.1	-10.2 ± 6.3	Calculated via equation #2 & #3
d15n surface bulk soil	NA	8.5 ± 1.0	NA	9.1 ± 1.4	Measured

Table 3. Description of the source of uncertainty and assumed variable distribution for each variable in the isotopic N mass balance.

	DWM	**Non DWM**	Source of Uncertainty	Assumed Distribution
Variable	Mass (kg/ha)	Mass (kg/ha)		
Fertilizer N Input	213 ± 21.0	213 ± 21.0	Assumed 10% error	Normal
Atmospheric N Input	8.2 ± 1.3	8.2 ± 1.3	NADP averaged across two years	Normal
Irrigation N Input	4.2 ± 0.5	4.2 ± 0.5	Variation across time (n=2)	Normal
Hydrologic N Export	10.2 ± 3.4	29.1 ± 1.2	Variation across replicate (n=2)	Normal
Crop N Export	118 ± 12	118 ± 12	Variation of %N across replicate (n=4)	Normal
Gaseous N Export	97.5 ± 23.8	78.3 ± 24.1	Propogation of error	Calculated
	DWM	**Non-DWM**	Source of Uncertainty	Assumed Distribution
Variable	d15n (‰)	d15n (‰)		
Fertilizer N Input	0.0 ± 2.0	0.0 ± 2.0	Literature uncertainty	Normal
Atmospheric N Input	0.0 ± 2.0	0.0 ± 2.0	Literature uncertainty	Normal
Irrigation N Input	7.5 ± 0.2	7.5 ± 0.2	Variation across time (n=2)	Normal
Hydrologic N Export	13.3 ± 2.1	12.6 ± 2.4	Variation across replicate (n=2)	Normal
Crop N Export	3.7 ± 0.4	3.7 ± 0.4	Variation across replicate (n=4)	Normal
Gaseous N Export	-6.0 ± 5.0	-10.2 ± 6.3	Propogation of error	Calculated
d15n surface bulk soil	8.5 ± 1.0	9.1 ± 1.4	Variation across replicate (n=2)	Normal

Table 4. Results of sensitivity analysis of different scenarios representing reductions in uncertainties of fertilizer N input and crop N export.

	Gaseous N Export (kg/ha)	
Gaseous N Export Mean Value	97.5	78.3
Uncertainty Variable Scenario	**DWM**	**Non-DWM**
Original table 2 Fert N input (± 21) and Crop N export (± 12)	± 23.8	± 24.1
Original with 50% of Fert N input uncertanity (± 10.5)	± 16.4	± 16.0
Original with 10% of Fert N input uncertanity (± 2.1)	± 12.6	± 12.2
Original with 50% of Crop N export uncertainty (± 6)	± 22.0	± 21.8
Original with 10% of Crop N export uncertainty (± 1.2)	± 21.2	± 20.9
Original with 50% of Fert N (± 10.5) and crop N (± 6) uncertainties	± 12.8	± 12.2

3.7 Figures

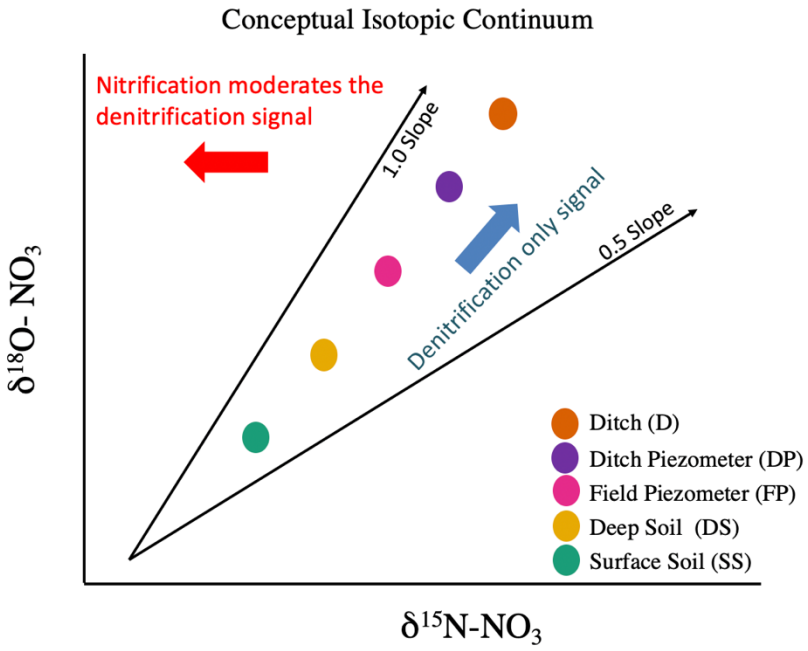

Figure 1. Conceptual isotopic continuum along an idealized hydrological flow path from soil surface to ground water to ditch. The dots indicate spatial sampling positions and correspond with Figures 2 and 3 in the methods section. The slopes represent the bounds of denitrification inference.

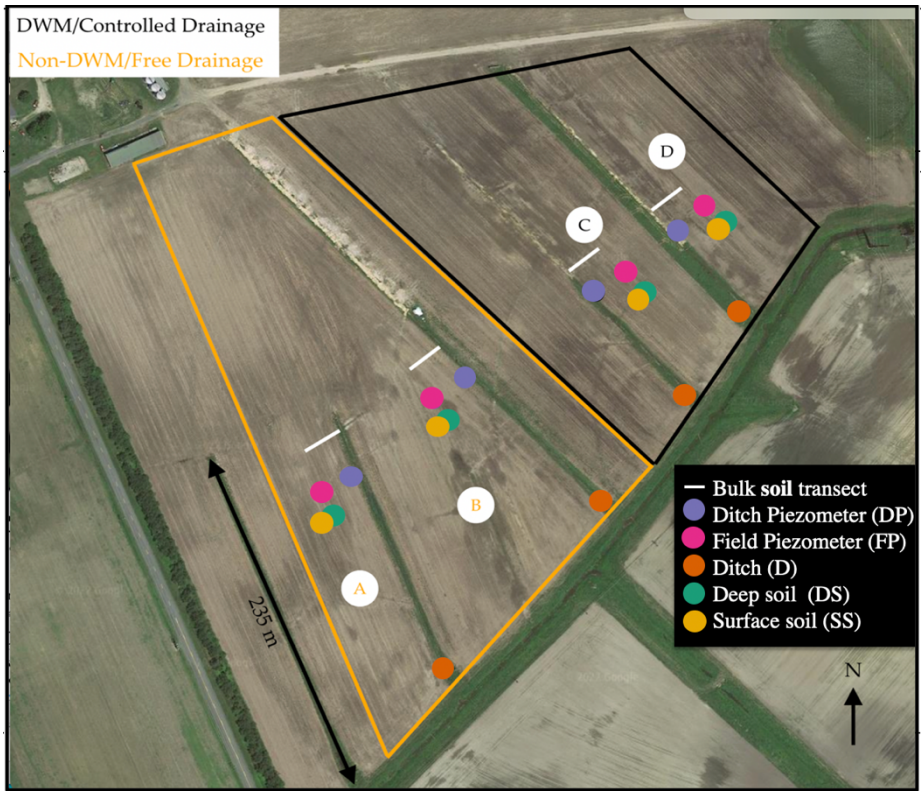

Figure 2. Aerial view of research site indicating treatment plots and approximate locations of sampling sites. Aerial image was taken during an early planting cropping period. See Figure 3 for cross sectional view.

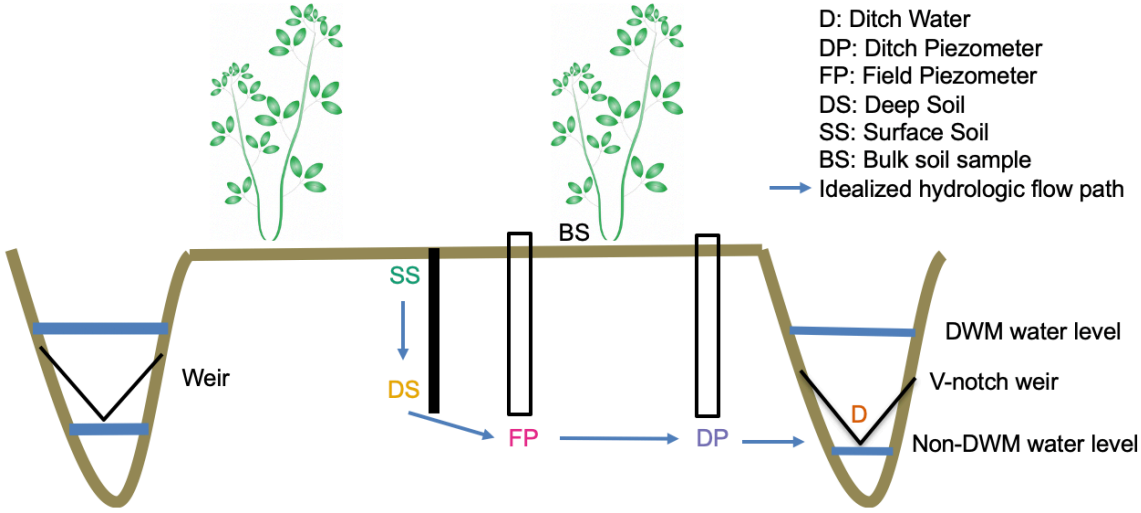

Figure 3. Cross sectional view of sampling locations. Theoretical water level by treatment is shown in ditches.

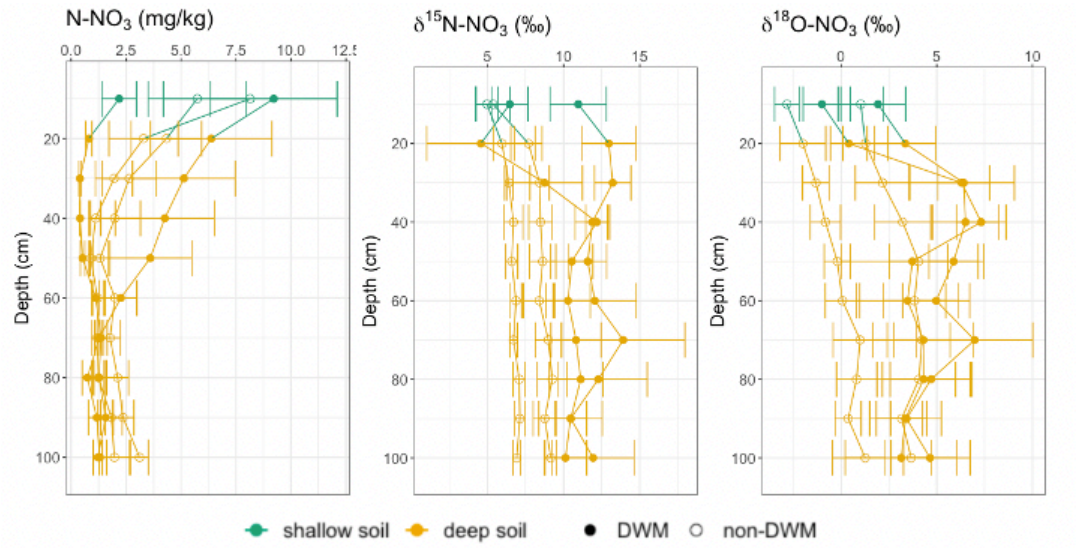

Figure 4. The mean ± SD for each constituent where solid fill circles represent the two DWM replicate fields, hollow circles the two non-DWM replicate fields, and color represents location of sample within the conceptual isotopic continuum shown in Figures 1-3.

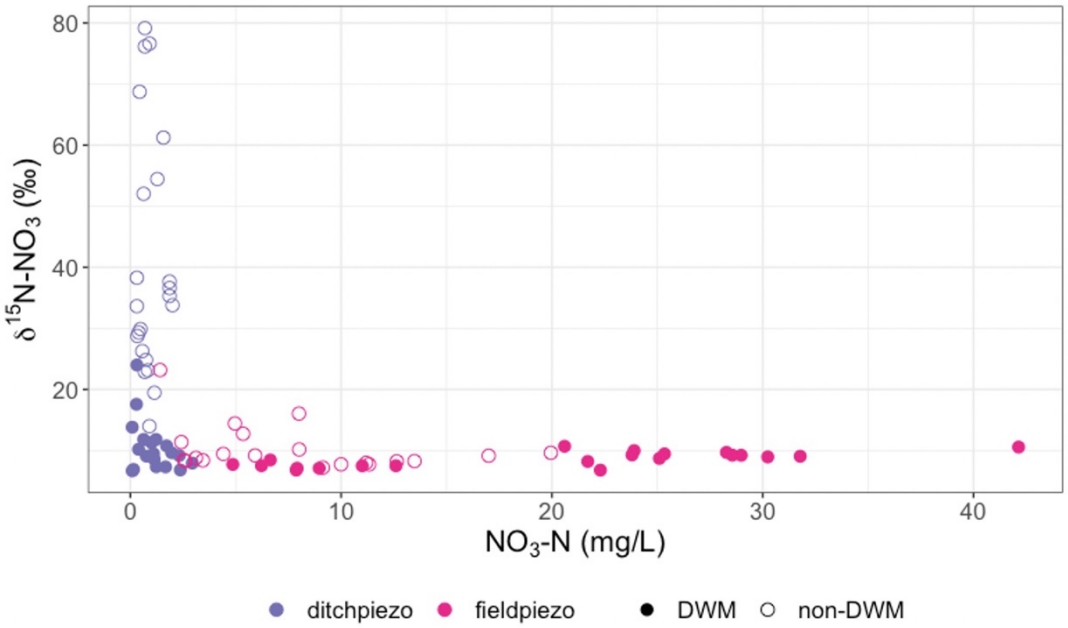

Figure 5. Relationship between NO_3^--N concentration and $\delta^{15}N$-NO_3^- value for the field and ditch piezometers. Shape (solid fill versus unfilled) represents treatment and color represents spatial location in the isotopic continuum. The spread of data represents variation by sampling date and replicate (Figure S4)

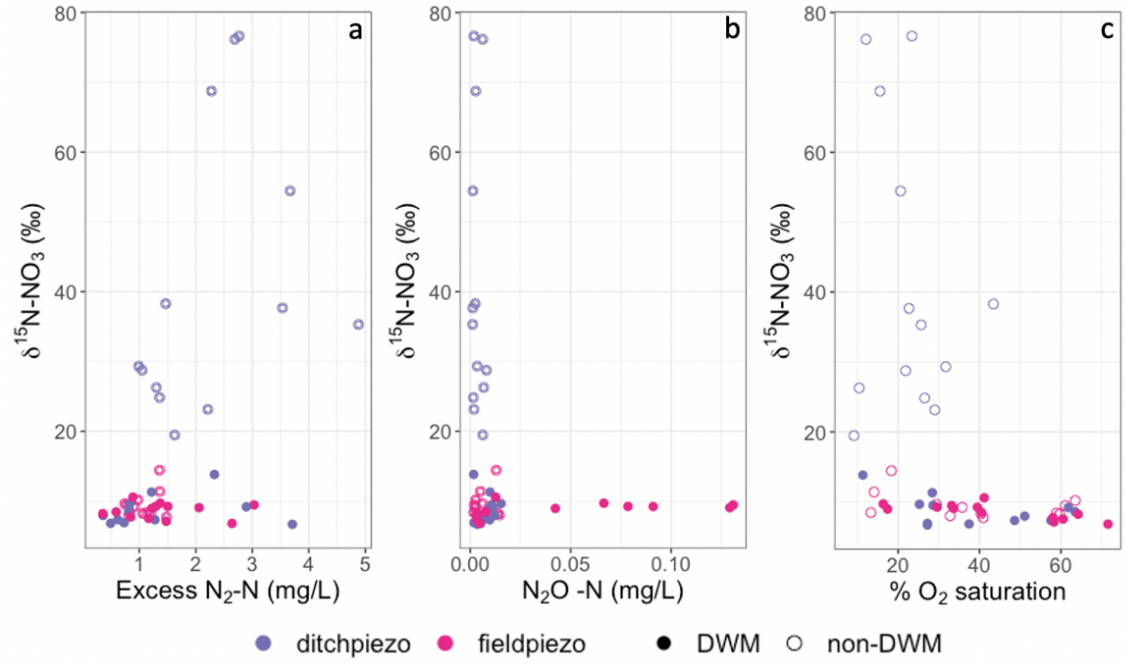

Figure 6. Relationship between $\delta^{15}N\text{-}NO_3^-$ and dissolved excess N_2-N (a), N_2O-N (b), and % O_2 saturation (c). Shape (solid fill versus unfilled) represents treatment and color represents location within the conceptual isotopic continuum shown in Figs. 1-3. The spread of data represents variation by sampling date and replicate (Figure S5)

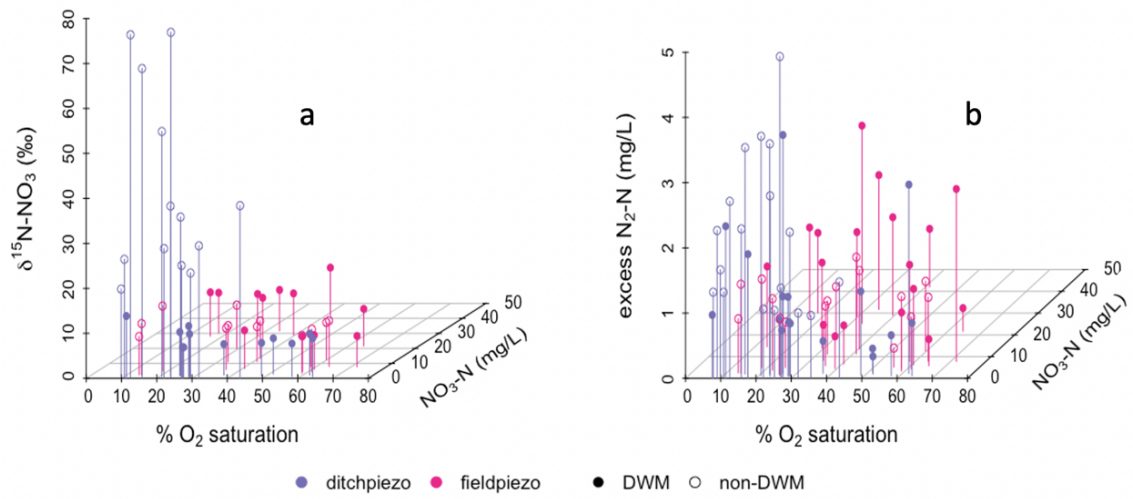

Figure 7. Relationships of $\delta^{15}N\text{-}NO_3^-$ (a) and excess N_2-N concentrations (b) with % O_2 saturation and NO_3^--N concentrations. Shape (solid fill versus unfilled) represents treatment and color represents location within the conceptual isotopic continuum shown in Figs. 1-3.

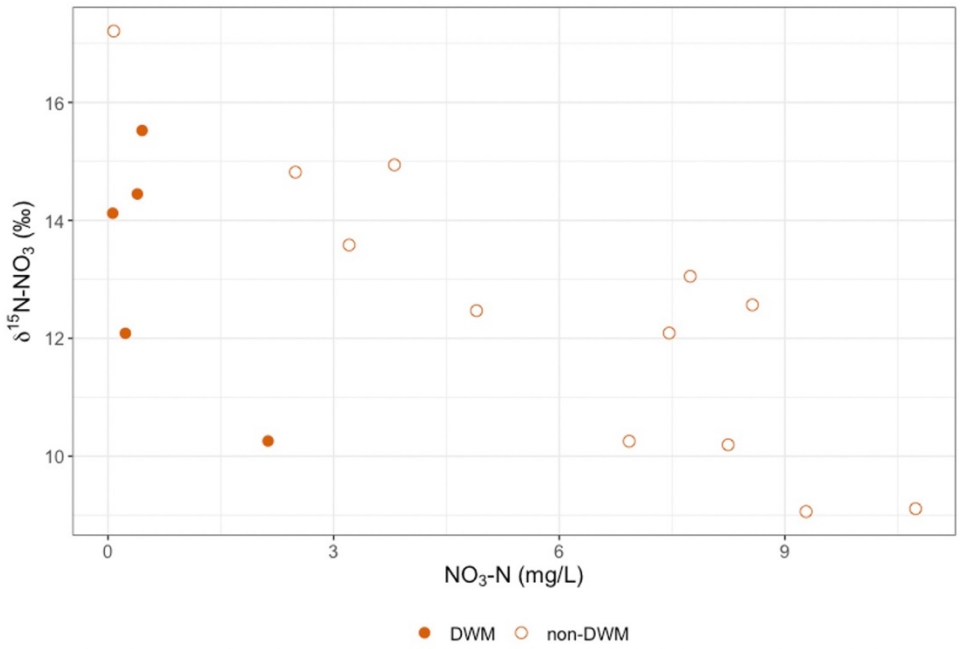

Figure 8. Relationship between NO_3^--N concentration and $\delta^{15}N\text{-}NO_3^-$ value for ditch discharge samples. Shape (solid fill versus unfilled) represents treatment and color represents spatial location in the isotopic continuum. The spread of data represents variation by sampling date and replicate (Figure S6).

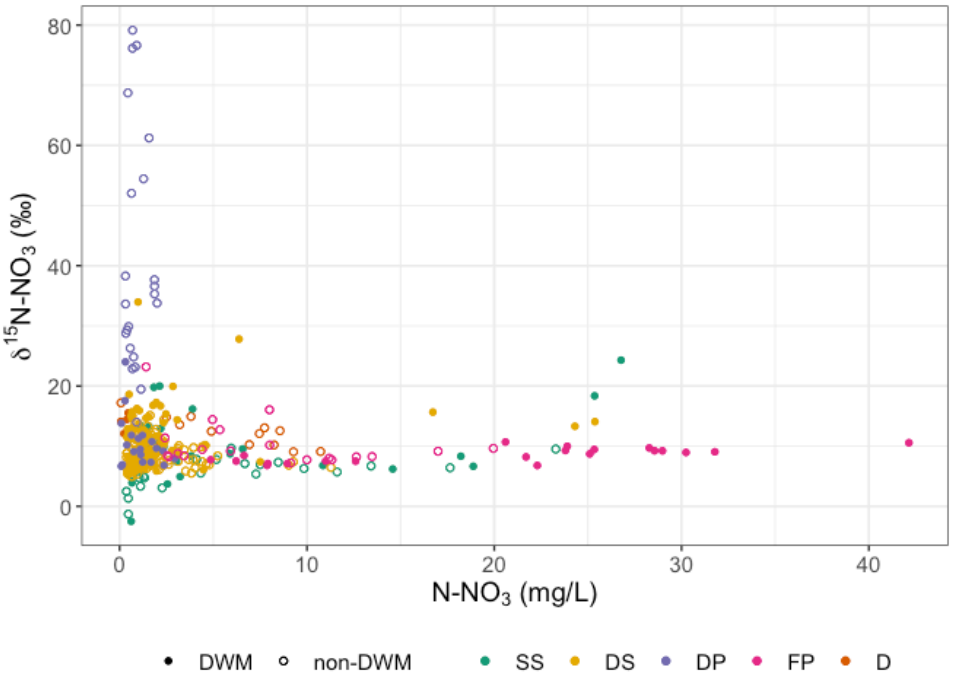

Figure 9. Figure showing the relationship between residual NO_3^--N concentration and $\delta^{15}N\text{-}NO_3^-$. Color represents location along conceptual isotopic continuum (SS = surface soil, DS= deep soil, DP= ditch piezometer, FP=field piezometer, D= ditch; same abbreviations as in Fig. 3). Shape (solid fill versus unfilled) represents treatment.

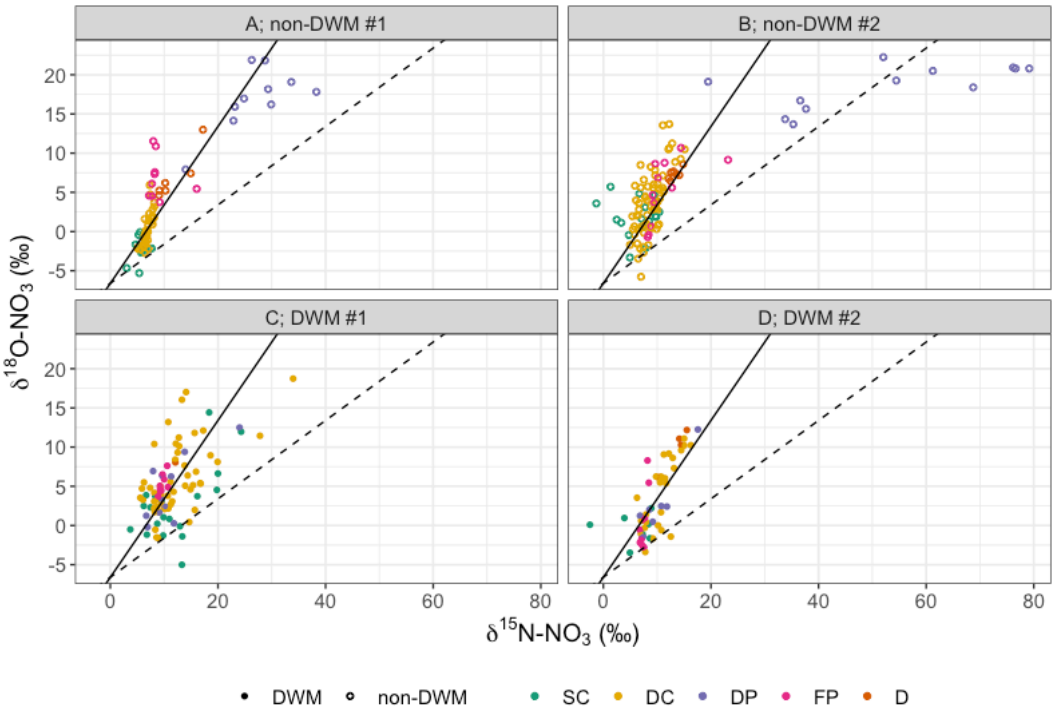

Figure 10. Relationship between $\delta^{18}O\text{-}NO_3^-$ and $\delta^{15}N\text{-}NO_3^-$ at different sampling sites along the conceptual isotopic continuum aggregated by treatment replicate. The lines, 1.0 slope (solid) and 0.5 slope (dashed), represent the bounds and range of denitrification signal assuming an origin $\delta^{15}N$ value of 0.0 ‰ from synthetic fertilizer and the lowest measured $\delta^{18}O\text{-}NO_3^-$ value. Color represents the location within the conceptual isotopic continuum (SS = surface soil, DS= deep soil, DP= ditch piezometer, FP=field piezometer, D= ditch; same abbreviations as in Fig. 3).

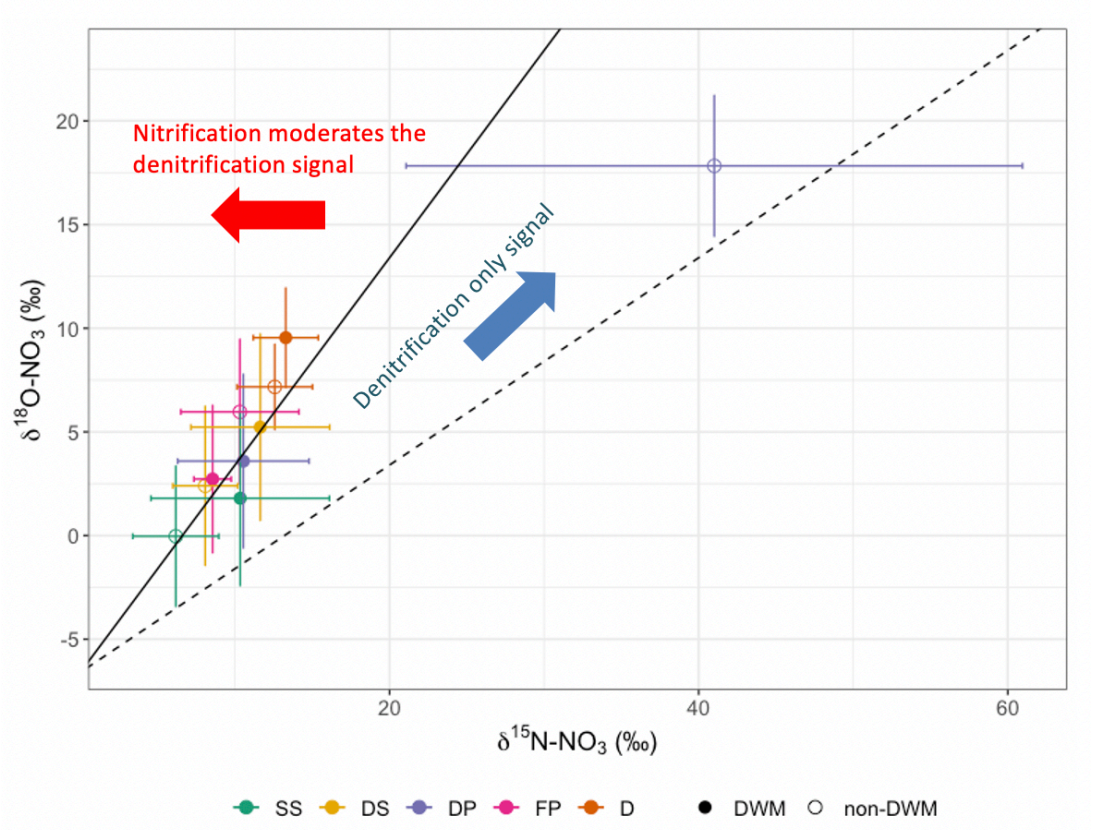

Figure 11. Relationship between $\delta^{18}O\text{-}NO_3^-$ and $\delta^{15}N\text{-}NO_3^-$ values (mean ± SD) aggregated by different sampling locations along the conceptual isotopic continuum (color) and treatment (shape). The lines, 1.0 (solid) and 0.5 (dotted) slope, represent the bounds and range of denitrification signal assuming an origin of $\delta^{15}N$ value of 0.0 ‰ from synthetic fertilizer and the lowest measured $\delta^{18}O\text{-}NO_3^-$. This figure is in the same format as the conceptual diagram in Figure 1.

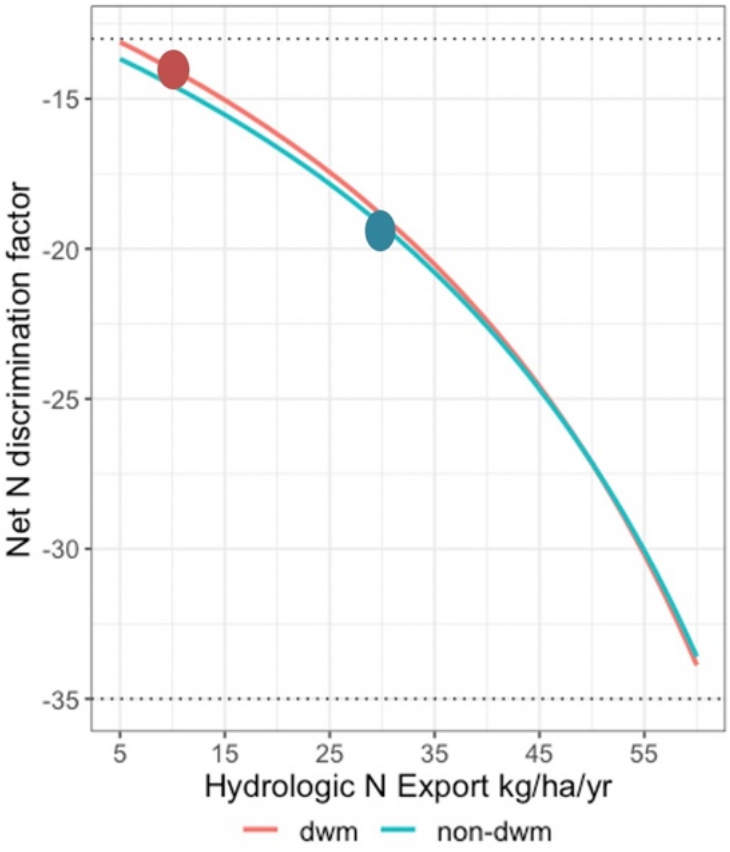

Figure 12. Sensitivity analysis results assessing how increases in hydrologic N export impacts the net N discrimination factor. Colored points correspond to calculated hydrologic N export values found in Table 2 for each treatment. Horizontal dotted lines represent the range of denitrification isotope discrimination factors reported in the literature.

.

3.8 Supplementary Figures

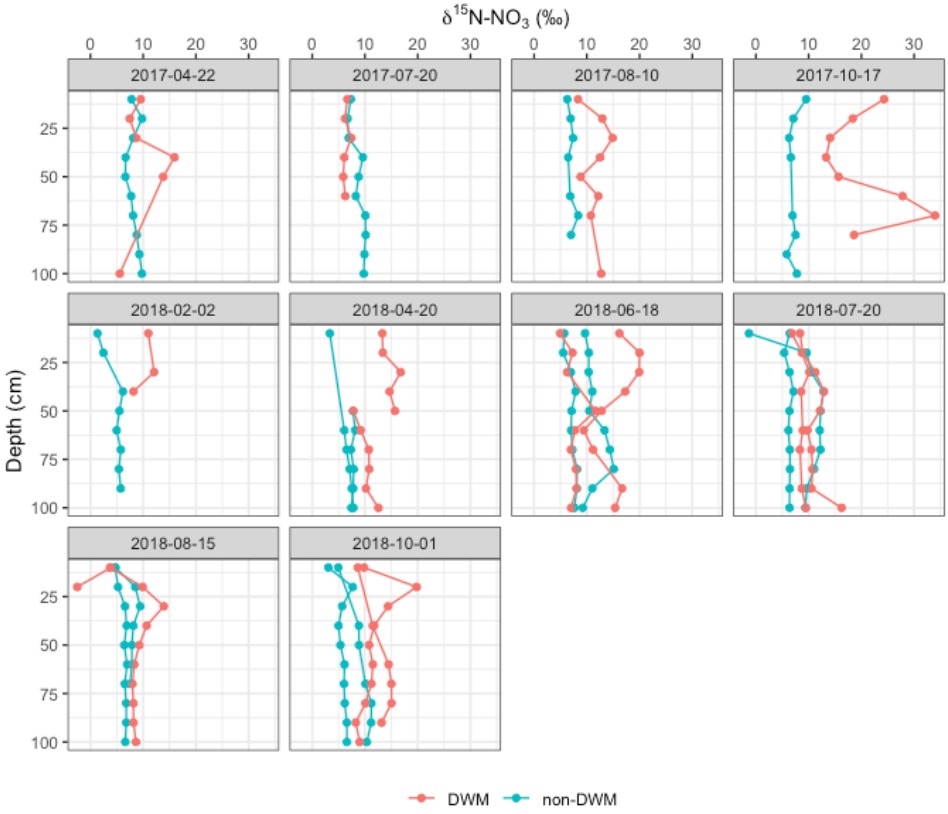

Figure S1. Relationship between soil profile KCL extraction $\delta^{15}N\text{-}NO_3^-$ value and depth. Aggregated by date and replicate; colored by treatment.

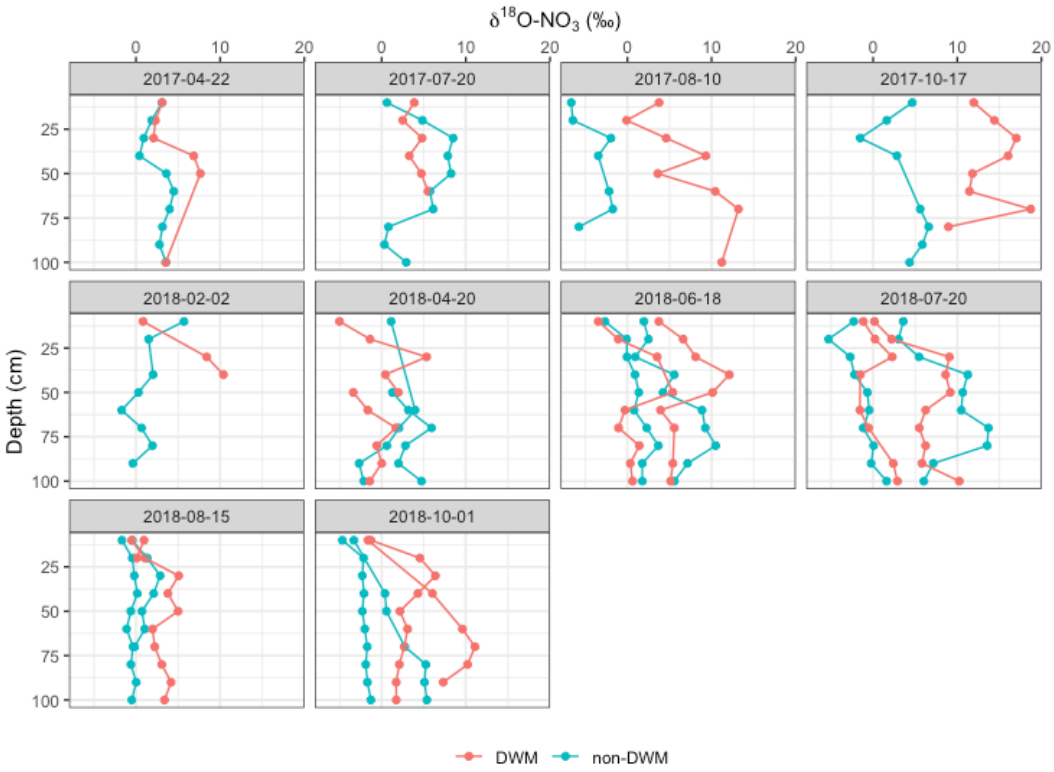

Figure S2. Relationship between soil profile KCL extraction $\delta^{18}O\text{-}NO_3^-$ value and depth. Aggregated by date and replicate; colored by treatment.

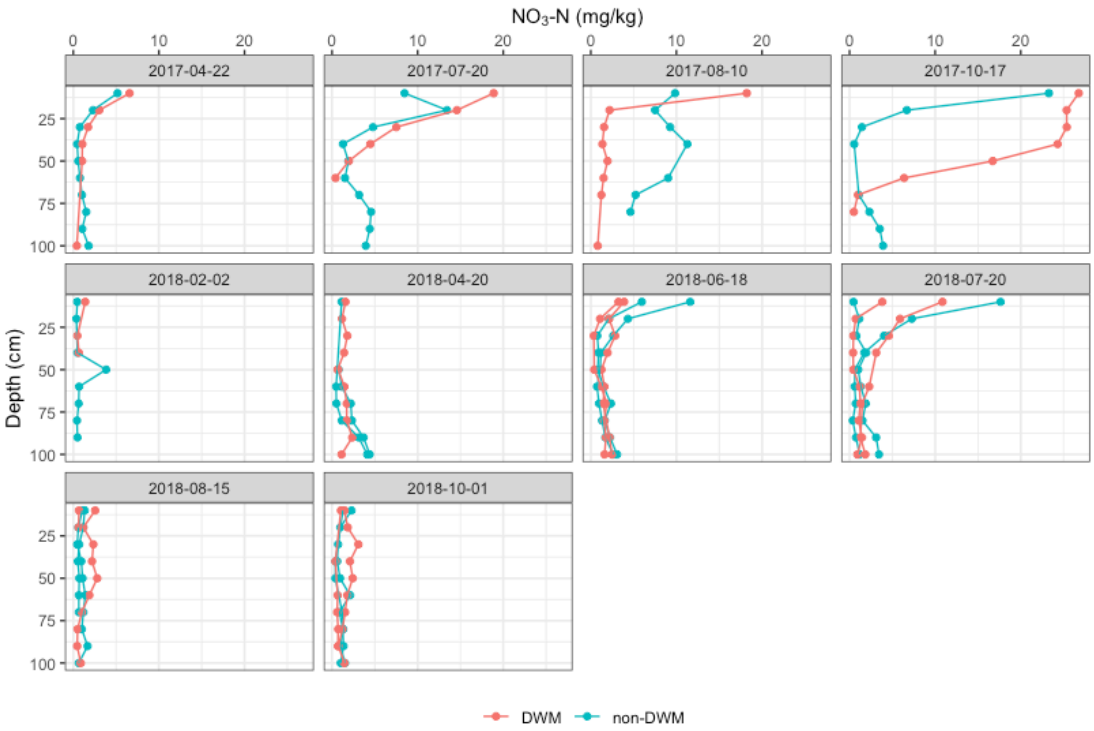

Figure S3. Relationship between soil profile KCL extraction NO_3-N (mg kg^{-1}) and depth. Aggregated by date and replicate; colored by treatment.

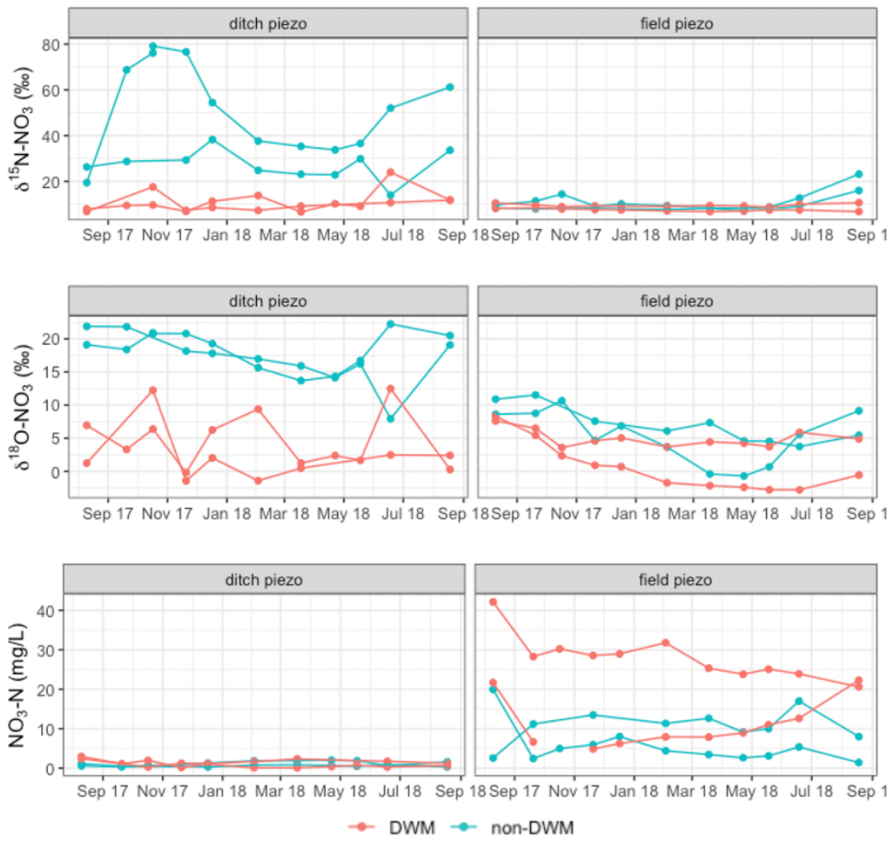

Figure S4. Temporal assessment of piezometer NO_3-N (mg L^{-1}), $\delta^{18}O$-NO_3^- value, and $\delta^{15}N$-NO_3^- value. Aggregated by piezometer location and replicate; colored by treatment.

Figure S5. Temporal assessment of piezometer % O_2 saturation, dissolved excess N_2-N (mg L^{-1}) and dissolved N_2O-N (mg L^{-1}). Aggregated by piezometer location and replicate; colored by treatment. A break in the lines represents a dry piezometer when no sample could be collected.

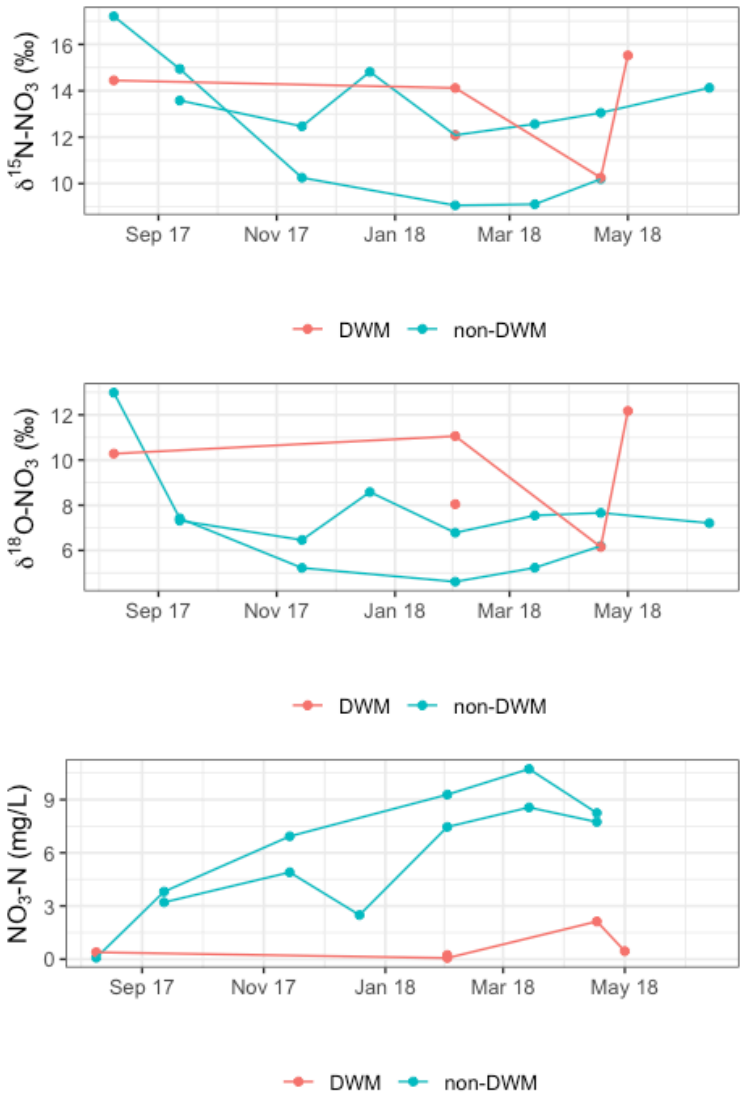

Figure S6. Temporal assessment of ditch water NO_3-N (mg L^{-1}), $\delta^{18}O$-NO_3^- value, and $\delta^{15}N$-NO_3^- value. Aggregated by replicate; colored by treatment.

Chapter 4: Assessment of Nitrogen Dynamics in an Agriculture Drainage Water Management System: A Synthesis of Budget Parameters

Chapter Note

This chapter serves as a synthesis chapter that incorporates data and findings from chapters 2 and 3 for the purposes of broadly evaluating N cycling dynamics within a field scale agricultural drainage water management system. Sections of this chapter will be combined with chapter 3 for submission of a manuscript to *Biogeochemistry* journal.

Abstract

Complete nitrogen (N) budgets in agroecosystems are important tools for assessing how N moves, transforms, and is impacted by farm management practices. Despite advancements in measurement techniques, complete N budgets remain elusive because of challenges in measuring gaseous N emissions, particularly the uncertainty surrounding the spatial and temporal heterogeneity, and the processes that control those emissions, such as denitrification. Within the context of a plant-soil system we synthesized a variety of N budget parameters to evaluate how the best management practice of drainage water management (DWM) impacted N fates and transformations. We supplemented isotopic N mass balance derived total gaseous N export values with groundwater dissolved N_2 and N_2O gas estimates, and soil N_2O flux measurements to explore the specific impacts of denitrification. While the mean

values suggested that DWM increased denitrification, the uncertainty of the gaseous N export components were often greater than the differences between treatments. However, the N mass balance revealed that gaseous N export was large and that soil N_2 export likely dominated. Most budget parameter magnitudes and ratios aligned with previous literature. This study was the first that examines an agricultural soil-plant system to estimate total gaseous N export and differentiate among fluxes of N_2 and N_2O via soil surface emissions and groundwater transport.

4.1 Introduction

In agroecosystems, nitrogen (N) is one of the most important nutrients for crop production, but intensive use of fertilizer-N, synthetic and organic, has led to severe environmental issues, including local water pollution and global climate change (Fowler et al., 2013, Zhang et al., 2021). To improve the efficacy of N application and general understanding of N cycling in agroecosystems, it is imperative to measure and monitor the fates of N. Nitrogen budgets are useful tools for understanding the magnitudes and movement of N in different ecosystems and can be used to identity and quantify missing N sources and sinks or assess the environmental impacts of N losses from a defined system (Zhang et al., 2020; Meisinger et al., 2008). However, accurately characterizing certain processes and pools of N has remained challenging (Groffman et al., 2006, Davidson et al., 2006)

One reason that constructing N budgets remains challenging is the quantification of gaseous N emissions. Under a variety of environmental conditions, multiple N cycling processes like denitrification, nitrification, and volatilization can produce gases, including dinitrogen (N_2), nitrous oxide (N_2O), nitric oxide (NO), and

ammonia (NH_3). Technology for plot scale measurements of N_2O, NO, and NH_3 has been developed and applied, but because of high ambient atmospheric N_2 concentration, N_2 is technologically difficult to measure from the soil surface (Fisher et al., 2019). This is unfortunate because N_2 is typically the most abundant gas produced by denitrification, a microbially driven process of nitrate (NO_3^-) reduction. This is why many denitrification and N_2 production estimates are calculated from N budgets by difference, which requires the propagation of error of all other N budget terms, leading to large uncertainty in the N_2 gas estimate, even though it can be a large fraction of total N export (Meisinger et al., 2008).

A complicating factor is that many of these processes that produce N gas emissions are spatially and temporally heterogeneous, being characterized as having hot spots and hot moments of emission (Groffman et al., 2009; McClain et al., 2003). This high variability requires careful consideration in sampling design to account for the spatial and temporal heterogeneity when measuring N gas emissions. Identifying key landscape locations more prone to gaseous N production and scaling those measurements to field, watershed, or regional areas often requires modeling approaches (Oehler et al., 2009; Boyer et al., 2006; David et al., 2009).

Another reason for the N budget challenge is that soil represents a large pool of N and a small fractional change to such a large pool could be important in a N mass balance, but small changes to large pools are difficult to quantify. This is important because most N budgets and mass balances require the assumption that the defined system is at steady state and that the internal cycling is at equilibrium (Van Meter et al., 2016). This assumption allows for mass balance of inputs and outputs to

determine sinks or sources of N flows and pools. Under this assumption, soil N content remains constant, even though it is understood that there are internal cycling processes like mineralization and immobilization that might not be at equilibrium, at least over certain time scales. However, measuring the total soil N stock with soil heterogeneity in both the vertical and horizontal directions, is burdensome on short time scales and likely results in sampling error greater than actual change of N stocks (Zhang et al., 2020)

For this research, the defined system for which a complete N budget was created was in a fertilized N plant-soil system at the field scale implemented with the best management practice (BMP) of drainage water management (DWM). The system has been in corn/soybean rotation since 2004 and DWM since 2006 and therefore may have reached a quasi-equilibrium resulting from a consistent, long-term cropping system. The purpose of DWM is to retain water in agriculture fields for a longer period by slowing water discharge at the outlet with the intent of inducing denitrification (Skaggs et al., 2012). Increased denitrification would consume more NO_3^-, thereby reducing dissolved NO_3^- export that can cause water pollution issues such as eutrophication and drinking water hazards (Fisher et al., 2010; Drury et al., 1996). However, increased denitrification could also increase gaseous emissions of N_2O and N_2, impacting the N budget. Increased production of the greenhouse gas N_2O would have implications for pollution swapping of dissolved NO_3^- reduction for an increase in greenhouse gas emissions.

The focus on undesired N export is common among N budgets. Most N budgets conducted in fertilized agricultural setting were designed for the purpose of

understanding the impact of fertilizer N inputs on hydrologic N export and denitrification rates because of the implications for environmental degradation from eutrophication (hydrologic NO_3^- export) and greenhouse gas production (N_2O from denitrification) (Allison et al., 1955; Anderson et al., 2014; Barry et al., 1993; David et al., 1997; Van Bremmen et al., 2002). Because of the concern of agricultural N_2O production, an abundance of studies have measured fertilized agriculture soil N_2O emissions to characterize the magnitudes, occurrence, and controls on those emissions, as done in chapter 2 (Hagedorn et al., 2022; Baggs et al., 2003; Parkin et al., 2006; Davidson et al., 1996; Fisher et al., 2018). While these N_2O measurements are commonly compared to total N fertilization rates and crop export rates (Eagle et al., 2020), they are not commonly conducted in conjunction with a complete N budget analysis that quantifies total denitrification. There have been no complete agricultural N budget analyses quantifying denitrification that also included the fractional breakdown of soil N_2 and N_2O emissions within that estimate. While this is lacking in agriculture context, it has been done in forested or grassland ecosystems (Enanga et al., 2017; Yanai et al., 2013). Although export of N_2O dissolved in groundwater entering agricultural drains has been recognized for several decades (Dowdell et al., 1979), few studies have included losses via biogenic N gases dissolved in drainage water in complete N budgets (Gardner et al., 2016; Gentry et al., 2009).

The primary objective of this chapter was to synthesize measurements and calculations from chapter 2 and chapter 3 into an N budget to estimate soil N_2 emissions within the DWM context. A secondary objective was to broadly evaluate the relationships between gaseous components of N export and their fit within the

agricultural N budget. Chapter 2 provided soil gas N_2O emission estimates while chapter 3 provided evidence for denitrification and N mass balance budget. This chapter combines the aforementioned pieces with annual estimates of dissolved N_2 and N_2O gas in groundwater entering agricultural ditches to constrain the gaseous N export components of the N budget.

4.2 Methods

4.2.1 Experimental Design

An experimental design with two replicates per treatment (DWM and non-DWM) was implemented. The site description, sampling regime, and analytical methodologies for measuring the major inputs and outputs to create the N budget parameters (fertilizer input, irrigation input, atmospheric deposition input, crop export, hydrologic export, and gaseous export) are described in detail in chapters 2 and 3. A brief summary of where and what measurements were taken is described below and associated with Figure 1.

Hydrology: V-notch weirs were placed at the end of the ditches to quantify hydrologic discharge. To assess shallow groundwater, two piezometers were installed in each plot. One piezometer, called ditch piezometer, was placed adjacent to the ditch and the other, a field piezometer, was placed about 20 meters inward, perpendicular to the ditch piezometer. At all these locations, water was sampled and measured for total dissolved nitrogen (TDN) and nitrate (NO_3^-) content. Dissolved N_2 and N_2O gas measurements were also obtained from the piezometers.

Soil: An 8 chamber transect was placed near the piezometer set, running perpendicular to the ditches, to measure N_2O soil gas emissions. Methodology was described in chapter 2.

Fertilizer, Crops and Irrigation: All three of these parameters were recorded and reported by the collaborating farmer. N content of the crop export and irrigation input was measured via methodology described in chapters 2 and 3.

4.2.2 Measured Constituents of Gaseous N Export

Since the objective of this chapter was to frame and explore the gaseous N export component of the N budget, the primary constituents described below were evaluated for the period of April 2017 to March 2018.

1. Total Gaseous N Export: The N budget summary (Table 1) contains various N inputs and N outputs assessed in an isotopic N mass balance for each treatment. The estimate for gaseous N export was obtained from the results of the N mass balance described in chapter 3. This gaseous N export value also incorporates residual error of the mass balance.

2. Soil N_2O Emissions: Annual estimates for soil N_2O gas emissions were quantified in chapter 2 from static soil chambers. Three different interpolation techniques were used to quantify annual estimates (Chapter 2, Table 3). The seasonally-based interpolation was selected and incorporated into this chapter's analysis because it best captured the impact of the post-fertilization increases in soil N_2O emissions. The values were 6.4 ± 1.1 N_2O-N kg ha^{-1} yr^{-1} for DWM and 4.3 ± 0.8 N_2O-N kg ha^{-1} yr^{-1} for non-DWM.

3. Dissolved N_2O and N_2: Dissolved excess N_2 and N_2O gas concentrations were taken at the ditch piezometers approximately monthly during the study period by the collaborating project team from Horn Point Laboratory. Dissolved N_2 concentrations and excess N_2 was measured and calculated according to the membrane inlet mass spectroscopy and N_2O by gas chromatography methods described in chapter 3. For annual estimates, it was assumed that the concentrations in the ditch piezometer represented the dissolved N gas concentrations entering the open ditches via groundwater. It was also assumed that the hydrologic discharge from groundwater into the ditch was the same volume as the hydrologic discharge from the v-notch weir. It is possible that more groundwater entered the ditch than discharged through the v-notch because of ditch evapotranspiration, which would likely result in a small underestimate of dissolved gas flux into the ditches. A mean value of the ditch piezometer gas concentrations (mg L^{-1}) observed throughout the year (Figure S1) was multiplied by the volume of water (L) discharged over the v-notch weir to obtain an estimate of the dissolved N_2O and excess N_2 mass exported from the field in groundwater. The masses were then converted to kg N ha^{-1} yr^{-1}, based on the drainage area of each ditch, which was determined by the Horn Point team using the Soil and Water Assessment Tool (SWAT) to delineate watershed boundaries using a digital elevation model and LiDAR data in ArcGIS.

4.2.3 Statistics

A Monte Carlo analysis was conducted to calculate the presumptive soil N_2-N emissions using equation 1, where the total gaseous N export term was derived from chapter 3 (Table 2 of chapter 3). Normal distributions were constructed from mean

values and standard deviations for each of the input variables and then randomly selected to solve for the output variable. This calculation was done 10,000 times to yield a distribution of values for the presumptive soil N_2-N emissions by treatment.

Equation 1. (Eq. 1)

$$\text{Presumptive Soil } N_2\text{-N Emissions} = \text{Total Gaseous N Export} - \text{dissolved } N_2 - \text{dissolved } N_2O - \text{soil } N_2O \text{ emissions}$$

4.3 Results

4.3.1 Dissolved N Gas Estimates

Among all individual dissolved gas concentrations at the ditch piezometer, regardless of treatment, excess N_2 concentrations were 29 to 2900 times larger than dissolved N_2O concentrations, with a median of 282 times larger. As a result, the annual estimates for the dissolved gases showed much higher excess N_2-N compared to N_2O-N (Table 2). There was variation by treatment replicate, with field B (non-DWM) having the highest annual excess N_2-N value. N_2O-N did not have as much variation among replicates.

4.3.2 Gaseous N Export Partitioning

The gaseous N export, dissolved N_2O-N and excess N_2-N gases, and soil N_2O gas emissions were aggregated by treatment (Table 4). The presumptive soil N_2-N emissions values were calculated by subtracting the dissolved groundwater excess

N_2-N, dissolved groundwater N_2O-N and soil N_2O emissions from the gaseous N export value (Eq. 1). The soil emissions N_2O-N/(N_2O-N + N_2-N) ratio was 0.07 for DWM and 0.06 for non-DWM. The groundwater dissolved N_2-N was 7% (DWM) and 18% (non-DWM) of total N_2-N emissions (groundwater dissolved + soil).

The input and output values for the DWM treatment from Table 1 and 3 are illustrated in Figure 2. The fertilizer N was the largest input, while the crop N was the largest output. The total gaseous N was the second largest output, dominated by soil N_2 emissions.

4.4 Discussion

4.4.1 Dissolved Gas Estimates

This study's estimates of dissolved N_2O-N (0.02 to 0.06 kg N_2O-N ha^{-1} yr^{-1}) agreed with literature values. Within agricultural systems, Parkin et al. (2016) found 0.04 to 0.07 kg N_2O-N ha^{-1} yr^{-1} while Davis et al. (2019) measured dissolved N_2O-N export to be (0.06 to 0.24 kg N ha^{-1} yr^{-1}). At the watershed scale, Gardner et al. (2016) found dissolved N_2O-N export to be 0.085 kg N ha^{-1} yr^{-1}. In disturbed forested systems, Davidson and Swank (1990) found that at maximum the N_2O-N export was 0.056 kg ha^{-1} yr^{-1}.

Only one other study was found that measured annual dissolved excess N_2 in groundwater in an agricultural watershed; it was conducted in the Choptank Basin on the Eastern Shore, near the present study area (Gardner et al., 2016). It estimated dissolved excess N_2 export from groundwater to be 8.3 kg N ha^{-1} yr^{-1} which is

intermediate between the 6.3 kg N ha^{-1} yr^{-1} (DWM) and 13.9 kg N ha^{-1} yr^{-1} (non-DWM) estimated in this study.

4.4.2 Denitrification and Total Gaseous N Export

This study estimated total gaseous N export, which is largely comprised of N_2 and N_2O that was either dissolved in groundwater or emitted from soil. N_2O can be produced by both nitrification and denitrification but this study was not designed to measure the difference between nitrification and denitrification sources of N_2O emissions measured at the soil surface. A tracer experiment by Panek et al. (2000) found that, depending upon soil moisture content, nitrification N_2O emissions could be equal to denitrification N_2O emissions. Morse et al. (2013) also found that nitrification N_2O could equal or exceed denitrification N_2O, even in drained agricultural systems. If this finding were applied in this study, the nitrification-derived soil N_2O emissions would be 3.2/2.2 (DWM/non-DWM) kg N ha^{-1} yr^{-1}. Because this represents only a small fraction of total gaseous N export (97.5/78.3 kg ha^{-1} yr^{-1}) and because the presumptive soil N_2-N emissions dominate (84.6/60.0 kg ha^{-1} yr^{-1}), which nitrification does not impact, it was assumed that the calculated total gaseous N export was the upper limit of the denitrification rate in this system.

Making an assumption that nearly all gaseous N export was a product of denitrification (whether dissolved in groundwater or emitted from soils), the upper limit of the denitrification rate would be (DWM/non-DWM) 97/78 kg N ha^{-1} yr^{-1}, or 42%/34% of the N inputs (225 kg N ha^{-1} yr^{-1}, Table 1). This upper limit denitrification value is elevated compared to other studies which found denitrification to be 38 to 65 kg N ha^{-1} yr^{-1} (Duncan et al., 2013), 27 kg N ha^{-1} yr^{-1} (Gentry et al.,

2009), 26 kg N ha^{-1} yr^{-1} (Sigler et al., 2022), and 15 to 20 kg N ha^{-1} yr^{-1} (Billen et al., 2021). A metanalysis of global agriculture soils indicated that poorly drained upland crop systems with similar N fertilization rates have between 30-75 kg N ha^{-1} yr^{-1} of denitrification, depending on the measurement method (Hofstra et al., 2005). Although the present denitrification estimate is higher than these reported values, the calculated denitrification percentage as a fraction of the total N inputs from fertilizer, atmospheric deposition, and irrigation (42%/34%) aligns with the similar percentages reported in other studies: ~40% (Boyer et al., 2006), 34% (Van Breemen et al., 2002), 16-27% (Duncan et al., 2013), 25-61% (Jahangir et al., 2012) and ~50% (Torber et al., 1992). The N fertilization rate in the present study was over 200 kg N ha^{-1} yr^{-1}, which explains how a similar percentage of inputs lost via denitrification results in a large value of gaseous N export.

4.4.3 Denitrification N_2 and N_2O Fractions

The gaseous N export value or upper limit of denitrification serves as a starting point for assessing the measured gaseous N components at this site. Subtracting the other measured N gas estimates (dissolved excess N_2 and N_2O, and soil N_2O emissions) from the total gaseous N export value results in 84.6/60.0 kg N ha^{-1} yr^{-1} (DWM/non-DWM) of unaccounted-for N within the N budget. If this unaccounted-for N represents the N_2 gas emissions from the soil surface, then N_2 efflux from the soil surface would account for 35%/27% of the N inputs. This result aligns with Zistl-Schlingmann et al. (2019), who found that measured N_2 emissions in soil cores were 31-42% of N inputs. This soil N_2 fraction was compared with the measured soil N_2O fraction for a $N_2O/(N_2O+N_2)$ ratio of 0.07 (DWM) and 0.06 (non-

DWM), falling on the low end of the range of common literature values between 0.04 and 0.28 (Butterbach-Bahl et al., 2013; Billen et al., 2021), and below the range Schlesinger (2009) found for fertilized agriculture systems (0.16 ± 0.07). The below average $N_2O/(N_2O+N_2)$ ratio calculated in the present study may reflect that the study site was naturally a wetland and still has groundwater relatively close to the surface, which would promote more complete denitrification to N_2.

4.4.4 Limitations of Presumptive Soil N_2-N Export Estimate

While the aforementioned discussion sections assumed that all gaseous N export was a product of denitrification and that all unaccounted-for gaseous N export was presumed to be soil surface N_2 gas emissions, other N transformation processes and N gas species need to be considered. For example, while N_2O and N_2 gaseous fractions usually dominate emissions from denitrification, NH_3 or NO are also N gases that can also contribute to total gaseous N export. Therefore, the presumed soil N_2-N value could be an overestimate, including and masking over some unmeasured fractions of gaseous N production.

Because the average soil pH at this site was 6.12, we speculate that NH_3 emissions were a minimal part of the total gaseous N export because acidic soils minimize volatilization compared to high pH conditions (Nelson et al., 1982). For NO, because of the site's mesic climate, the emissions are likely to be lower than the measured N_2O soil emissions (Davidson and Verchot, 2000).

Another potential explanation for some of the presumed soil N_2-N export are N export processes that are not associated with gas production, such as N leaching via deeper groundwater seepage or underflow. This study assumed that all hydrologic N

export was measured by the discharge at the weir, but there could have been seepage around the DCS or underflow at the end of the ditches. This was explored in the sensitivity analysis (chapter 3) which examined how changes of hydrologic N export could impact the net N discrimination factor. There was a limit to how much hydrologic N export could increase (~ 60 kg ha^{-1} yr^{-1}), and subsequently gaseous N export decrease, before the net N isotopic discrimination factor was unrealistically out of range of literature values.

Finally, another potential explanation for unaccounted-for N is an increase in soil N storage. The original mass balance technique (chapter 3) assumed that the soil N pool was at steady where all internal N cycling processes were in equilibrium. While the soil N status might not be at steady state in any given year, this research site has most likely approached a long-term equilibrium as the farm management regime (crop rotation and fertilization rates) has been the same since 2004.

4.5 Conclusion

At the agricultural field scale, this study is the first to combine multiple gaseous N export measurements, particularly incorporating dissolved biogenic N gas production, into a N budget to help account for the "missing N" commonly associated with N mass balances. Common measures of N export, such as total denitrification as a fraction of total N inputs and $N_2O/(N_2O+N_2)$, fell within or near the ranges reported in previous literature from a variety of ecosystems. Within the context of DWM, the gaseous production and denitrification estimates suggest a potential increase in denitrification in the DWM treatment, but uncertainties of estimates were too large to conclude definitively that DWM increased denitrification and gas production. For soil

N_2 and total gaseous N export, the difference between treatments was less than the uncertainty of the estimate itself. In both DWM and non-DWM treatments, mass balance and isotopic analyses indicated that gaseous export was large and likely dominated by N_2. Based on measurements of excess N_2 dissolved in piezometers near the drainage ditches, about 7-18% of the estimated N_2 production was likely exported hydrologically, with the remainder emitted from the soil surface. Although uncertainties exist for each measured and calculated budget term, this mass balance puts each into perspective quantitatively. Multiple constraints and comparisons with existing literature provide corroboration that the calculated N_2 emissions from the cropland soil surface must be a quantitatively important component of the annual N budget of this agricultural system, following N exported in the crop harvest as the second largest output budget term.

4.6 Tables

Table 1. Obtained from chapter 3, table 2. The inputs and outputs were measured or approximated to derive a gaseous N export value.
.

	DWM		Non-DWM		Type of Data
Variable	Mass (kg ha^{-1})	$\delta^{15}N$ (‰)	Mass (kg ha^{-1})	$\delta^{15}N$ (‰)	
Fertilizer N Input	213 ± 21.0	0.0 ± 2.0	213 ± 21.0	0.0 ± 2.0	Measured
Atmospheric N Input	8.2 ± 1.3	0.0 ± 2.0	8.2 ± 1.3	0.0 ± 2.0	Literature values
Irrigation N Input	4.2 ± 0.5	7.5 ± 0.2	4.2 ± 0.5	7.5 ± 0.2	Measured
Hydrologic N Export	10.2 ± 3.4	13.3 ± 2.1	29.1 ± 1.2	12.6 ± 2.4	Measured
Crop N Export	118 ± 12	3.7 ± 0.4	118 ± 12	3.7 ± 0.4	Measured
Gaseous N Export	97.5 ± 23.8	-6.0 ± 5.0	78.3 ± 24.1	-10.2 ± 6.3	Calculated via equation #2 & #3

Table 2. Summary of dissolved N gas annual estimates (mean ± SD) by field. A/B are non-DWM treatment and C/D are DWM treatment. The SD represents the variation in dissolved gas concentration from multiple sampling dates.

kg ha^{-1} yr^{-1}	Groundwater delivered Dissolved Gas Load	
Field	N_2-N	N_2O-N
A	8.4 ± 5.0	0.02 ± 0.01
B	19.4 ± 6.5	0.05 ± 0.05
C	8.9 ± 4.3	0.06 ± 0.04
D	3.7 ± 1.7	0.04 ± 0.01

Table 3. Summary table of gaseous N export, dissolved gases, and soil N_2O emissions with Monte Carlo analysis for presumptive soil N_2-N emissions.

Component (kg ha^{-1} yr^{-1})	DWM	Non-DWM	Derivation	Location
Total Gaseous N Export	97.5 ± 23.8	78.3 ± 24.1	Mass N Balance	Chap 3
Excess N_2-N export dissolved in groundwater	6.3 ± 3.7	13.9 ± 7.8	Dissolved gas data and extrapolation	Chap 4
N_2O-N export dissolved in groundwater	0.05 ± 0.01	0.04 ± 0.02	Dissolved gas data and extrapolation	Chap 4
Soil N_2O-N emissions	6.4 ± 1.1	4.3 ± 0.8	Soil chambers and extrapolation	Chap 2
Presumptive soil N_2-N emissions	84.6 ± 24.1	60.0 ± 25.2	By difference, Equation 1	Chap 4

4.7 Figures

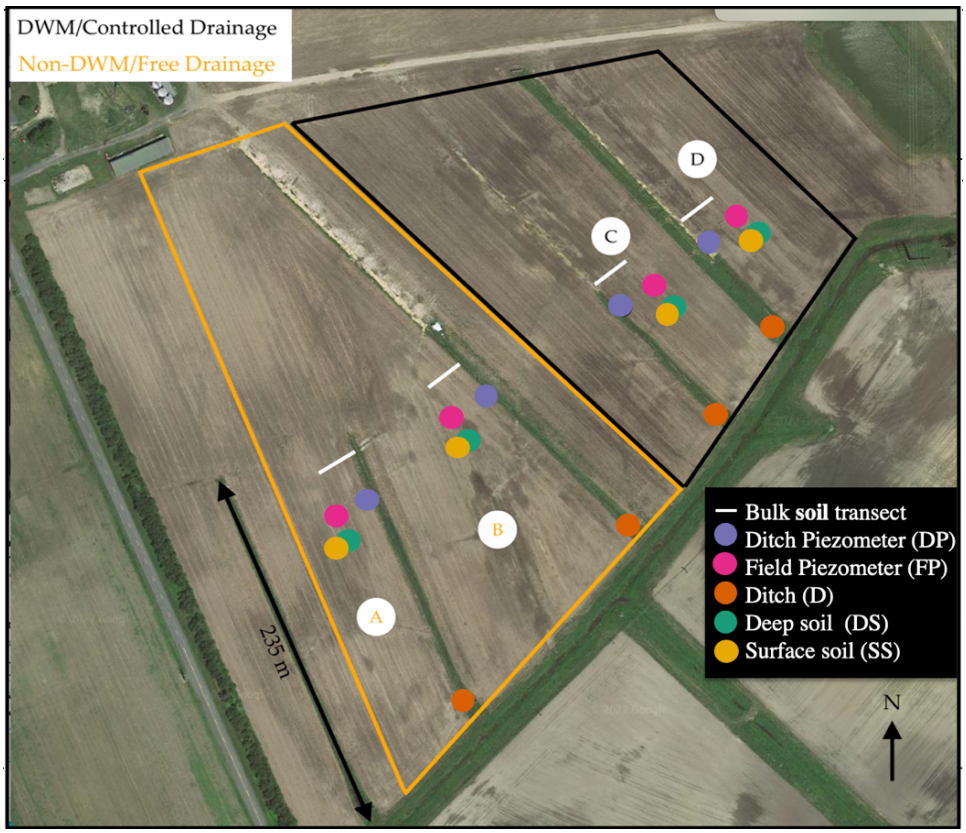

Figure 1. Aerial view of research site indicating treatment plots and approximate locations of sampling sites. Aerial image was taken during an early planting cropping period.

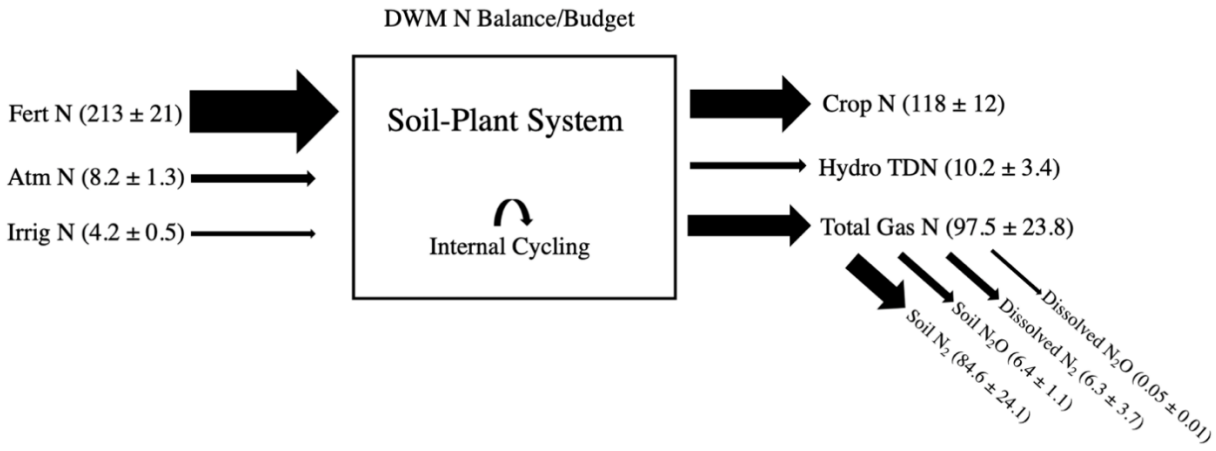

Figure 2. Summary N budget graphic detailing measured inputs and outputs of the soil-plant system in the Drainage Water Management treatment from Tables 1 and 3. The thickness of the arrow is proportional to the magnitude of the inputs and outputs.

4.8 Supplementary Figures

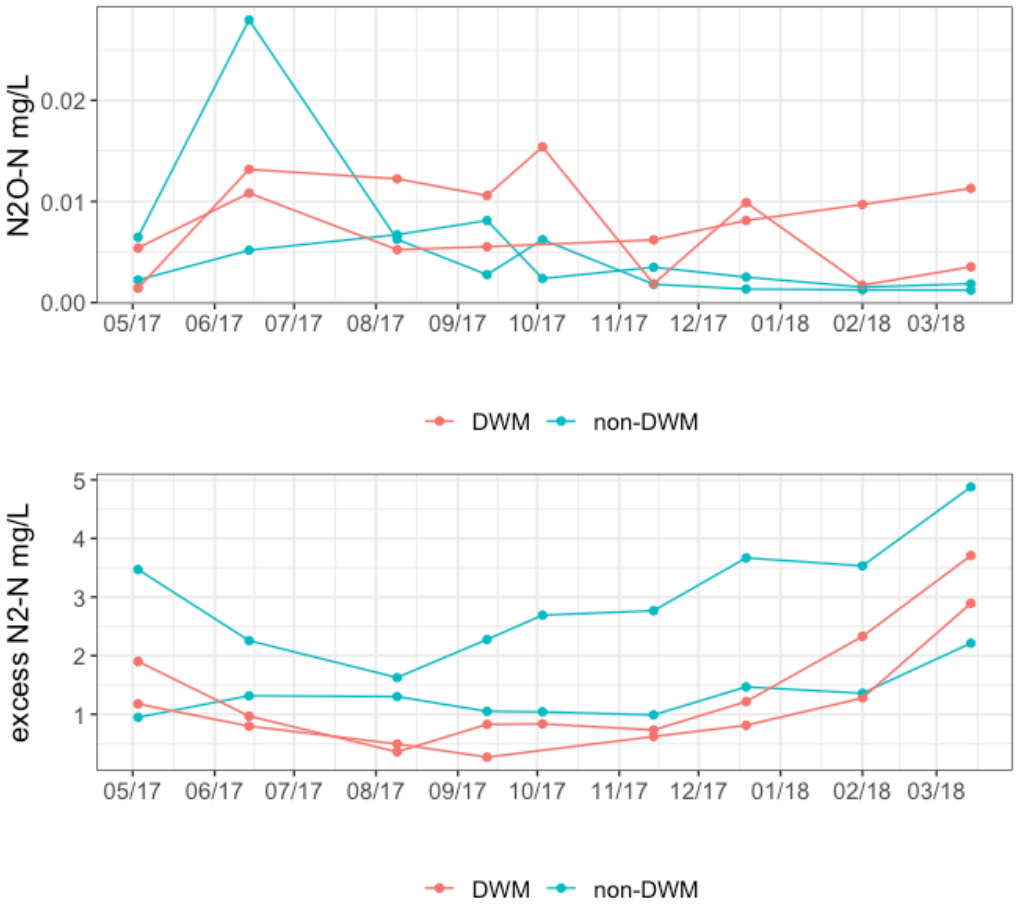

Figure S1. Temporal variation in ditch piezometer dissolved N_2O-N (top panel) and N_2-N (bottom panel) from April 2017 to March 2018. Grouped by replicate field and colored by treatment.

Bibliography

Allison, F. E. (1955). The enigma of soil nitrogen balance sheets. Advances in agronomy, 7, 213-250.

Amundson, R. G., & Davidson, E. A. (1990). Carbon dioxide and nitrogenous gases in the soil atmosphere. *Journal of Geochemical Exploration*, *38*(1-2), 13-41.

Anderson, T. R., Goodale, C. L., Groffman, P. M., & Walter, M. T. (2014). Assessing denitrification from seasonally saturated soils in an agricultural landscape: A farm-scale mass-balance approach. *Agriculture, ecosystems & environment*, *189*, 60-69.

Ator, S. W., & Denver, J. M. (2015). Understanding the nutrients in the Chesapeake Bay watershed and implications for management and restoration: The eastern shore.

Baggs, E.M.; Stevenson, M.; Pihlatie, M.; Regar, A.; Cook, H.; Cadisch, G. Nitrous oxide emissions following application of residues and fertiliser under zero and conventional tillage. *Plant Soil* 2003, *254*, 361–370.

Bai, E., Houlton, B. Z., & Wang, Y. P. (2012). Isotopic identification of nitrogen hotspots across natural terrestrial ecosystems. Biogeosciences, 9(8), 3287-3304.

Barford, C. C., Montoya, J. P., Altabet, M. A., & Mitchell, R. (1999). Steady-state nitrogen isotope effects of N2 and N2O production in Paracoccus denitrificans. *Applied and Environmental Microbiology*, *65*(3), 989-994.

Barry, D. A. J., Dave Goorahoo, and Michael J. Goss. Estimation of nitrate concentrations in groundwater using a whole farm nitrogen budget. Vol. 22. No. 4. American Society of Agronomy, Crop Science Society of America, and Soil Science Society of America, 1993.

Basso, B.; Shuai, G.; Zhang, J.; Robertson, G.P. Yield stability analysis reveals sources of large-scale nitrogen loss from the US Midwest *Sci. Rep.* 2019, *9*, 1–9.

Bateman, E.J.; Baggs, E.M. Contributions of nitrification and denitrification to N2O emissions from soils at different water-filled pore space. *Biol. Fertil. Soils* 2005, *41*, 379–388.

Bernhardt, E. S., Blaszczak, J. R., Ficken, C. D., Fork, M. L., Kaiser, K. E., & Seybold, E. C. (2017). Control points in ecosystems: moving beyond the hot spot hot moment concept. Ecosystems, 20(4), 665-682.

Billen, G., & Garnier, J. (2021). Nitrogen biogeochemistry of water-agro-food systems: the example of the Seine land-to-sea continuum. *Biogeochemistry*, *154*(2), 307-321.

Böhlke, J. K., & Denver, J. M. (1995). Combined use of groundwater dating, chemical, and isotopic analyses to resolve the history and fate of nitrate contamination in two agricultural watersheds, Atlantic coastal plain, Maryland. *Water Resources Research*, *31*(9), 2319-2339.

Böhlke, J. K., Mroczkowski, S. J., & Coplen, T. B. (2003). Oxygen isotopes in nitrate: New reference materials for 18O: 17O: 16O measurements and observations on nitrate-water equilibration. *Rapid Communications in Mass Spectrometry*, *17*(16), 1835-1846.

Bolker, B.M.; Brooks, M.E.; Clark, C.J.; Geange, S.W.; Poulsen, J.R.; Stevens, M.H.H.; White, J.-S.S. Generalized linear mixed models: A practical guide for ecology and evolution. *Trends Ecol. Evol.* 2009, *24*, 127–135.

Boyer, E. W., Alexander, R. B., Parton, W. J., Li, C., Butterbach-Bahl, K., Donner, S. D., ... & Grosso, S. J. D. (2006). Modeling denitrification in terrestrial and aquatic ecosystems at regional scales. *Ecological Applications*, *16*(6), 2123-2142.

Bremner, J.M.; Breitenbeck, G.A.; Blackmer, A.M. Effect of nitrapyrin on emission of nitrous oxide from soil fertilized with anhydrous ammonia. *Geophys. Res. Lett.* 1981, *8*, 353–356.

Brevik, E. C. (2012). Soils and climate change: gas fluxes and soil processes. *Soil Horizons*, *53*(4), 12-23.

Burns, D. A., Boyer, E. W., Elliott, E. M., & Kendall, C. (2009). Sources and transformations of nitrate from streams draining varying land uses: evidence from dual isotope analysis. *Journal of environmental quality*, *38*(3), 1149-1159.

Butterbach-Bahl, K., Baggs, E. M., Dannenmann, M., Kiese, R., & Zechmeister-Boltenstern, S. (2013). Nitrous oxide emissions from soils: how well do we understand the processes and their controls?. *Philosophical Transactions of the Royal Society B: Biological Sciences*, *368*(1621), 20130122.

Carstensen, M.V.; Hashemi, F.; Hoffmann, C.C.; Zak, D.; Audet, J.; Kronvang, B. Efficiency of mitigation measures targeting nutrient losses from agricultural drainage systems: A review. *Ambio* 2020, *49*, 1820–1837.

Carstensen, M. V., Poulsen, J. R., Ovesen, N. B., Børgesen, C. D., Hvid, S. K., & Kronvang, B. (2016). Can controlled drainage control agricultural nutrient emissions? Evidence from a BACI experiment combined with a dual isotope approach. *Hydrology and Earth System Sciences Discussions*, 1-17.

Carstensen, M. V., Børgesen, C. D., Ovesen, N. B., Poulsen, J. R., Hvid, S. K., & Kronvang, B. (2019). Controlled drainage as a targeted mitigation measure for nitrogen and phosphorus. *Journal of environmental quality*, *48*(3), 677-685.

Casciotti, K. L., Sigman, D. M., Hastings, M. G., Böhlke, J. K., & Hilkert, A. (2002). Measurement of the oxygen isotopic composition of nitrate in seawater and freshwater using the denitrifier method. *Analytical chemistry*, *74*(19), 4905-4912.

Casciotti, K. L., Sigman, D. M., & Ward, B. B. (2003). Linking diversity and stable isotope fractionation in ammonia-oxidizing bacteria. *Geomicrobiology Journal*, *20*(4), 335-353.

Castellano, M. J., Schmidt, J. P., Kaye, J. P., Walker, C., Graham, C. B., Lin, H., & Dell, C. J. (2010). Hydrological and biogeochemical controls on the timing and magnitude of nitrous oxide flux across an agricultural landscape. Global Change Biology, 16(10), 2711-2720.

Chapin, F. S., Matson, P. A., Mooney, H. A., & Vitousek, P. M. (2002). Principles of terrestrial ecosystem ecology.

Christiansen, J.R.; Outhwaite, J.; Smukler, S.M. Comparison of CO_2, CH_4 and N_2O soil-atmosphere exchange measured in static chambers with cavity ring-down spectroscopy and gas chromatography. *Agric. For. Meteorol.* 2015, *211*, 48–57.

Clague, J. C., Roland Stenger, and U. Morgenstern. "The influence of unsaturated zone drainage status on denitrification and the redox succession in shallow groundwater." *Science of the Total Environment* 660 (2019): 1232-1244.

Colt, J. 1984. Computation of dissolved gas concentrations in water as functions of temperature, salinity, and pressure. Bethesda, MD: American Fisheries Society.

Conant, R.T.; Berdanier, A.B.; Grace, P.R. Patterns and trends in nitrogen use and nitrogen recovery efficiency in world agriculture. *Glob. Biogeochem. Cycles* 2013, *27*, 558–566.

Courtois, E.A.; Stahl, C.; Burban, B.; Van den Berge, J.; Berveiller, D.; Bréchet, L.; Soong, J.L.; Arriga, N.; Peñuelas, J.; Janssens, I.A. Automatic high-frequency measurements of full soil greenhouse gas fluxes in a tropical forest. *Biogeosciences* 2019, *16*, 785–796.

Cowan, N., Maire, J., Krol, D., Cloy, J. M., Hargreaves, P., Murphy, R., ... & Drewer, J. (2021). Agricultural soils: A sink or source of methane across the British Isles?. *European Journal of Soil Science*, *72*(4), 1842-1862.

Craine, J. M., Brookshire, E. N. J., Cramer, M. D., Hasselquist, N. J., Koba, K., Marin-Spiotta, E., & Wang, L. (2015). Ecological interpretations of nitrogen isotope ratios of terrestrial plants and soils. Plant and Soil, 396(1), 1-26.

Crézé, C.M.; Madramootoo, C.A. Water table management and fertilizer application impacts on CO_2, N_2O and CH_4 fluxes in a corn agro-ecosystem. *Sci. Rep.* 2019, *9*, 1–13.

Datta, A.; Smith, P.; Lal, R. Effects of long-term tillage and drainage treatments on greenhouse gas fluxes from a corn field during the fallow period. *Agric. Ecosyst. Environ.* 2013, *171*, 112–123.

David, M. B., & Gentry, L. E. (2000). Anthropogenic inputs of nitrogen and phosphorus and riverine export for Illinois, USA. Journal of Environmental Quality, 29(2), 494-508.

David, M. B., Drinkwater, L. E., & McIsaac, G. F. (2010). Sources of nitrate yields in the Mississippi River Basin. Journal of environmental quality, 39(5), 1657-1667.

David, M. B., McIsaac, G. F., Royer, T. V., Darmody, R. G., & Gentry, L. E. (2001). Estimated historical and current nitrogen balances for Illinois. TheScientificWorldJOURNAL, 1, 597-604.

David, M. B., Del Grosso, S. J., Hu, X., Marshall, E. P., McIsaac, G. F., Parton, W. J., ... & Youssef, M. A. (2009). Modeling denitrification in a tile-drained, corn and soybean agroecosystem of Illinois, USA. *Biogeochemistry*, *93*(1), 7-30.

David, Mark B., et al. Nitrogen balance in and export from an agricultural watershed. Vol. 26. No. 4. American Society of Agronomy, Crop Science Society of America, and Soil Science Society of America, 1997.

Davidson, E. A., & Seitzinger, S. (2006). The enigma of progress in denitrification research. Ecological Applications, 16(6), 2057-2063.

Davidson, E. A., & Swank, W. T. (1990). Nitrous oxide dissolved in soil solution: an insignificant pathway of nitrogen loss from a southeastern hardwood forest. Water resources research, 26(7), 1687-1690.

Davidson, E. A., & Verchot, L. V. (2000). Testing the hole-in-the-pipe model of nitric and nitrous oxide emissions from soils using the TRAGNET database. Global Biogeochemical Cycles, 14(4), 1035-1043.

Davidson, E. A., Hart, S. C., Shanks, C. A., & Firestone, M. K. (1991). Measuring gross nitrogen mineralization, and nitrification by 15 N isotopic pool dilution in intact soil cores. *Journal of Soil Science*, *42*(3), 335-349.

Davidson, E. A., Matson, P. A., & Brooks, P. D. (1996). Nitrous oxide emission controls and inorganic nitrogen dynamics in fertilized tropical agricultural soils. *Soil Science Society of America Journal*, *60*(4), 1145-1152.

Davidson, E. A., Keller, M., Erickson, H. E., Verchot, L. V., & Veldkamp, E. (2000). Testing a conceptual model of soil emissions of nitrous and nitric oxides: using two

functions based on soil nitrogen availability and soil water content, the hole-in-the-pipe model characterizes a large fraction of the observed variation of nitric oxide and nitrous oxide emissions from soils. *Bioscience*, *50*(8), 667-680.

Denk, T. R., Mohn, J., Decock, C., Lewicka-Szczebak, D., Harris, E., Butterbach-Bahl, K., ... & Wolf, B. (2017). The nitrogen cycle: A review of isotope effects and isotope modeling approaches. *Soil Biology and Biochemistry*, *105*, 121-137.

Dobbie, K.E.; McTaggart, I.P.; Smith, K.A. Nitrous oxide emissions from intensive agricultural systems: Variations between crops and seasons, key driving variables, and mean emission factors. *J. Geophys. Res. Atmos.* 1999, *104*, 26891–26899.

Drury, C. F., Tan, C. S., Gaynor, J. D., Oloya, T. O., & Welacky, T. W. (1996). Influence of controlled drainage-subirrigation on surface and tile drainage nitrate loss. Journal of environmental Quality, 25(2), 317-324.

Drury, C. F., Tan, C. S., Welacky, T. W., Reynolds, W. D., Zhang, T. Q., Oloya, T. O., ... & Gaynor, J. D. (2014). Reducing nitrate loss in tile drainage water with cover crops and water-table management systems. Journal of Environmental Quality, 43(2), 587-598.

Drury, C.F.; Tan, C.S.; Reynolds, W.D.; Welacky, T.W.; Oloya, T.O.; Gaynor, J.D. Managing tile drainage, subirrigation, and nitrogen fertilization to enhance crop yields and reduce nitrate loss. *J. Environ. Qual.* 2009, *38*, 1193–1204.

Duncan, Jonathan M., Peter M. Groffman, and Lawrence E. Band. "Towards closing the watershed nitrogen budget: Spatial and temporal scaling of denitrification." Journal of Geophysical Research: Biogeosciences 118.3 (2013): 1105-1119.

Eagle, A.J.; McLellan, E.L.; Brawner, E.M.; Chantigny, M.H.; Davidson, E.A.; Dickey, J.B.; Linquist, B.A.; Maaz, T.M.; Pelster, D.E.; Pittelkow, C.M.; et al. Quantifying on-farm nitrous oxide emission reductions in food supply chains. *Earth's Future* 2020, *8*, e2020EF001504.

Elliott, E. M., Kendall, C., Wankel, S. D., Burns, D. A., Boyer, E. W., Harlin, K., ... & Butler, T. J. (2007). Nitrogen isotopes as indicators of NO x source contributions to atmospheric nitrate deposition across the midwestern and northeastern United States. *Environmental Science & Technology*, *41*(22), 7661-7667.

Elmi, A.; Burton, D.; Gordon, R.; Madramootoo, C. Impacts of water table management on N_2O and N_2 from a sandy loam soil in southwestern Quebec, Canada. *Nutr. Cycl. Agroecosystems* 2005, *72*, 229–240.

Enanga, E. M., Casson, N. J., Fairweather, T. A., & Creed, I. F. (2017). Nitrous oxide and dinitrogen: the missing flux in nitrogen budgets of forested catchments?. *Environmental Science & Technology*, *51*(11), 6036-6043.

Evans, R. O., Bass, K. L., Burchell, M. R., Hinson, R. D., Johnson, R., & Doxey, M. (2007). Management alternatives to enhance water quality and ecological function of channelized streams and drainage canals. Journal of Soil and Water Conservation, 62(4), 308-320.

Evans, R.O.; Skaggs, R.W.; Gilliam, J.W. Controlled versus conventional drainage effects on water quality. *J. Irrig. Drain. Eng.* 1995, *121*, 271–276.

Fang, Y., Koba, K., Makabe, A., Takahashi, C., Zhu, W., Hayashi, T., ... & Yoh, M. (2015). Microbial denitrification dominates nitrate losses from forest ecosystems. Proceedings of the National Academy of Sciences, 112(5), 1470-1474.

Fernández, F.G.; Venterea, R.T.; Fabrizzi, K.P. Corn nitrogen management influences nitrous oxide emissions in drained and undrained soils. *J. Environ. Qual.* 2016, *45*, 1847–1855.

Filoso, S., & Palmer, M. A. (2011). Assessing stream restoration effectiveness at reducing nitrogen export to downstream waters. *Ecological Applications*, *21*(6), 1989-2006.

Firestone, M. K. (1982). Biological denitrification. *Nitrogen in agricultural soils*, *22*, 289-326.

Firestone, M.K.; Davidson, E.A. Microbiological basis of NO and N 2 O production and consumption in soil. *Exch. Trace Gases Between Terr. Ecosyst. Atmos.* 1989, *47*, 7–21.

Fisher, T. R., E. Koontz, A. B. Gustafson, R. J. Fox, J. Hagedorn, Q. Zhu, J. Lewis, M. Castro, E. Davidson. in prep. The effects of drainage control structures on the hydrology of an agricultural field. (in prep).

Fisher, T. R., Fox, R. J., Knee, K. L., & Jordan, T. E. (2019). Watershed Nitrogen Budgets. Encyclopedia of Water: Science, Technology, and Society, 1-13.

Fisher, T.R.; Fox, R.J.; Gustafson, A.B.; Lewis, J.; Millar, N.; Winstene, J.R. Fluxes of nitrous oxide and nitrate from agricultural fields on the Delmarva Peninsula: N biogeochemistry and economics of field management. *Agric. Ecosyst. Environ.* 2018, *254*, 162–178.

Fisher, T.R.; Jordan, T.E.; Staver, K.W.; Gustafson, A.B.; Koskelo, A.I.; Fox, R.J.; Sutton, A.J.; Kana, T.; Beckert, K.A.; Stone, J.P.; et al. The Choptank Basin in transition: Intensifying agriculture, slow urbanization, and estuarine eutrophication. In *Coastal Lagoons: Systems of Natural and Anthropogenic Change*; Kennish, M.J., Paerl, H.W., Eds.; CRC Press: Boca Raton, FL, USA, 2010; pp. 135–165.

Fisher, T. R., Fox, R. J., Gustafson, A. B., Lewis, J., Millar, N., & Winsten, J. R. (2018). Fluxes of nitrous oxide and nitrate from agricultural fields on the Delmarva

Peninsula: N biogeochemistry and economics of field management. *Agriculture, Ecosystems & Environment*, *254*, 162-178.

Fisher, T. R., Fox, R. J., Gustafson, A. B., Koontz, E., Lepori-Bui, M., & Lewis, J. (2021). Localized water quality improvement in the choptank estuary, a tributary of Chesapeake Bay. *Estuaries and Coasts*, *44*(5), 1274-1293.

Foley, J. A., Ramankutty, N., Brauman, K. A., Cassidy, E. S., Gerber, J. S., Johnston, M., ... & Zaks, D. P. (2011). Solutions for a cultivated planet. *Nature*, *478*(7369), 337-342.

Fowler, D., Coyle, M., Skiba, U., Sutton, M. A., Cape, J. N., Reis, S., ... & Voss, M. (2013). The global nitrogen cycle in the twenty-first century. Philosophical Transactions of the Royal Society B: Biological Sciences, 368(1621), 20130164.

Fox, R. J., Fisher, T. R., Gustafson, A. B., Koontz, E. L., Lepori-Bui, M., Kvalnes, K. L., ... & Silaphone, K. (2021). An evaluation of the Chesapeake Bay management strategy to improve water quality in small agricultural watersheds. *Journal of Environmental Management*, *299*, 113478.

Fox, R. J., Fisher, T. R., Gustafson, A. B., Jordan, T. E., Kana, T. M., & Lang, M. W. (2014). Searching for the missing nitrogen: biogenic nitrogen gases in groundwater and streams. *The Journal of Agricultural Science*, *152*(S1), 96-106.

Galloway, J. N., Aber, J. D., Erisman, J. W., Seitzinger, S. P., Howarth, R. W., Cowling, E. B., & Cosby, B. J. (2003). The nitrogen cascade. Bioscience, 53(4), 341-356.

Gardner, J. R., Fisher, T. R., Jordan, T. E., & Knee, K. L. (2016). Balancing watershed nitrogen budgets: accounting for biogenic gases in streams. Biogeochemistry, 127(2), 231-253.

Gavlak, R.; Horneck, D.; Miller, R.O. *Soil, Plant and Water Reference Methods for the Western Region*; WREP-125; Western Region Extension Publication: Logan, UT, USA, 2005.

Gentry, L. E., David, M. B., Below, F. E., Royer, T. V., & McIsaac, G. F. (2009). Nitrogen mass balance of a tile-drained agricultural watershed in east-central Illinois. *Journal of environmental quality*, *38*(5), 1841-1847.

Gilliam, J. W., & Skaggs, R. W. (1986). Controlled agricultural drainage to maintain water quality. *Journal of Irrigation and Drainage Engineering*, *112*(3), 254-263.

Gilliam, J. W., Skaggs, R. W., & Weed, S. B. (1979). Drainage control to diminish nitrate loss from agricultural fields. Journal of Environmental Quality, 8(1), 137-142.

Glibert, P.M. From hogs to HABs: Impacts of industrial farming in the US on nitrogen and phosphorus and greenhouse gas pollution. *Biogeochemistry* 2020, *150 (2)*, 139–180.

Granger, J., Sigman, D. M., Rohde, M. M., Maldonado, M. T., & Tortell, P. D. (2010). N and O isotope effects during nitrate assimilation by unicellular prokaryotic and eukaryotic plankton cultures. *Geochimica et Cosmochimica Acta*, *74*(3), 1030-1040.

Granger, J., Sigman, D. M., Lehmann, M. F., & Tortell, P. D. (2008). Nitrogen and oxygen isotope fractionation during dissimilatory nitrate reduction by denitrifying bacteria. Limnology and Oceanography, 53(6), 2533-2545.

Granger, J., & Wankel, S. D. (2016). Isotopic overprinting of nitrification on denitrification as a ubiquitous and unifying feature of environmental nitrogen cycling. *Proceedings of the National Academy of Sciences*, *113*(42), E6391-E6400.

Groffman, P. M., Altabet, M. A., Böhlke, H., Butterbach-Bahl, K., David, M. B., Firestone, M. K., ... & Voytek, M. A. (2006). Methods for measuring denitrification: diverse approaches to a difficult problem. Ecological applications, 16(6), 2091-2122.

Groffman, P. M., Butterbach-Bahl, K., Fulweiler, R. W., Gold, A. J., Morse, J. L., Stander, E. K., ... & Vidon, P. (2009). Challenges to incorporating spatially and temporally explicit phenomena (hotspots and hot moments) in denitrification models. Biogeochemistry, 93(1), 49-77.

Groffman, P. M. (2012). Terrestrial denitrification: challenges and opportunities. *Ecological Processes*, *1*(1), 1-11.

Groffman, P. M., Butterbach-Bahl, K., Fulweiler, R. W., Gold, A. J., Morse, J. L., Stander, E. K., ... & Vidon, P. (2009). Challenges to incorporating spatially and temporally explicit phenomena (hotspots and hot moments) in denitrification models. *Biogeochemistry*, *93*(1), 49-77.

Hagedorn JG, Davidson EA, Fisher TR, Fox RJ, Zhu Q, Gustafson AB, Koontz E, Castro MS, Lewis J. Effects of Drainage Water Management in a Corn–Soy Rotation on Soil N2O and CH4 Fluxes. Nitrogen. 2022; 3(1):128-148.

Hagedorn, J.; Davidson, E.; Fox, R.; Koontz, E.; Fisher, T.; Castro, M.; Zhu, Q.; Gustafson, A. Pollution Swapping of N_2O and CH_4 Emissions with Dissolved Nitrogen and Phosphorus Export in Drainage Water Managed Agricultural Field. In Proceedings of the AGU 2019 Fall Meeting, San Francisco, CA, USA, 9–13 December 2019; https://doi.org/10.1002/essoar.10501940.1.

Hall, S. J., Weintraub, S. R., & Bowling, D. R. (2016). Scale-dependent linkages between nitrate isotopes and denitrification in surface soils: implications for isotope measurements and models. Oecologia, 181(4), 1221-1231.

Helmers, M. J., Abendroth, L., Reinhart, B., Chighladze, G., Pease, L., Bowling, L., ... & Strock, J. (2022). Impact of controlled drainage on subsurface drain flow and nitrate load: A synthesis of studies across the US Midwest and Southeast. *Agricultural Water Management*, *259*, 107265.

Hergoualc'H, K.; Mueller, N.; Bernoux, M.; Kasimir, Ä.; van der Weerden, T.J.; Ogle, S.M. Improved accuracy and reduced uncertainty in greenhouse gas inventories by refining the IPCC emission factor for direct N_2O emissions from nitrogen inputs to managed soils. *Glob. Change Biol.* 2021, *27*, 6536–6550.

Hobbie, E. A., & Ouimette, A. P. (2009). Controls of nitrogen isotope patterns in soil profiles. *Biogeochemistry*, *95*(2), 355-371.

Hofstra, N., & Bouwman, A. F. (2005). Denitrification in agricultural soils: summarizing published data and estimating global annual rates. *Nutrient Cycling in Agroecosystems*, *72*(3), 267-278.

Högberg, P. (1997). Tansley review no. 95 15N natural abundance in soil–plant systems. *The New Phytologist*, *137*(2), 179-203

Houlton, B. Z., Sigman, D. M., & Hedin, L. O. (2006). Isotopic evidence for large gaseous nitrogen losses from tropical rainforests. Proceedings of the National Academy of Sciences, 103(23), 8745-8750.

Howarth, R. W., Billen, G., Swaney, D., Townsend, A., Jaworski, N., Lajtha, K., ... & Zhao-Liang, Z. (1996). Regional nitrogen budgets and riverine N & P fluxes for the drainages to the North Atlantic Ocean: Natural and human influences. In Nitrogen cycling in the North Atlantic Ocean and its watersheds (pp. 75-139). Springer, Dordrecht.

Hutchinson, G. L., & Davidson, E. A. (1993). Processes for production and consumption of gaseous nitrogen oxides in soil. *Agricultural ecosystem effects on trace gases and global climate change*, *55*, 79-93.

Jahangir, M. M., Khalil, M. I., Johnston, P., Cardenas, L. M., Hatch, D. J., Butler, M., ... & Richards, K. G. (2012). Denitrification potential in subsoils: a mechanism to reduce nitrate leaching to groundwater. *Agriculture, Ecosystems & Environment*, *147*, 13-23.

Jankowski, K.; Neill, C.; Davidson, E.A.; Macedo, M.N.; Costa, C.; Galford, G.L.; Santos, L.M.; Lefebvre, P.; Nunes, D.; Cerri, C.E.P.; et al. Deep soils modify environmental consequences of increased nitrogen fertilizer use in intensifying Amazon agriculture. *Sci. Rep.* 2018, *8*, 1–11.

Jaynes, D. B., Colvin, T. S., Karlen, D. L., Cambardella, C. A., & Meek, D. W. (2001). Nitrate loss in subsurface drainage as affected by nitrogen fertilizer rate. *Journal of environmental quality*, *30*(4), 1305-1314.

Jung, H., Koh, D. C., Kim, Y. S., Jeen, S. W., & Lee, J. (2020). Stable isotopes of water and nitrate for the identification of groundwater flowpaths: A review. *Water*, *12*(1), 138.

Kaiser, J., Hastings, M. G., Houlton, B. Z., Röckmann, T., & Sigman, D. M. (2007). Triple oxygen isotope analysis of nitrate using the denitrifier method and thermal decomposition of N2O. *Analytical Chemistry*, *79*(2), 599-607.

Kana, T. M., Darkangelo, C., Hunt, M. D., Oldham, J. B., Bennett, G. E., & Cornwell, J. C. (1994). Membrane inlet mass spectrometer for rapid high-precision determination of N2, O2, and Ar in environmental water samples. *Analytical Chemistry*, *66*(23), 4166-4170.

Kanter, D.; Wagner-Riddle, C.; Groffman, P.M.; Davidson, E.A.; Galloway, J.N.; Gourevitch, J.D.; van Grinsven, H.J.M.; Houlton, B.Z.; Keeler, B.L.; Ogle, S.M.; et al. Improving the social cost of nitrous oxide. *Nat. Clim. Change* 2021, *11*, 1008–1010. https://doi.org/10.1038/s41558-021-01226-z.

Kelley, C. J., Keller, C. K., Evans, R. D., Orr, C. H., Smith, J. L., & Harlow, B. A. (2013). Nitrate–nitrogen and oxygen isotope ratios for identification of nitrate sources and dominant nitrogen cycle processes in a tile-drained dryland agricultural field. *Soil Biology and Biochemistry*, *57*, 731-738.

Kemp WM, Boynton WR, Adolf JE, Boesch DF, Boicourt WC, Brush G, Cornwell JC, Fisher TR, Glibert PM, Hagy JD. 2005. Eutrophication of Chesapeake Bay: Historical trends and ecological interactions. Marine Ecology Progress Series 303: 1-29.

Kendall, C., Elliott, E. M., & Wankel, S. D. (2007). Tracing anthropogenic inputs of nitrogen to ecosystems. *Stable isotopes in ecology and environmental science*, *2*(1), 375-449.

Kliewer, B.A.; Gilliam, J.W. Water table management effects on denitrification and nitrous oxide evolution. *Soil Sci. Soc. Am. J.* 1995, *59*, 1694–1701.

Knoll, A. H., Canfield, D. E., & Konhauser, K. O. (2012). What is geobiology. *Fundamentals of Geobiology*, 1-4.

Knowles, R. Methane: Processes of production and consumption. *Agric. Ecosyst. Eff. Trace Gases Glob. Clim. Change* 1993, *55*, 145–156.

Knowles, R. (1982). Denitrification. *Microbiological reviews*, *46*(1), 43-70.

Koba, K., Tokuchi, N., Wada, E., Nakajima, T., & Iwatsubo, G. (1997). Intermittent denitrification: the application of a 15N natural abundance method to a forested ecosystem. *Geochimica et Cosmochimica Acta*, *61*(23), 5043-5050.

Kravchenko, A.N.; Robertson, G.P. Statistical challenges in analyses of chamber-based soil CO_2 and N_2O emissions data. *Soil Sci. Soc. Am. J.* 2015, *79*, 200–211.

Kumar, S.; Nakajima, T.; Kadono, A.; Lal, R.; Fausey, N. Long-term tillage and drainage influences on greenhouse gas fluxes from a poorly drained soil of central Ohio. *J. Soil Water Conserv.* 2014, *69*, 553–563.

Lalonde, V.; Madramootoo, C.A.; Trenholm, L.; Broughton, R.S. Effects of controlled drainage on nitrate concentrations in subsurface drain discharge. *Agric. Water Manag.* 1996, *29*, 187–199.

Lassaletta, L.; Billen, G.; Grizzetti, B.; Anglade, J.; Garnier, J. 50 year trends in nitrogen use efficiency of world cropping systems: The relationship between yield and nitrogen input to cropland. *Environ. Res. Lett.* 2014, *9*, 105011.

Lavaire, T., Gentry, L. E., David, M. B., & Cooke, R. A. (2017). Fate of water and nitrate using drainage water management on tile systems in east-central Illinois. *Agricultural Water Management*, *191*, 218-228.

Lawrence, N. C., Tenesaca, C. G., VanLoocke, A., & Hall, S. J. (2021). Nitrous oxide emissions from agricultural soils challenge climate sustainability in the US Corn Belt. Proceedings of the National Academy of Sciences, 118(46), e2112108118.

Levy, P.E.; Gray, A.; Leeson, S.R.; Gaiawyn, J.; Kelly, M.P.C.; Cooper, M.D.A.; Dinsmore, K.J.; Jones, S.K.; Sheppard, L.J. Quantification of uncertainty in trace gas fluxes measured by the static chamber method. *Eur. J. Soil Sci.* 2011, *62*, 811–821.

Mariotti, Andre, et al. "Experimental determination of nitrogen kinetic isotope fractionation: some principles; illustration for the denitrification and nitrification processes." *Plant and soil* 62.3 (1981): 413-430.

Matson, P.A.; Billow, C.; Hall, S.; Zachariassen, J. Fertilization practices and soil variations control nitrogen oxide emissions from tropical sugar cane. *J. Geophys. Res. Atmos.* 1996, *101*, 18533–18545.

Matson, P. A., Parton, W. J., Power, A. G., & Swift, M. J. (1997). Agricultural intensification and ecosystem properties. *Science*, *277*(5325), 504-509.

Maynard, D.G.; Kalra, Y.P.; Crumbaugh, J.A. Nitrate and exchangeable ammonium nitrogen. In *Soil Sampling and Methods of Analysis*; CRC Press: Boca Raton, FL, USA, 1993; Volume 1.

McClain, M. E., Boyer, E. W., Dent, C. L., Gergel, S. E., Grimm, N. B., Groffman, P. M., ... & Pinay, G. (2003). Biogeochemical hot spots and hot moments at the interface of terrestrial and aquatic ecosystems. Ecosystems, 301-312.

Meisinger, J. J., Calderón, F. J., & Jenkinson, D. S. (2008). Soil nitrogen budgets. Nitrogen in agricultural systems, 49, 505-562.

Mengis, M., Schif, S. L., Harris, M., English, M. C., Aravena, R., Elgood, R. J., & MacLean, A. (1999). Multiple geochemical and isotopic approaches for assessing ground water NO3− elimination in a riparian zone. *Groundwater*, *37*(3), 448-457.

Michalski, G., Kolanowski, M., & Riha, K. M. (2015). Oxygen and nitrogen isotopic composition of nitrate in commercial fertilizers, nitric acid, and reagent salts. *Isotopes in environmental and health studies*, *51*(3), 382-391.

Morse, J. L., Ardón, M., & Bernhardt, E. S. (2012). Using environmental variables and soil processes to forecast denitrification potential and nitrous oxide fluxes in coastal plain wetlands across different land uses. Journal of Geophysical Research: Biogeosciences, 117(G2).

Murphy, R. R., Keisman, J., Harcum, J., Karrh, R. R., Lane, M., Perry, E. S., & Zhang, Q. (2021). Nutrient improvements in chesapeake bay: direct effect of load reductions and implications for coastal management. *Environmental Science & Technology*, *56*(1), 260-270.

Nangia, Vinay; Sunohara, M.; Topp, E.; Gregorich, E.; Drury, C.; Gottschall, N.; Lapen, D. Measuring and modeling the effects of drainage water management on soil greenhouse gas fluxes from corn and soybean fields. *J. Environ. Manag.* 2013, *129*, 652–664.

National Atmospheric Deposition Program, 2022. Total Deposition Maps, v2021.01.

Needelman, B. A., Kleinman, P. J., Strock, J. S., & Allen, A. L. (2007). Drainage Ditches: Improved management of agricultural drainage ditches for water quality protection: An overview. *Journal of Soil and Water Conservation*, *62*(4), 171-178

Nelson, D. W. (1982). Gaseous losses of nitrogen other than through denitrification. Nitrogen in agricultural soils, 22, 327-363.

Nestler, A., Berglund, M., Accoe, F., Duta, S., Xue, D., Boeckx, P., & Taylor, P. (2011). Isotopes for improved management of nitrate pollution in aqueous resources: review of surface water field studies. *Environmental Science and Pollution Research*, *18*(4), 519-533.

Nickerson, N. *Evaluating Gas Emission Measurements using Minimum Detectable Flux (MDF)*; Eosense Inc.: Dartmouth, Canada, 2016.

Nömmik, H. (1956). Investigations on denitrification in soil. *Acta Agriculturae Scandinavica*, *6*(2), 195-228.

Nykänen, H., Alm, J., Silvola, J., Tolonen, K., & Martikainen, P. J. (1998). Methane fluxes on boreal peatlands of different fertility and the effect of long-term experimental lowering of the water table on flux rates. Global biogeochemical cycles, 12(1), 53-69.

Oehler, F., Durand, P., Bordenave, P., Saadi, Z., & Salmon-Monviola, J. (2009). Modelling denitrification at the catchment scale. *Science of the total environment*, *407*(5), 1726-1737.

Osaka, K. I., Ohte, N., Koba, K., Yoshimizu, C., Katsuyama, M., Tani, M., ... & Nagata, T. (2010). Hydrological influences on spatiotemporal variations of δ15N and δ18O of nitrate in a forested headwater catchment in central Japan: Denitrification plays a critical role in groundwater. *Journal of Geophysical Research: Biogeosciences*, *115*(G2).

Ostrom, N. E., Knoke, K. E., Hedin, L. O., Robertson, G. P., & Smucker, A. J. (1998). Temporal trends in nitrogen isotope values of nitrate leaching from an agricultural soil. *Chemical Geology*, *146*(3-4), 219-227.

Pachauri, R. K., Allen, M. R., Barros, V. R., Broome, J., Cramer, W., Christ, R., ... & van Ypserle, J. P. (2014). Climate change 2014: synthesis report. Contribution of Working Groups I, II and III to the fifth assessment report of the Intergovernmental Panel on Climate Change.

Panek, J. A., Matson, P. A., Ortiz-Monasterio, I., & Brooks, P. (2000). Distinguishing nitrification and denitrification sources of N2O in a Mexican wheat system using 15N. *Ecological Applications*, *10*(2), 506-514.

Parkin, T. B., & Kaspar, T. C. (2006). Nitrous oxide emissions from corn–soybean systems in the Midwest. Journal of environmental quality, 35(4), 1496-1506.

Parkin, T.B.; Kaspar, T.C. Nitrous oxide emissions from corn–soybean systems in the Midwest. *J. Environ. Qual.* 2006, *35*, 1496–1506.

Phillips, R. L. (2008). Denitrification in cropping systems at sub-zero soil temperatures. A review. *Agronomy for sustainable development*, *28*(1), 87-93.

Prather, M.J.; Hsu, J.; DeLuca, N.M.; Jackman, C.H.; Oman, L.; Douglass, A.R.; Fleming, E.L.; Strahan, S.E.; Steenrod, S.D.; Søvde, O.A.; et al. Measuring and modeling the lifetime of nitrous oxide including its variability. *J. Geophys. Res. Atmos.* 2015, *120*, 5693–5705.

Pribyl, A. L., Mccutchan, J. H., Lewis, W. M., & Saunders Iii, J. F. (2005). Whole-system estimation of denitrification in a plains river: a comparison of two methods. Biogeochemistry, 73(3), 439-455.

Reddy, S., Panichelli, L., Waterworth, R. M., Federici, S., Green, C., Jonckheere, I., Kahuri, S., Kurz, W. A., de Ligt, R., Ometto, J. P., Petersson, H., Takahiro, E., Paul, T., Tullis, J., Somogyi, Z., Pandya, M., Rocha, M. T., & Suzuki, K. (2019). Chapter 3: Consistent representation of land. In E. Calvo Buendia, K. Tanabe, A. Kranjc, J. Baasansuren, M. Fukuda, S. Ngarize, A. Osako, Y. Pyrozhenko, P. Shermanau, & S. Federici (Eds.), 2019 Refinement to the 2006 IPCC guidelines for national

greenhouse gas inventories—Volume 4 agriculture, forestry and other land use (sec. 3.1–3.55). Intergovernmental Panel on Climate Change.

Reinhardt, M., Müller, B., Gächter, R., & Wehrli, B. (2006). Nitrogen removal in a small constructed wetland: an isotope mass balance approach. *Environmental science & technology*, *40*(10), 3313-3319

Robertson, G.P.; Coleman, D.C.; Sollins, P.; Bledsoe, C.S. *Standard Soil Methods for Long-Term Ecological Research*; Oxford University Press: Oxford, UK, 1999; Volume 2.

Rochette, P., Angers, D. A., Chantigny, M. H., Gasser, M. O., MacDonald, J. D., Pelster, D. E., & Bertrand, N. (2013). NH3 volatilization, soil concentration and soil pH following subsurface banding of urea at increasing rates. *Canadian Journal of Soil Science*, *93*(2), 261-268.

Roy, E.D.; Wagner, C.R.H.; Niles, M.T. Hot spots of opportunity for improved cropland nitrogen management across the United States. *Environ. Res. Lett.* 2021, *16*, 035004.

Sabo, R.D.; Clark, C.M.; Bash, J.; Sobota, D.; Cooter, E.; Dobrowolski, J.P.; Houlton, B.Z.; Rea, A.; Schwede, D.; Morford, S.L.; et al. Decadal shift in nitrogen inputs and fluxes across the contiguous United States: 2002–2012. *J. Geophys. Res. Biogeosciences* 2019, *124*, 3104–3124.

Sabo, R. D., Sullivan, B., Wu, C., Trentacoste, E., Zhang, Q., Shenk, G. W., ... & Linker, L. C. (2022). Major point and nonpoint sources of nutrient pollution to surface water have declined throughout the Chesapeake Bay watershed. *Environmental Research Communications*, *4*(4), 045012.

Schlesinger, W. H. (2009). On the fate of anthropogenic nitrogen. *Proceedings of the National Academy of Sciences*, *106*(1), 203-208.

Schmidt, J. P., Dell, C. J., Vadas, P. A., & Allen, A. L. (2007). Nitrogen export from coastal plain field ditches. *Journal of Soil and Water Conservation*, *62*(4), 235-243.

Schott, L., Lagzdins, A., Daigh, A. L. M., Craft, K., Pederson, C., Brenneman, G., & Helmers, M. J. (2017). Drainage water management effects over five years on water tables, drainage, and yields in southeast Iowa. *Journal of Soil and Water Conservation*, *72*(3), 251-259.

Schwede, D. B., & Lear, G. G. (2014). A novel hybrid approach for estimating total deposition in the United States. *Atmospheric Environment*, *92*, 207-220.

Seitzinger, S., Harrison, J. A., Böhlke, J. K., Bouwman, A. F., Lowrance, R., Peterson, B., ... & Drecht, G. V. (2006). Denitrification across landscapes and waterscapes: a synthesis. *Ecological applications*, *16*(6), 2064-2090.

Sigler, W. A., Ewing, S. A., Wankel, S. D., Jones, C. A., Leuthold, S., Brookshire, E. N. J., & Payn, R. A. (2022). Isotopic signals in an agricultural watershed suggest denitrification is locally intensive in riparian areas but extensive in upland soils. *Biogeochemistry*, *158*(2), 251-268.

Sigman, D. M., Casciotti, K. L., Andreani, M., Barford, C., Galanter, M. B. J. K., & Böhlke, J. K. (2001). A bacterial method for the nitrogen isotopic analysis of nitrate in seawater and freshwater. *Analytical chemistry*, *73*(17), 4145-4153.

Skaggs, R.W.; Breve, M.A.; Gilliam, J.W. Hydrologic and water quality impacts of agricultural drainage*. *Crit. Rev. Environ. Sci. Technol.* 1994, *24*, 1–32.

Skaggs, R.W.; Fausey, N.R.; Evans, R.O. Drainage water management. *J. Soil Water Conserv.* 2012, *67,* 167A–172A.

Skiba, U. M., Sheppard, L. J., MacDonald, J., & Fowler, D. (1998). Some key environmental variables controlling nitrous oxide emissions from agricultural and semi-natural soils in Scotland. Atmospheric environment, 32(19), 3311-3320.

Smil, V. Nitrogen in crop production: An account of global flows. *Glob. Biogeochem. Cycles* 1999, *13*, 647–662.

Smith, E.L.; Kellman, L.M. Nitrate loading and isotopic signatures in subsurface agricultural drainage systems. *J. Environ. Qual.* 2011, *40*, 1257–1265.

Snider, D. M., Venkiteswaran, J. J., Schiff, S. L., & Spoelstra, J. (2015). From the ground up: Global nitrous oxide sources are constrained by stable isotope values. *PloS one*, *10*(3), e0118954.

Soil Survey Staff, Natural Resources Conservation Service, United States Department of Agriculture. Web Soil Survey. Available online at http://websoilsurvey.nrcs.usda.gov/. Accessed [06/11/2022].

Soper, F. M., Taylor, P. G., Wieder, W. R., Weintraub, S. R., Cleveland, C. C., Porder, S., & Townsend, A. R. (2018). Modest gaseous nitrogen losses point to conservative nitrogen cycling in a lowland tropical forest watershed. *Ecosystems*, *21*(5), 901-912.

Sunohara, M.D.; Craiovan, E.; Topp, E.; Gottschall, N.; Drury, C.F.; Lapen, D.R. Comprehensive nitrogen budgets for controlled tile drainage fields in eastern Ontario, Canada. *J. Environ. Qual.* 2014, *43*, 617–630.

Sutton, A. J., Fisher, T. R., & Gustafson, A. B. (2010). Effects of restored stream buffers on water quality in non-tidal streams in the Choptank River basin. *Water, air, and soil pollution*, *208*(1), 101-118.

Testa, J. M., Clark, J. B., Dennison, W. C., Donovan, E. C., Fisher, A. W., Ni, W., ... & Ziegler, G. (2017). Ecological forecasting and the science of hypoxia in Chesapeake Bay. *BioScience*, *67*(7), 614-626.

Tiedje, J. M. (1988). Ecology of denitrification and dissimilatory nitrate reduction to ammonium. *Biology of anaerobic microorganisms*, 179-244.

Topp, G.C.; Davis, J.L.; Annan, A.P. Electromagnetic determination of soil water content: Measurements in coaxial transmission lines. *Water Resour. Res.* 1980, *16*, 574–582.

Torbert, H.A., R.G. Hoeft, R.M. Vandenheuvel, and R.L. Mulvaney. (1992). Effect of moisture regime on recovery and utilization of fertilizer N applied to corn. Commun. Soil Sci. Plant Anal. 13:1409–1426.

Ullah, S.; Moore, T.R. Biogeochemical controls on methane, nitrous oxide, and carbon dioxide fluxes from deciduous forest soils in eastern Canada. *J. Geophys. Res. Biogeosciences* 2011, Vol. *116*.

Unkovich, M., Herridge, D. A. V. I. D., Peoples, M., Cadisch, G., Boddey, B., Giller, K., ... & Chalk, P. (2008). *Measuring plant-associated nitrogen fixation in agricultural systems*. Australian Centre for International Agricultural Research (ACIAR).

US-EPA. .Inventory of US Greenhouse Gas Emissions and Sinks, 1990–2019. *US Environmental Protection Agency.* https://www. epa. gov/ghgemissions/inventory-us-greenhouse-gas-emissions-and-sinks. Access date: 11/13/2021.

Van Breemen, N. V., Boyer, E. W., Goodale, C. L., Jaworski, N. A., Paustian, K., Seitzinger, S. P., ... & Billen, G. (2002). Where did all the nitrogen go? Fate of nitrogen inputs to large watersheds in the northeastern USA. *Biogeochemistry*, *57*(1), 267-293.

Van der Weerden, T.J.; Noble, A.N.; Luo, J.; de Klein, C.A.M.; Saggar, S.; Giltrap, D.; Gibbs, J.; Rys, G. Meta-analysis of New Zealand's nitrous oxide emission factors for ruminant excreta supports disaggregation based on excreta form, livestock type and slope class. *Sci. Total Environ.* 2020, *732*, 139235.

Van Meter, K. J., Basu, N. B., Veenstra, J. J., & Burras, C. L. (2016). The nitrogen legacy: emerging evidence of nitrogen accumulation in anthropogenic landscapes. *Environmental Research Letters*, *11*(3), 035014.

Van Zandvoort, A.; Lapen, D.; Clark, I.; Flemming, C.; Craiovan, E.; Sunohara, M.; Boutz, R.; Gottschall, N. Soil CO_2, CH_4, and N_2O fluxes over and between tile drains on corn, soybean, and forage fields under tile drainage management. *Nutr. Cycl. Agroecosystems* 2017, *109*, 115–132.

Venterea, R.T.; Coulter, J.A. Split application of urea does not decrease and may increase nitrous oxide emissions in rainfed corn. *Agron. J.* 2015, *107*, 337–348.

Verchot, L.V.; Davidson, E.; Cattanio, J.H.; Ackerman, I.L.; Erickson, H.E.; Keller, M. Land use change and biogeochemical controls of nitrogen oxide emissions from soils in eastern Amazonia. *Glob. Biogeochem. Cycles* 1999, *13*, 31–46.

Vitousek, P. M., Aber, J. D., Howarth, R. W., Likens, G. E., Matson, P. A., Schindler, D. W., ... & Tilman, D. G. (1997). Human alteration of the global nitrogen cycle: sources and consequences. *Ecological applications*, *7*(3), 737-750.

Walter, K. M., Zimov, S. A., Chanton, J. P., Verbyla, D., & Chapin, F. S. (2006). Methane bubbling from Siberian thaw lakes as a positive feedback to climate warming. Nature, 443(7107), 71-75.

Webb, J. R., Clough, T. J., & Quayle, W. C. (2021). A review of indirect N2O emission factors from artificial agricultural waters. *Environmental Research Letters*, *16*(4), 043005

Weiss, R. F., & Price, B. A. (1980). Nitrous oxide solubility in water and seawater. *Marine chemistry*, *8*(4), 347-359.

Weitzman, J. N., Groffman, P. M., Adler, P. R., Dell, C. J., Johnson, F. E., Lerch, R. N., & Strickland, T. C. (2021). Drivers of hot spots and hot moments of denitrification in agricultural systems. *Journal of Geophysical Research: Biogeosciences*, *126*(7), e2020JG006234.

Wexler, S. K., Goodale, C. L., McGuire, K. J., Bailey, S. W., & Groffman, P. M. (2014). Isotopic signals of summer denitrification in a northern hardwood forested catchment. *Proceedings of the National Academy of Sciences*, *111*(46), 16413-16418.

Wieczorek, M.E.; LaMotte, A.E. *Attributes for NHDPlus Catchments (Version 1.1) for the Conterminous United States: Nutrient Application (Phosphorus and Nitrogen) for Fertilizer and Manure Applied to Crops (Cropsplit), 2002*; Data Series DS-490-08; U.S. Geological Survey Digital: Reston, VA, USA, 2010.

Williams, M.R.; King, K.W.; Fausey, N.R. Drainage water management effects on tile discharge and water quality. *Agric. Water Manag.* 2015, *148*, 43–51.

Xu, R.; Tian, H.; Pan, N.; Thompson, R.L.; Canadell, J.G.; Davidson, E.A.; Nevison, C.; Winiwarter, W.; Shi, H.; Pan, S.; et al. Magnitude and uncertainty of nitrous oxide emissions from North America based on bottom-up and top-down approaches: Informing future research and national inventories. *Geophys. Res. Lett.* 2021, *48*, e2021GL095264.

Xu, S. Q., Liu, X. Y., Sun, Z. C., Hu, C. C., Wanek, W., & Koba, K. (2021). Isotopic elucidation of microbial nitrogen transformations in forest soils. *Global Biogeochemical Cycles*, *35*(12), e2021GB007070.

Yanai, R. D., Vadeboncoeur, M. A., Hamburg, S. P., Arthur, M. A., Fuss, C. B., Groffman, P. M., ... & Driscoll, C. T. (2013). From missing source to missing sink: long-term changes in the nitrogen budget of a northern hardwood forest. *Environmental science & technology*, *47*(20), 11440-11448.

Yu, L., Mulder, J., Zhu, J., Zhang, X., Wang, Z., & Dörsch, P. (2019). Denitrification as a major regional nitrogen sink in subtropical forest catchments: Evidence from multi-site dual nitrate isotopes. *Global change biology*, *25*(5), 1765-1778.

Zhang, X., Davidson, E. A., Zou, T., Lassaletta, L., Quan, Z., Li, T., & Zhang, W. (2020). Quantifying nutrient budgets for sustainable nutrient management. Global Biogeochemical Cycles, 34(3), e2018GB006060.

Zhang, Xin; Davidson, E.A.; Mauzerall, D.L.; Searchinger, T.D.; Dumas, P.; Shen, Y. Managing nitrogen for sustainable development. *Nature* 2015, *528*, 51–59.

Zhang, Xin; Zou, T.; Lassaletta, L.; Mueller, N.D.; Tubiello, F.N.; Lisk, M.D.; Lu, C.; Conant, R.T.; Dorich, C.D.; Gerber, J.; et al. Quantification of global and national nitrogen budgets for crop production. *Nat. Food* 2021, *2,* 529–540.

Zhang, X., Zou, T., Lassaletta, L., Mueller, N. D., Tubiello, F. N., Lisk, M. D., ... & Davidson, E. A. (2021). Quantification of global and national nitrogen budgets for crop production. *Nature Food*, *2*(7), 529-540.

Zistl-Schlingmann, M., Feng, J., Kiese, R., Stephan, R., Zuazo, P., Willibald, G., ... & Dannenmann, M. (2019). Dinitrogen emissions: an overlooked key component of the N balance of montane grasslands. *Biogeochemistry*, *143*(1), 15-30.